Development of HZSM-5-based Catalysts for In-situ Catalytic Upgrading of Bio-oil Derived from Fast Pyrolysis of Biomass

Nichaboon Chaihad

A Dissertation Submitted in Partial Fulfillment of the Requirements for the Degree of Doctor of Engineering

GRADUATE SCHOOL OF SCIENCE AND TECHNOLOGY

HIROSAKI UNIVERSITY

2022

Abstract

Fast pyrolysis of biomass to produce bio-oils has attracted great attention because it is an effective technology to convert most of biomass components directly into liquid fuel. However, the bio-oils obtained from the pyrolysis process always have highly complex oxygenated compounds with high viscosity, serious corrosivity, and rather instability. Thus, before the raw bio-oils are used as fuel or chemical feedstock, they must be upgraded, especially deoxygenated. Cracking of bio-oils over protonated zeolites such as HY, H-Beta, H-ferrierite and HZSM-5 at ambient pressure could be an effective way for the bio-oil upgrading, in which hydrogen gas is not necessary. Especially, among various protonated zeolites, HZSM-5 has been considered the most effective one in the deoxygenation of bio-oils with more aromatic species in the upgraded bio-oils. However, HZSM-5 itself is limited by low mass-transfer rates of large reactants as well as products due to its micropore structure. During the deoxygenation process, the easy blockage of open micropores always leads to the sharp catalyst deactivation. To deal with this issue, three main strategies could be applied. First one is metal modification, which is a facile method to optimize the acidity of the HZSM-5 for the promoting of deoxygenation and meanwhile, the reducing of the further reactions to form coke on the catalyst and thereby slowing down the catalyst deactivation rate. However, this method cannot reduce the diffusion limitation of the micropores in the zeolites. Thus, the second strategy, i.e., construction of HZSM-5 with a hierarchical structure, could solve diffusion limitations. The third one is the synthesis of special ZSM-5 morphologies such as HZSM-5 catalysts with hollow structure or core/shell structure. In this dissertation, the above three strategies were used for the preparation of HZSM-5-based zeolite catalysts for the in-situ upgrading of bio-oils derived from the fast pyrolysis of biomass. While, the mechanisms influencing catalytic performance and catalyst preparation were proposed and discussed. The main conclusions are summarized as follows:

(1) A study on in-situ upgrading of bio-oil from the fast pyrolysis of biomass over Cu/ZSM-5

prepared using the wet impregnation method. It is found that Cu/HZSM-5 with low Cu loading amounts preserved HZSM-5 crystalline structure as well as its acid sites and provided the best textural properties which enhanced deoxygenation performance. 0.5 wt.% Cu/ZSM-5 exhibited the best catalytic performance with a high relative amount of aromatic hydrocarbons of 73.2 % and a yield of specific aromatic hydrocarbons as high as 56.5 mg/g-biomass (d.a.f), which were much higher than those based on the parent HZSM-5. Moreover, the 0.5 wt.% Cu loaded HZSM-5 catalyst also showed excellent catalytic reusability and regeneration property.

(2) Hierarchical structured HZSM-5 catalysts were synthesized by desilication of commercial HZSM-5 in aqueous NaOH solution with the assistance of tetrapropylammonium hydroxides (TPAOH) and applied for upgrading of bio-oil derived from fast pyrolysis of biomass. In comparison to traditional HZSM-5 and those hierarchical structured HZSM-5 zeolite catalysts prepared under other conditions, the hierarchical HZSM-5 prepared by using concentrations of 0.2 M NaOH with 0.25 M TPAOH showed the maximum catalytic performance, resulting in the highest production of aromatic hydrocarbons. With the help of a small amount of TPAOH, the formation of mesopores can be highly controlled, resulting in more surface area and suitable acid content. However, the coke generated on the catalyst surface led to the deactivation of catalysts. To solve this issue, hierarchical HZSM-5 zeolite catalysts were modified by various metals with different loading amounts. It was found that 0.25 wt.% Cu loaded hierarchical HZSM-5 further increased the yield of aromatic hydrocarbons with reduced coke formation.

(3) To further improve the catalytic performance, HZSM-5 zeolites with hollow structure were prepared by using the hydrothermal method. In the presence of tetrapropylammonium hydroxide (TPAOH), it was found that the obtained hollow HZSM-5 zeolite catalyst had a mesoporous shell. When the optimum catalyst was used for the upgrading of bio-oils derived from the fast pyrolysis of cellulose and hemicellulose, aromatic hydrocarbon yields of

78.49–78.67 % were achieved, which were much higher than the case using traditional HZSM-5 (61.06–68.26 %). Moreover, when real biomass (cedar) with an optimum biomass/catalyst weight ratio of 1:2 was used, the yield of aromatic hydrocarbons was up to 80.16%. In addition, this catalyst also exhibited excellent reusability and regeneration properties.

Acknowledgements

Table of Contents

List of Tables

List of Figures

List of Schemes

Chapter 1 Introduction

1.1 Upgrading of bio-oil process

The bio-oil obtained from the pyrolysis of biomass has a dark brown appearance with a distinctive smoky smell. Due to its poor quality including high viscosity, high water content, high oxygen concentration, low heating value and instability, upgrading of bio-oil is necessary before it can be used as a transportation fuel and chemical feedstocks [1]. Catalytic pyrolysis, hydrodeoxygenation, and esterification are typical bio-oil upgrading processes. However, they can generate different products.

1.1.1 Catalytic pyrolysis

Catalytic pyrolysis is a potential technology for directly converting biomass or polymers into commercially valuable hydrocarbons with the assistance of catalysts, in which hydrogen is not needed and the process is operated at atmospheric pressure [2, 3]. By the assistance of catalysts, the quality of pyrolysis oil can be improved, and the decomposition temperature can be decreased with the increase in the selectivity to the desired product. Such a catalytic pyrolysis process is always controlled by various factors such as pyrolysis operating conditions, in particular the temperature, heating rate, and residence time.

1.1.1.1 Classification of the pyrolysis process

Pyrolysis processes are often broadly classified into three types, i.e., slow ($\leq$ 500 ºC), fast (425-600ºC) and flash (650-1300ºC) based on the heating rate [4]. The slow pyrolysis process always results in the production of more biochar with a small yield of liquids [5]. In contrast, the fast pyrolysis performing with a short vapor residence time (2 s.), which can lead to 60-75 % of bio-fuel yield with less other products like gas and solid char [4, 6]. In the presence of catalysts, aromatics such as BTX (benzene, toluene and xylene) can be effectively generated

from the fast pyrolysis process, which has gained great attention in the biomass-related petrochemical industry. While, flash pyrolysis or very fast pyrolysis with rapid heating rates (>1000 °C/s) has been proven to provide high yield of bio-oil as well as high conversion efficiency even over 70% [7].

1.1.1.2 Operation modes of pyrolysis

Generally, there are two types of operation modes: *in situ* catalytic pyrolysis, in which the feedstock and catalyst are thoroughly mixed and the catalyst is exposed to pyrolysis vapor. In this case, the pyrolysis vapor diffuses promptly into the catalyst pore, where it undergoes a series of processes including cracking, deoxygenation, aromatization, and condensation [2].

However, if the catalyst placed in the reactor is separated by quartz wool to separate the catalyst and biomass on top (before the reaction) or char (the experimental product after the reaction) and only allow pass through of pyrolysis vapors which reacted further on the catalyst layer. The name given to this process is in situ catalytic upgrading. The other mode is *ex situ* pyrolysis, which requires at least two reactors, where the pyrolysis vapor is produced from biomass without the use of a catalyst in the primary reactor and then passed to the secondary reactor for catalytic upgrading [8]. In this case, the temperatures of the two reactors can be regulated individually to achieve the best operation conditions for pyrolysis and catalysis processes, which allows for greater control over product distribution and selectivity [9].

1.1.1.3 Chemical reactions in catalytic fast pyrolysis

A catalytic pyrolysis process can be used to upgrade bio-oil by removing oxygen from those

oxygenated compounds, which is also called deoxygenation. There are three common types of deoxygenation reactions: dehydration, decarboxylation and decarbonylation. In the bio-oils, a considerable number of components with -OH group exist. A dehydration reaction can remove oxygen from those oxygenated compounds in the form of water, in which Brønsted acid sites on the catalysts have primary influence, that is, they can donate protons to the hydroxyl group of oxygenates to generate water. The decarboxylation is a process to remove oxygen from those fatty acids and fatty acid methyl esters in the form of carbon dioxide. The decarbonylation is a process to remove oxygen in the form of carbon monoxide, in which the carbonyl groups can be removed from those aldehydes and ketone compounds. Meanwhile, some carbon and hydrogen could be lost by coke formation over the catalysts and/or the generation of gaseous hydrocarbons by the bio-oil vapor cracking [10]. There are also other reactions involved in the upgrading of bio-oils, such as cracking, aldol condensation, ketonization and aromatization. Such a combined complex pyrolysis process will finally achieve the conversion of oxygenated compounds to hydrocarbons, thereby enhancing bio-oil quality [11].

 In particular, the aromatization is a chemical reaction by which those olefins and low molecular weight oxygenates, such as acids, alcohols, aldehydes, esters, ethers, and furans will convert to aromatic hydrocarbons. During the aromatization process, other reactions may occur simultaneously, such as cracking, dehydrogenation, oligomerization and cyclization. Aromatization generally takes place within the pores of catalysts such as zeolites. Two typical examples of aromatization are: the combination of propylene and furan to produce toluene or the reaction of benzene with furan to the form naphthalene via Diels-Alder condensation reaction [12]. **Fig.1.1** shows reactions in bio-oil upgrading from catalytic fast pyrolysis.
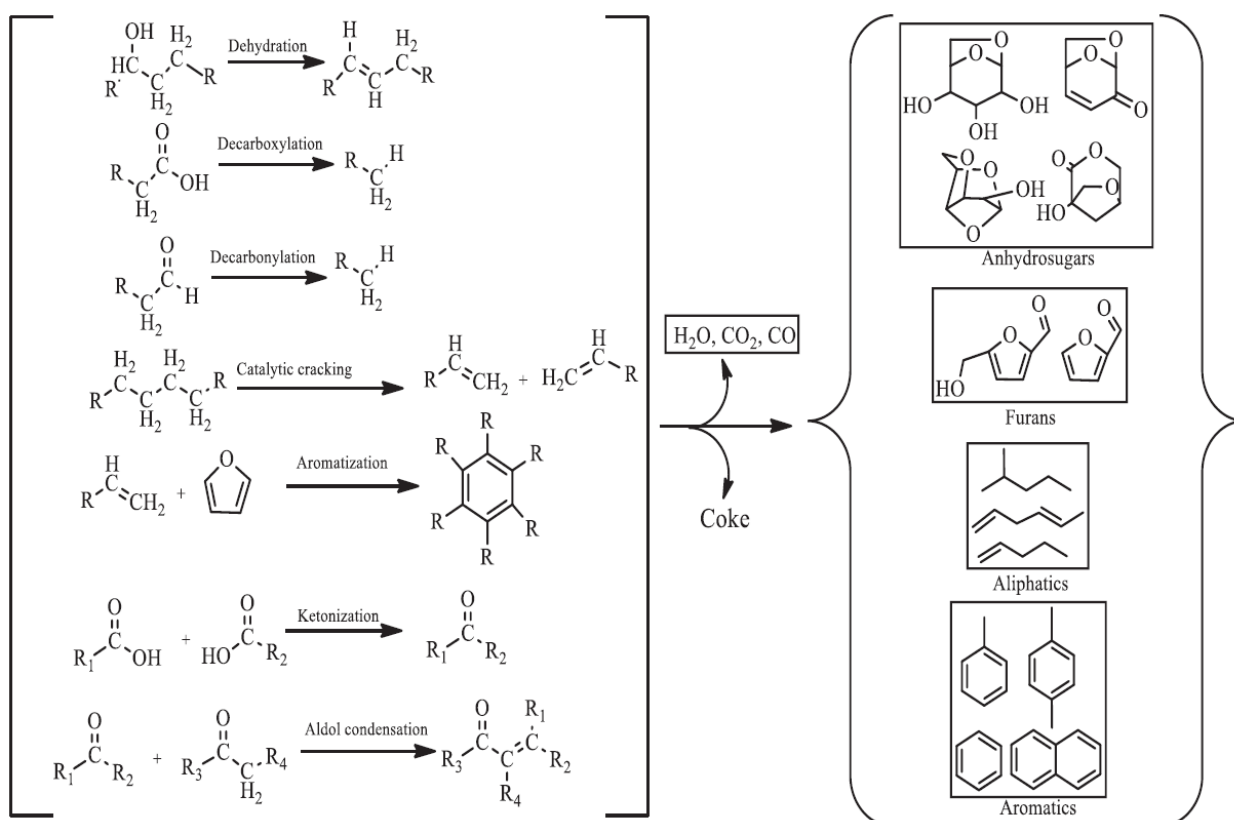
Fig. 1.1 Possible reactions in bio-oil upgrading from catalytic fast pyrolysis [12]

1.1.2 Hydrodeoxygenation

HDO is a bio-oil upgrading process that uses high-pressure (50-150 bar) hydrogen with catalysts at a moderate temperature to create saturated C-C bonds with the generation of water [13, 14]. In this case, high pressure can result in higher reaction rate and lower coke formation on the catalyst surface [15, 16]. However, the purification in the manufacturing of high-pressure hydrogen always consumes abundant energy, thus the cost is high [17]. As such, it is necessary to develop high-performance catalysts to reduce hydrogen consumption. Also, it is important to understand the mechanism and kinetics in the HDO process. In addition, development of a low-pressure process should be interesting in the industrial bio-oil HDO process. To date, noble and transition metals such as Pt, Ru Co, Mo, Ni and V, sulfides, nitrides, metal oxides, and metal supported alumina or aluminosilicate have been employed as industrially petrochemical catalysts [18-20]. However, since bio-oil always contain high water

4

content, some catalysts having alumina or aluminosilicate exhibit instability, especially for those bio-oils containing up to 50-60 wt.% of oxygen, resulting in rapid catalyst deactivation during the hydroprocessing [21].

In the HDO process, other reactions such as water separation, dehydration, condensation, polymerization, decarboxylation, hydrogenation and hydrocracking could occur together, which involve the breakdown of large molecules into smaller molecules [22, 23]. A possible mechanism for HDO can be described in **Scheme 1.1** as an example:

Scheme 1.1 Possible pathways of guaiacol hydrodeoxygenation [24]

1.1.3 Esterification

Esterification is an effective method that transforms organic acids like carboxylic acid in bio-oil into esters by reacting them with alcohol under milder conditions [25]. Numerous catalysts including mineral acids (sulfuric acid, hydrochloride acid, and phosphoric acid) and solid acid catalyst such as metal oxides (TiO_2, ZrO_2, SiO_2-TiO_2) and zeolites have been applied in the esterification of those organic acids in the bio-oil for upgrading [26]. Among them, solid acid catalysts should be more suitable for practical application because they are non-corrosive and easy to be separated [27].

1.2 Fundamentals of ZSM-5 based catalysts

ZSM-5 is a microporous aluminosilicate zeolite with characteristics suitable for aromatic and olefin production in the petrochemical industries due to its adequate combination of acid strength and shape selectivity. Similarly, ZSM-5 based catalysts have been widely employed in the upgrading of bio-oil obtained from the pyrolysis of a variety of biomass materials by enhancing a number of reactions including as decarboxylation, decarbonylation, dehydration, isomerization, and aromatization for the transforming of biomass-derived oxygenates into aromatic hydrocarbons [28]. Irwan *et al*. [29] investigated the *in-situ* catalytic upgrading of bio-oil derived from fast pyrolysis of lignin over different catalysts and concluded that ZSM-5 was a more active catalyst among all catalysts which improved the quality of bio-oil in terms of the highest selectivity towards monoaromatic hydrocarbons, and simultaneously, the use of ZSM-5 resulted in the highest yield of light oil and the lowest yield of coke. Generally, due to the bio-oil compositions, it is considered undesirable for use as transport fuel if it contains only fewer aromatics than those oxygenated species. Aho *et al*. [30] studied the catalytic pyrolysis of pine wood biomass in a fluidized bed reactor at 450°C utilizing various catalysts, including Beta, Y, ZSM-5, and Mordenite. The results showed that by the use of ZSM-5 resulted in the formation of lower acid and alcohol contents than that by using other zeolites, indicating that the variety of products could be influenced by the different zeolite structures. Furthermore, coke deposition on ZSM-5 appeared to be lower than that on other catalysts. Due to its adequate balance between acid strength and shape selectivity, ZSM-5 has been extensively used to convert biomass-derived oxygenated compound into aromatic hydrocarbons.

1.3 Influencing factors in catalytic fast pyrolysis over ZSM-5 based catalysts

The catalytic pyrolysis over ZSM-5 based catalysts could be influenced by several factors, especially not only the properties of the ZSM-5 based catalysts in terms of shape selectivity, pore size, surface area and acidity, but also the biomass type, catalyst to biomass ratio, and

reaction temperature.

1.3.1 Effect of ZSM-5 various properties on catalytic pyrolysis

Important properties of ZSM-5 such as pore size, surface area, acidity, shape selectivity and stability always greatly affect catalytic activity and the product distribution.

1.3.1.1 Acidity

The acid strength and acid site density of ZSM-5 catalyst vary with the SiO_2/Al_2O_3 ratio which determine the catalyst activity, deactivation, and product distribution during the pyrolysis process [31]. There are two types of acid sites of ZSM-5, i.e., Brønsted acid site and the Lewis acid site. High acidity with low Si/Al ratio is controlled especially by the Brønsted acid site, which becomes more active in the cracking process, leading to the production of more aromatics such as BTX or light olefins with the reducing of heavy oil fraction [32, 33]. However, the higher acidity will result in secondary reactions to produce more polyaromatic and form coke on the catalyst surface, thereby causing the deactivation of the catalyst. Polyaromatic hydrocarbons (PAH) have been reported as the precursor of coke. With the decrease in the SiO_2/Al_2O_3 molar ratio of zeolite, more polyaromatic hydrocarbons (PAH) and water will be generated with the reduced amount of light bio-oil yield [32, 34]. Thus, proper adjustment of acidity to make ZSM-5 suitable for the aromatic production has been proposed by using several techniques such as ion exchange, desilication, and dealumination [21, 35, 36]

1.3.1.2 Surface area

Surface area is one of main factors affecting the catalytic efficiency. Typically, ZSM-5 zeolites have specific BET surface areas in the range of 350-450 m^2/g [37]. In fact, the surface area is also strongly correlated with the acidity, thereby affecting catalytic activity. Especially, those ZSM-5 catalysts with higher surface area as well as larger pore size and shorter diffusion length will exhibit higher activity. The reactions over ZSM-5 catalysts include consecutive depolymerization of biomass products to form monocyclic aromatics such as BTX. It has been reported that the nanosheet ZSM-5 catalysts had better textural properties than the

conventional ZSM-5 with higher BET surface area, larger mesopore volume, and higher concentration of external Brønsted acid sites, thereby resulting in better performance for catalytic cracking reactions [38]. Generally, the acid sites on the external surface are vital in catalytic cracking of large molecules whereas those acid sites on the internal surface cannot effectively catalyse the macromolecule cracking due to the abundance of micropores, causing in rapid coke formation on the outlet of micropore and finally resulting in the gradual deactivation of ZSM-5 catalysts [39]. In other words, if the surface area and pore size can be increased, those large molecules in the bio-oil can easily diffuse into the pore and contact with more active sites, allowing them to be rapidly converted to hydrocarbons. Furthermore, the ZSM-5 catalysts with a high surface area could be more easily modified by metal loading since the metal loading can significantly reduce the surface area and clog the opening pores due to metal agglomerations [40]. In addition, large surface area could delay the deactivation of ZSM-5 catalysts caused by coke formation and deposition on the exterior surface. While, the coke deposition within the zeolite pore could inhibit the capillary and diffusion flow of reactants, finally lowering the aromatics yielding reaction rate [12].

1.3.1.3 Pore size

The mass transfer ability of bulky reactants and products to pass through the micropore in the zeolite is determined by the pore size, thereby significantly affecting the catalytic activity. ZSM-5 has micropores consisting of two intersecting three-dimensional channels of 10-membered rings with one straight channels (5.1 Å × 5.5 Å) and sinusoidal channels (5.3 Å × 5.6 Å) [41, 42]. The mass transfer ability of bulky reactants and products to pass through the micropore of ZSM-5 is determined by the pore size, thereby significantly affecting the catalytic activity. When the cracking reaction occurs within the pore, if the formed product can only diffuse slowly out of the pore, a small amount of product will be obtained. While, those molecules larger than the pore size of ZSM-5 such as levoglucosan, and 5-

hydroxymethyl furfural could be more likely to be converted to coke outside the pores since they cannot enter the ZSM-5 pores [43]. Thus, the mass transfer will be improved by increasing the pore size of ZSM-5 [44, 45]. However, it has also been reported that the zeolites with large pores have low stability, leading to the generation of undesirable compounds, which is the primary cause of the deactivation [35].

1.3.1.4 Shape selectivity

ZSM-5 is a hydrated silicoaluminate constructed of linked aluminate and silicate species tetrahedra (i.e., AlO_4 and SiO_4) [46]. Different crystalline structures and open cavities have been used to classify zeolites. For ZSM-5 zeolite, it has a hexagonal-shaped MFI crystal structure with dimensions of 2-4 m in length and 1-2 m in width [47]. The conversion of biomass-derived oxygenates to aromatics in catalytic fast pyrolysis depends on the reactant entering the pore, conversion in the pore, and pore shape selection of the product to diffuse out of the zeolite pores [48]. That is, poor shape selectivity and diffusion limitation could hinder the reactant to access the catalytic active sites of the zeolite, which is a frequent problem with zeolite catalyst for the desired product in terms of quantity and quality. Although Brønsted acid sites exist on both the external and internal surfaces of zeolites, the external surface contributes to a minor fraction of the total surface area. As a result, the chemical reactions catalyzed by zeolites are assumed to take place mostly within the internal pore of the zeolites. Thus, only the pyrolysis vapor captured by the narrow pores of ZSM-5 can convert oxygenated compounds to aromatic hydrocarbons through shape selectivity in the catalytic pyrolysis, where the acidity of ZSM-5 determines the catalytic activity for the deoxygenation and aromatic formation. It has been reported that among zeolite catalysts of H-β, HY/USY, and HZSM-5, HZSM-5 was the most effective zeolite catalyst in promoting the yield of aromatic hydrocarbon obtained from catalytic fast pyrolysis of lignin, attributing to its well-balanced acidity and shape selectivity [47].

1.3.1.5 Stability against coking

The stability of ZSM-5 catalysts is of great importance to their performances. The deactivation of ZSM-5 catalysts is always caused by coke-induced blockage of reactants and products on active sites and/or the sintering of active species on the catalyst surface. Thus, the high-performance ZSM-5 must be durable and capable of preventing self-accumulating coke or sintering, or even in the case that coke deposition or sintering does occur, it has little effect on the catalytic activity and still has good catalytic efficiency [2].

1.3.1.5.1 Coking

ZSM-5 often suffers from the coke formation due to its small micropore and the cracking over the acid sites on the external surface [49]. During catalytic fast pyrolysis, many reactions occur, of which the coke formation is mainly resulted from the polymerization of aromatics and olefin, leading to the blockage of pore opening and finally the deactivation of HZSM-5 catalyst [50]. Herein, the high acidity affects not only the catalytic activity but also the deactivation by the promoting of coke deposition. The ZSM-5 catalysts with high stability could be achieved by tuning the acid sites by adjusting the aluminum speciation on the external surface [51, 52]. For example, dealumination from ZSM-5 structure can be realized by treatment with acid solutions (e.g., HCl, HNO_3 and HF solutions) [51, 53, 54]. The dealumination can decrease Brønsted acidity, resulting in lower polymerization and less coke formation [54]. While, the introduction of mesopore into the structure of ZSM-5 catalysts by post-treatment with alkaline solution is also one way to reduce the coke formation. In this case, the bulk Si/Al ratio, micropore volume, and crystallinity can be decreased while the Lewis acidity is increased to improve the coking resistance [55].

1.3.1.5.2 Sintering

The agglomeration of metal species on the ZSM-5 zeolite during the reaction is known as catalysis species sintering. It has been reported that some noble metal species doped on the ZSM-5 catalysts are easily accumulated, causing the deactivation of catalyst since the sintering

results in loss of active sites and blockage of the zeolite pores. Herein, excessive amount of metal loading and low metal species dispersion could lead to the high accumulation of metal species during the reaction, leading to the decreases in mass transfer as well as catalytic activity.

1.3.2 Effect of biomass types

The kind of biomass has a major impact on the composition of the product due to the different compositions of cellulose, hemicellulose and lignin, as well as different ash contents with inorganic minerals especially alkali and alkaline earth metal (AAEM) species. In general, the decompositions of cellulose and hemicellulose occur at relatively lower temperatures than that of lignin in the biomass. While, lignin is a more stable component, it normally begins to decompose at a temperature above 200 °C and leaves 40% of residual solid product at the end of pyrolysis. In addition, lignin is known to contain phenolic compounds, which is the most abundant source of aromatic hydrocarbons produced from the biomass [56]. **Table 1.1** presents a literature survey on the proximate analyses of different biomass feedstocks. Since different kind of biomass has different basic compositions of cellulose, hemicellulose and lignin, it is critical for the selection of biomass type to obtain target pyrolysis product distribution. Lignocellulosic biomass can be classified into hardwood (e.g., oak, beech), softwood (e.g., pine, cedar, corn stalk), and grasses (e.g., barley straw, bagasse). In general, softwood contains more lignin than hardwood, while grass biomass contains less lignin than woody biomass but has a higher ash content [57].

1.3.3 Effect of catalyst/ biomass weight ratio

It is always critical to choose a suitable catalyst-to-biomass ratio during the catalytic pyrolysis process for bio-oil production. When the proportion of the catalyst used is too small, the total pyrolysis vapor cannot completely contact the catalyst. Especially, some catalysts could have already deactivated during the initial stage of pyrolysis by cracking of previous pyrolysis vapor. As such, the obtained bio-oil will consist of both catalytic oil and non-catalytic oil, resulting

in a smaller quantity of desired high-quality bio-oil.

Table 1.1 Proximate and ultimate composition of various biomass

Feedstock	Fiber Analysis (%)			Proximate Analysis (%)		Ultimate Analysis (%)					Ref.
	Cellulose	Hemicellulose	Lignin	Moisture	Ash	C	H	N	S	O	
Pine	45.6	24.0	26.8	0.5	1.1	-	-	-	-	-	[58]
oak	43.2	21.9	35.4	0.6	0.2	-	-	-	-	-	[58]
Corn stalk	22.8	43.0	15.6	-	7.4	43.8	5.7	1.0	0.1	48.9	[59]
Sugar bagasse	44	32	24	8.5	9	45.1	6.1	0.3	-	42.8	[60]
Beech wood	45.8	31.8	21.9	9.7	0.7	46.9	6.2	0.3	0.7	45.9	[61]
Sawdust	46.3	27.6	8.2	7.8	1.3	47.1	6.1	0.4	-	46.4	[62]
Japanese cedar	38.7	23.2	33.8	-	0.3	-	-	-	-	-	[63]
Barley straw	48.6	29.7	27.7	6.9	9.8	41.4	6.2	0.6	0.01	51.7	[64]
Rice husk	31.3	24.3	14.3	-	23.5	36.9	5.0	0.4	-	37.9	[65]

1.3.4 Effect of temperature

The total products obtained from the pyrolysis process are heavily influenced by the reaction temperature. Pyrolysis is typically performed at temperatures in the range of 350-650ºC. At a lower temperature (<350ºC), it is always difficult to completely devolatilized the volatile compounds in the biomass. Moreover, a certain increase in vapor residence time as the temperature rises from 350ºC to 500ºC will result in a higher bio-oil yield. As the reaction temperature rises, vapor formation rises as well, resulting in greater vapor condensation and finally leading to a high bio-oil yield. However, with an increase in temperature over 650ºC,

some secondary reactions also occur, which will decrease the generation of more bio-oil since the secondary reactions predominate with the continuous increasing of gaseous products as shown in **Fig. 1.2**.
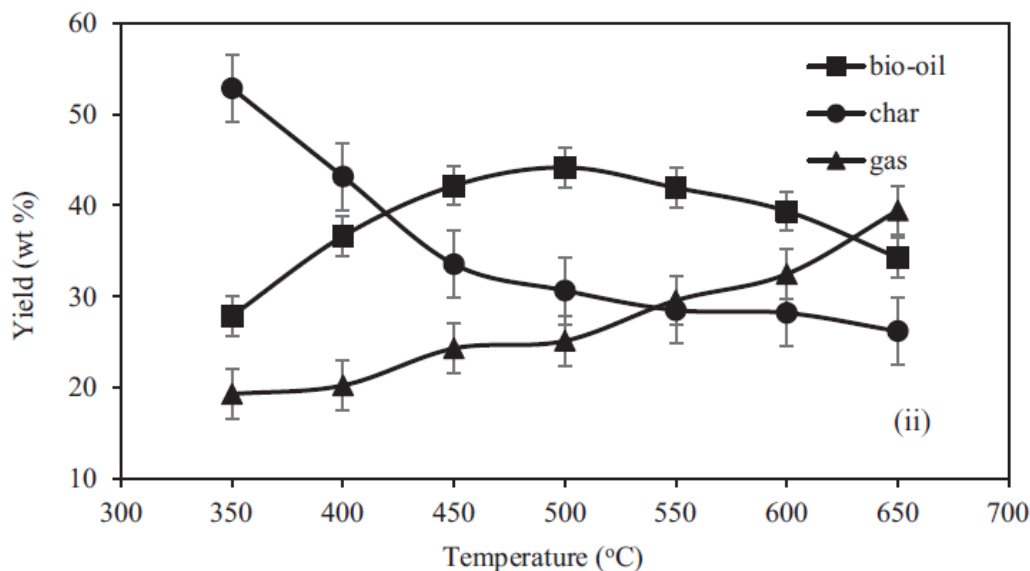
Fig. 1.2 Effect of pyrolysis temperature on bio-oil, char and gas yield using heating rate of 50ºC/min [66]

1.4 Strategies to improve ZSM-5 catalyst performance

Despite that ZSM-5 is the most popular zeolite among other types for deoxygenation of bio-oils to make aromatics because of its unique pore structure, better shape selectivity, and appropriate acid sites, the unique micropore structure of the ZSM-5 restricts the mass transfer of the reactant and product in the pore, which makes carbon deposition and catalyst deactivation easier. More crucially, the location of a large amount of acid sites inside the pore affected catalytic efficiency, always resulting in a lower yield of the desired product. As a result, the parent ZSM-5 is usually restructured to produce relatively large pores by introducing mesopore to the parent ZSM-5 structure or added new active sites by metal loading to increase the resistance to carbon deposition. Moreover, great efforts have been made to modify the Si/Al ratio framework by dealumination/alumination or desilication as it is directly

related to the catalytic performance.

1.4.1 Metal modification

It is found that HZSM-5 is the most efficient catalyst for production of aromatic compounds through catalytic conversion of biomass since it has suitable acidity, excellent heat tolerance, strong selective cracking ability with well isomerization property [67]. However, the coking rate over it is quite high, leading to a significant deactivation problem. As such, the aromatics generation rate is always significantly low. Thus, the parent HZSM-5 catalyst needs to be further modified to improve the upgrading performance. Currently, the parent HZSM-5 catalyst is usually improved by metal loading, which is an easy way for the catalyst performance improving due to the simple preparation procedure and high ability to alter the acidity of HZSM -5 for achieving the optimal upgrading [68]. While, it can decrease the formation of coke. Herein, the types of doping metal have been widely investigated. By doping of transition metal or noble metal on HZSM-5, it is feasible to boost deoxygenation capacity and produce more carbon oxides with less water, resulting in more hydrogen available for incorporation into hydrocarbons [69]. While, alkaline earth metal oxides such as MgO and CaO doping on HZSM-5 can behave as bases and their metal cations could function as Lewis acid sites, which allow tailoring the zeolite activity to avoid excessive cracking of the bio-oil, and in turn result in a higher yield of the deoxygenated compounds in the upgraded bio-oil with the decreasing of the formation of undesired polyaromatic hydrocarbons and coke [10].

1.4.1.1 Transition metal and noble metal loadings

Development of the HZSM-5 based catalyst by loading transition metals/noble metals for the catalytic pyrolysis process has been widely reported. For example, Ni- and Co-modified HZSM-5 catalysts were found to successfully reduce the oxygen content in the bio-oil, and especially, the Ni modified HZSM-5 resulted in the increase of the aromatic hydrocarbons content of upgraded bio-oil via in-situ catalytic pyrolysis of biomass [69]. While, the doping of 2wt% Zn on the HZSM-5 effectively increased the strong acid site content of the catalysts,

resulting in a high BTX yield during the bio-oil upgrading process. However, further doping of Zn (e.g.,10 wt.%) reduced the acidity and physical characteristics of the catalyst, resulting in poor reactant and product diffusion in the zeolite pore, thereby reducing the BTX yield [70]. Madiha *et al*. [71] doped various metal species (Co, Ni, Zn and Fe) on ZSM-5, and found that the doping of metal improved the catalytic selectivity towards monoaromatic hydrocarbons (MAHs), particularly for Fe-ZSM-5, which produced a most amount of MAHs with a highest deoxygenation potential. While, Sun *et al*. [72] also confirmed that Fe/ZSM-5 catalyst exhibited better deoxygenation catalytic activity than the parent ZSM-5 catalyst due to the formation of new active sites and simultaneously, it also inhibited repolymerization, leading to a large amount of aromatic polyaromatics and less coke formation with a high BTX selectivity. Yung *et al*. [73] tested the Ga-modified ZSM-5 in a fixed bed and fluidized-bed reactor. When compared to the upgraded bio-oil obtained by using ZSM-5, the production of hydrocarbons increased by about 30%. It is possible that the incorporation of Ga increased the dehydrogenation activity. While, Zheng *et al*. [68] reported that Ga/ZSM-5 catalysts produced a higher bio-oil yield with a lower amount of coke when compared with the parent ZSM-5 catalyst. In addition, it is found that a high yield of the single-ring aromatics can be obtained by using Zn/ZSM-5 catalyst. It is reported that 1wt.% Mo/HZSM-5 had the potential to produce a higher yield of aromatic hydrocarbons than the unmodified HZSM-5 [74]. A noble metal supported HZSM-5 exhibited a high selectivity towards monoaromatics in upgrated bio-oil [12]. Thangalazhy-Gopakumar *et al*. [75] impregnated metal species (Ni, Co, Mo, and Pt) in the HZSM-5 catalysts and investigated their effects in utilizing hydrogen for deoxygenation during the catalytic pyrolysis process. They found that Pt-HZSM-5 resulted in a highest BTX yield among the obtained catalysts.

1.4.1.2 AAEM loading

In general, alkaline metal loading can change acid site strength by increasing Lewis acid sites and decreasing in Brønsted acid sites, which could effectively prevent excessive cracking of

the bio-oil, resulting in a higher yield of the deoxygenated compounds in the upgraded bio-oil with the extension of catalyst lifetime. AAEMs including Na, Mg and Ca have been loaded on ZSM-5 for the upgrading of bio-oils. When Mg was loaded on ZSM-5 in the form of MgO, the obtained catalysts exhibited better selectivity towards monocyclic aromatics due to the creation of new Lewis acid sites and the reducing of Brønsted acid sites in the parent catalyst [10]. Ca loaded on ZSM-5 also altered acid strength by reducing of strong acid sites and increasing of weak acid sites. Due to the obvious acid strength change and BET surface area decrease, it promoted the production of xylenes but lowered BTX production in comparison to the parent ZSM-5 [70]. Williams *et al.* [76] investigated catalytic upgrading of bio-oil derived from biomass pyrolysis over Na/HZSM-5 and compared with HZSM-5, and found that the yield of single ring aromatic compounds in the upgraded bio-oils, especially BTX, increased from 15.9 wt.% for the HZSM-5 catalyst to 21.3 wt.% for the Na-ZSM-5 catalyst.

1.4.1.3 Effect of preparation method

As stated above, the catalytic performance of ZSM-5 can be improved by metal loading in catalytic upgrading of bio-oil. While, the preparation method could also influence the physicochemical properties and catalytic upgrading performance of the obtained catalysts even using the same metal to load. Several preparation methods have been used for the metal loading on ZSM-5, which include impregnation, ion exchange, precipitation, sol-gel, hydrothermal and the temperature programmed reaction methods. Both of the impregnation and precipitation methods have been extensively utilized. The impregnation method can be classified as the wet impregnation, in which an excessive amount of metal solution is used, and the dry impregnation, in which the volume of metal solution equals to the entire pore volume of ZSM-5 catalysts. While, impregnation time and the following drying process have also been reported to affect the efficiency of metal loading on the catalyst [77]. The short period of impregnation time and drying may cause weakly adsorbing metal species, resulting in metal deposition mainly on the support surface rather than within pores [78]. In contrast, in

the ion-exchange method, the excess metal precursor after ion-exchange process will be washed out by deionized water so that only the exchanged metal ions remain in the zeolite. Furthermore, co-impregnation, a process for manufacturing bimetal loaded ZSM-5, is more challenging than the single metal impregnation since different metal solubility and diffusivity could result in a varying degree of precipitation within the pores [77]. Due to the high dispersion ability of the precipitation method, it is more suitable for the preparation of metal-loaded ZSM-5 catalyst with a high metal loading amount. Herein, it should be noted that the nucleation and growth of metal particles will be induced by the supersaturation of precursor solution. In addition, the precipitation includes coprecipitation and deposition-precipitation. The coprecipitation method involves the dissolving and mixing metal precursors and support salts to allow nucleation and growth of combined precursor particles of active metal and support. In most cases, the combined precursor salts are insoluble metal carbonates or hydroxides that would promptly precipitate upon their formation [79].

1.4.2 Hierarchical ZSM-5 zeolite

Hierarchical zeolites are characterized by the presence of a bimodal porous structure, especially containing both micropores and mesopores/macropores. The exact definition of hierarchical structure of catalysts is a pore system of bi- or multimodal pores with different pore size where the large pores connect the small pores, i.e., small pores branch off from a continuous large pore [80]. Because of their exceptional properties, such materials have been attracted great attentions. Hierarchical ZSM-5 differ significantly from the conventional one in terms of improved diffusion, promoted mass transfer, enhanced resistance to deactivation [81]. The classical methods for introducing mesoporous structure into the ZSM-5 catalysts include single templating, double templating with soft/hard-template and post-treatment.

1.4.2.1 Single templating method

Typically, TPAOH is applied as a structure-directing agent as well as a micropores template for the preparation of ZSM-5. In the case of the addition of TPAOH alone during ZSM-5

synthesis, to obtain hierarchical structured ZSM-5, it requires base etching as the post-treatment process to the mesopore formation [82].

1.4.2.2 Double templating method

In the synthesis of mesoporous zeolite, two types of templates by selecting a template that has the shape of a three-dimensionally structured mesopore system and mixing it with the precursor chemicals including structure-directing agent of ZSM-5 in the first stage is necessary. In this case, mesopores can be produced during the crystallization stage, and the template will be decomposed by a calcination stage after the hydrothermal synthesis process [39]. It has been reported that using a small amount of mesopore template during the synthesis process always results in insufficient mesopore generation whereas using a large amount of template will hinder the crystal nucleation and growth [83]. Thus, it is needed to search the optimum mesopore template amount during the synthesis. In the production of hierarchical zeolites, both hard templates such as carbon black, carbon fibers, aerogels, and polymer aerogel and soft templates such as cationic polymers, amphiphilic organosilane surfactants, and silylated polymers can be applied [84, 85]. In this case, the morphology of mesopores may be accurately regulated. Compared to the chemical etching (acid or base treatment) for the generation of mesoporous or microporous structure, the employing of a secondary template could raise the cost and a calcination process to eliminate the template is also necessary.

1.4.2.3 Post-treatment method

In comparison to direct synthesis ways, the post-treatment method is more convenient, simple, and cost-effective for the introducing secondary meso-macropores in the zeolite catalysts structure by extraction of framework. Generally, an acid solution was employed for extracting Al atom while a base solution was employed for extracting Si atom, both of which can generate mesopores in the zeolite structure. The disadvantage of this method is the loss of micropore structure as a result of framework extraction for the generation of mesopore porosity, or the collapse of structure to lose the surface area in the case of over extraction.

1.4.2.3.1 Desilication/Alkaline etching

The preparation of hierarchical ZSM-5 catalysts by the alkaline etching method could result in improved surface properties. Since the small pores of the parent ZSM-5 always limit the mass transfer and diffusion of reactants and products, by introducing mesopores into the structure, the accessibility of acid sites can be improved, the diffusion length can be shortened and finally the catalyst lifetime can be enhanced [86]. Popular alkaline solutions used for the etching of ZSM-5 include sodium hydroxide (NaOH), tetrapropylammonium hydroxide (TPAOH), tetrabutylammonium hydroxide (TBAOH), sodium carbonate (Na_2CO_3) with NaOH solutions [87]. In this case, some Si-Al bonds may be disrupted, causing the zeolite to lose its location adjacent to Al and decrease the acidity. While, the obtained catalysts usually have a wide pore size distribution. For the bio-oil upgrading, it is reported that the ideal Si/Al ratio in the original ZSM-5 for the construction of a hierarchical structure by using alkaline solution should be 25-50. Herein, since the excessive aluminum content in ZSM-5 can surround the silicon to prevent the desilication for the mesopore creation [88]. On the other hand, when the aluminum content is low, a large amount of Si can be dissolved, resulting in low yield zeolite and large mesopore, which always negatively affect the catalytic cracking activity. Organic hydroxides such as TPAOH and TBAOH have lower ability for the Si dissolution than those inorganic hydroxides, which can better control Si species dissolution so that only a little change occur in the acid property after alkaline treatment [89]. Furthermore, it is reported that the hierarchical ZSM-5 catalysts by post-treatment using a mixture of inorganic and organic base solutions can result in a better control of the mesopore formation since the assistance of the organic base solution prevented the excessive extraction to maintain a better zeolite structure as shown in **Fig. 1.3**.
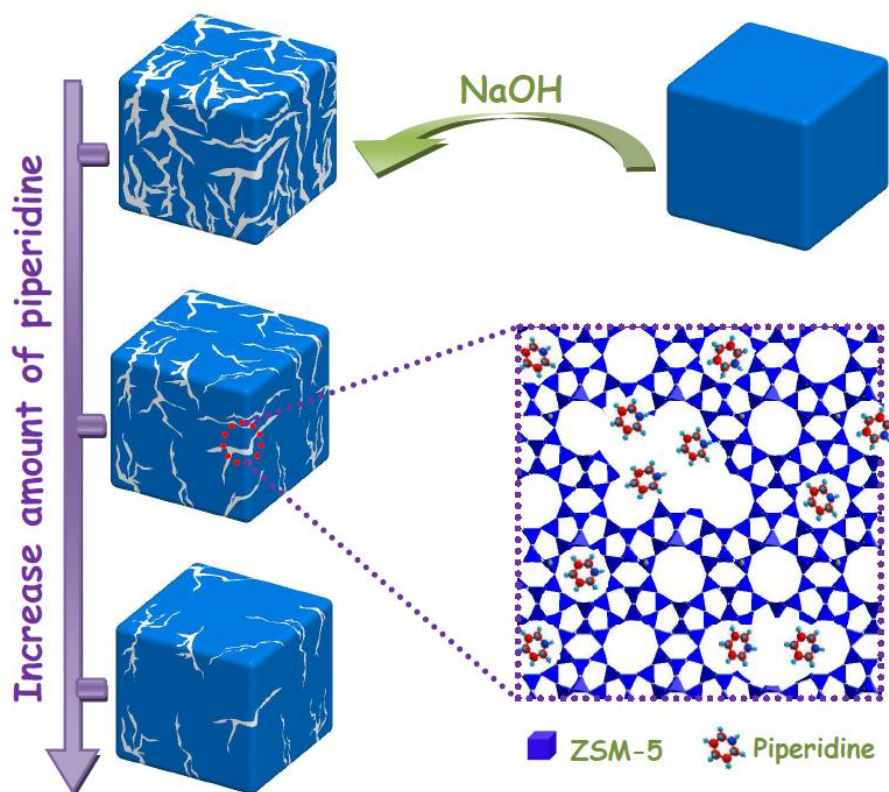
Fig. 1.3 The desilication and mesopore formation of ZSM-5 crystals with the assistance of an organic base solution (TPAOH) [90]

1.4.2.3.2 Dealumination/acid leaching

Dealumination is the process of removing Al from the zeolite framework using an acid solution. It is most typically employed for the post-treatment of parent ZSM-5 zeolites with a low Si/Al ratio (2.5-5), which usually have high acid density and strong acid strength and favor the coke generation, thereby causing catalyst deactivation [91, 92]. After the dealumination using acid solution, the Si/Al ratio in the zeolite framework will be increased, and a hierarchical structure with existing mesoporosity will be generated. In this case, the adjustment of zeolite acidity becomes more controllable. In addition, even if the zeolite is extremely dealuminated, partial extra-framework Al can be reinserted into the structure using the hydrothermal technique while the zeolite structure is preserved better than the case employing the alkaline etching method [93, 94]. However, the use of strong acid concentration will cause a decrease of Brønsted acid sites due to a significant decrease in the framework Al content,

and an increase in the Lewis acid site due to the detached Al which becomes an extra-framework Al floating in the environment as an extra-framework Al atom [95]. The most commonly used acids in the dealumination are hydrochloric acid (HCl), nitric acid (HNO$_3$), sulfuric acid (H$_2$SO$_4$) and hydrofluoric acid (HF) [96]. Herein, chemical etching with fluoride ions generated from NH$_4$-HF has been reported to create secondary porosity and increase the exterior surface area of hierarchical ZSM-5. However, the use of extremely concentrated HF solution could result in the decrease of Brønsted acidity due to the indiscriminate extraction of Al and Si [97]. **Fig. 1.4** presents an example of an SEM image of hierarchical ZSM-5 treated with an acid solution.
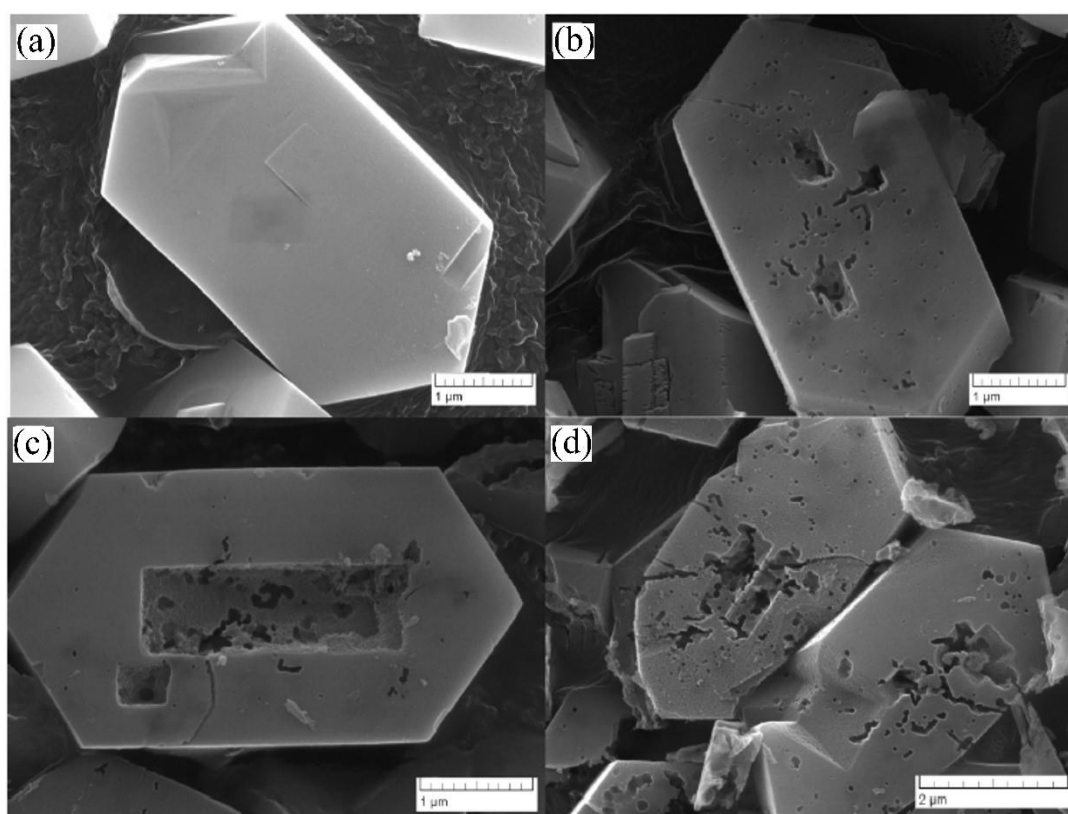
Fig. 1.4 SEM images of ZSM-5 crystals treated by different NH$_4$F-HF amounts varied from low to high [97]

1.4.3 ZSM-5 zeolite with special morphology

As stated above, owing to its acidity and shape-selective property of ZSM-5, it is considered

as one of the most effective catalysts for the deoxygenation of bio-oil, especially in the production of light aromatic hydrocarbons such as benzene, toluene and xylene (BTX). However, one of the major drawbacks of ZSM-5 is the fast deactivation due to the coke formation. In the upgrading of bio-oils, the mass transfer of large intermediate oxygenates in the bio-oil is restricted by the small pore diameter of ZSM-5 so that it is difficult to diffuse into the pore for reaction, which will result in the coking to lock the inner pore and finally cause ZSM-5 catalysts to be deactivated. Thus, ZSM-5 catalysts with special morphologies have been designed to reduce the diffusion length or increase the diffusion efficiency. To date, hollow ZSM-5 catalysts, core-shell ZSM-5/mesopore composite catalysts, nanosheet ZSM-5 catalysts have been developed.

1.4.3.1 Hollow ZSM-5

To improve the catalytic effectiveness and keep the shape-selective ability of micropores in the zeolites, interior hollow structured zeolites have been designed and fabricated. In this case, the hollows within the zeolite will assist to shorten the diffusion distance with a decrease in the unutilized quantity within the center of zeolites. Two ways have been applied to fabricate hollow zeolites. The first one is to assemble zeolite crystals with polycrystalline shells using a template followed by calcination at a high temperature to remove the template as shown in **Scheme 1.2**. Herein, the crystals are aggregated at random to form an interparticle cavity. Since the obtained shell thickness is only a few microns, the reactants and products could be more easily pass through it. Another example is to use mesoporous silica sphere as the sacrifice template, on which zeolite nanoparticles will subsequently coated on it during the synthesis process as shown in **Fig. 1.5**. Herein, the inner part of the particle is a jujube-like mesoporous silica spheres as Si and pre-seeded sources for the preparation of hollow zeolite.
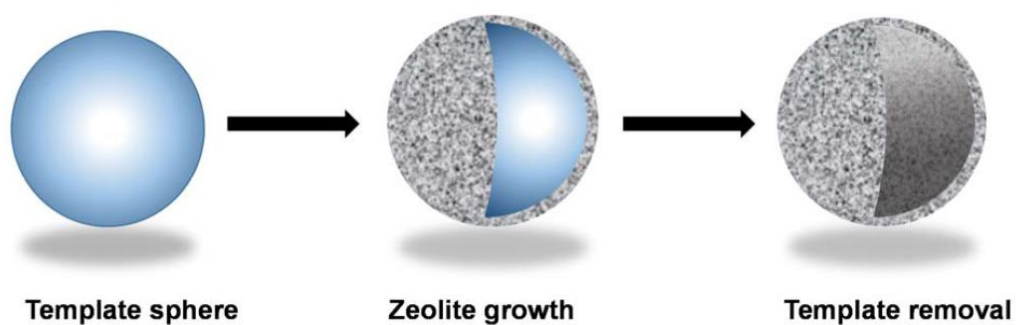
Scheme 1.2 Schematic representation of the formation of hollow zeolite using a solid template [98]
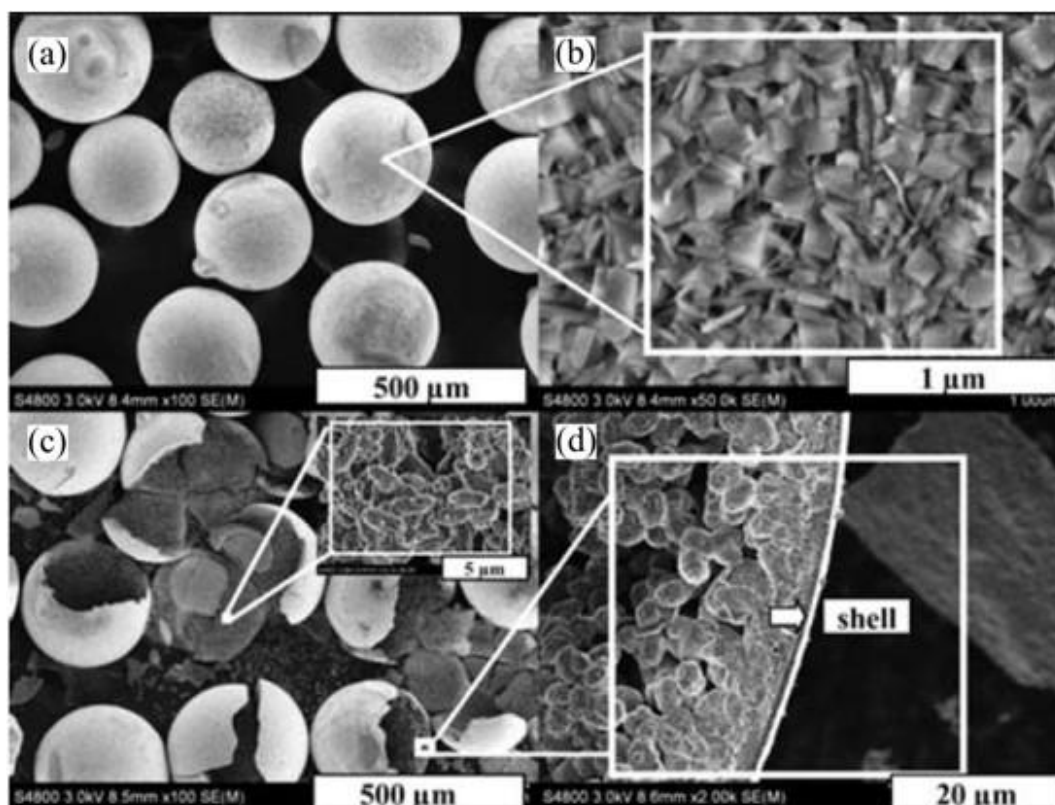
Fig. 1.5 SEM images of core-shell ZSM-5 spheres, overview, inside the spheres, crushing ZSM-5 spheres and sphere shell [99]

The other approach is to employ chemical etching to create hollow cavities in the zeolite catalysts. This method involves two-step: (i) using sol-gel route to form single zeolite crystals from a single nucleus; (ii) constructing a perfect hollow in the center of the zeolite crystal as well as a zeolite shell using etching with different chemical concentrations. For example, when

the parent ZSM-5 was desilicated by TPAOH, an internal hollow structure can be generated as shown in **Fig 1.6**.
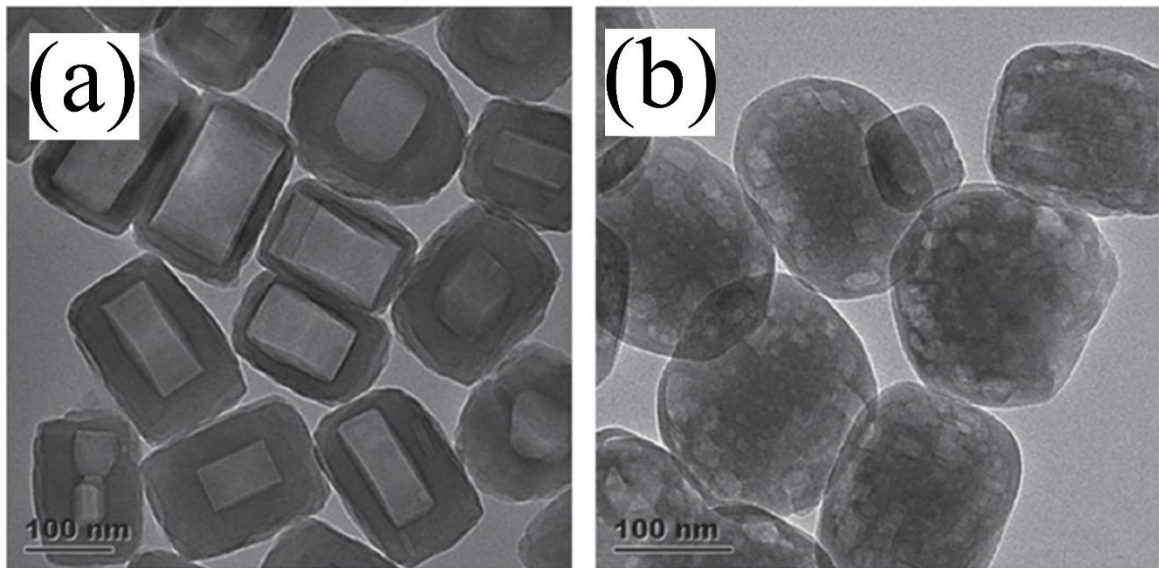
Fig. 1.6 TEM images of ZSM-5 with different parent Si/Al ratios after TPAOH etching [100].

1.4.3.2 Core-shell composites

ZSM-5/mesoporous material composite with a core/shell structure is considered to have following advantages: (i) the mesoporous structure is benefit for the better diffusion and can hinder the coke formation on the surface of ZSM-5 catalysts; (ii) the acidity and shape selectivity of ZSM-5 suitable for aromatic hydrocarbon production in catalytic upgrading process can be maintained. **Fig. 1.7** shows an example of the core/shell ZSM-5/mesoporous material composite. Li *et al*. [101] synthesized a ZSM-5 catalyst coated with a thin mesoporous silicalite-1 layer and tested their catalytic performance on catalytic fast pyrolysis of pine sawdust, which demonstrated high stability as well as a high p-xylene selectivity. Yu *et al*. [102] prepared MCM-41/ZSM-5 composites, in which ZSM-5 crystals were encapsulated in MCM-41 particles. When these composites were applied for the in-situ and ex-situ catalytic fast pyrolysis of miscanthus, the equivalent hydrocarbon yield as that from the pure ZSM-5 was obtained, but the MCM-41 shell worked as a barrier layer for coke deposition, which effectively protected the ZSM-5 from the severe coke formation. Herein, a

simple procedure for preparing the core/shell composite is the treatment of parent HZSM-5 zeolite with an alkaline solution to desilication of Si at first, and then the mesoporous material is synthesized as the shell of ZSM-5 by adding the mesoporous template in the hydrothermal synthesis process followed by calcination to remove the template. For the synthesis of mesoporous MCM-41 shell, cetyltrimethylammonium bromide is generally employed, as is the use of the triblock copolymer Pluronic P123 to create SBA-15.
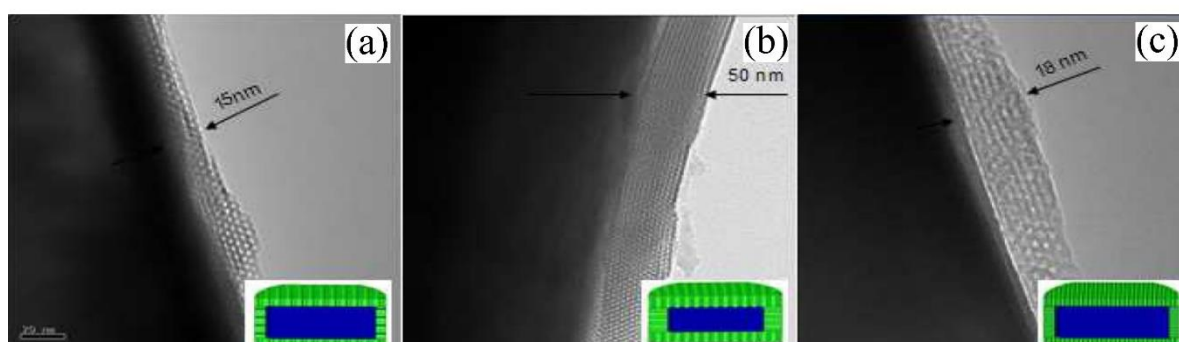
Fig. 1.7 TEM images for ZSM-5/MCM-41 Composite Zeolite with different NaOH concentration and crystallization time [103].

1.4.3.3 Nanosheet ZSM-5

The nanosheet ZSM-5 has a hierarchical pore structure with a thin sheet structure, which can overcome the disadvantages of the small and long porous diffusion path in the conventional ZSM-5 zeolite. Due to its size (only 5-10 nm) as small as the size of a unit cell, the diffusion length can allow the substrate to more easily diffuse through the ZSM-5, which could improve catalytic activity and lifetime of zeolite catalysts [104]. **Fig. 1.8** shows SEM images of zeolite nanosheets using the different tail of structure-directing agents [105], which is one of such nanosheet ZSM-5 catalysts. Herein, the tail of SDA is sufficiently hydrophobic to provide a substantial hydrophobic barrier in the micelle, limiting lamellar structure formation around the

hydrophilic tails and allowing effective control of nanosheet thickness.
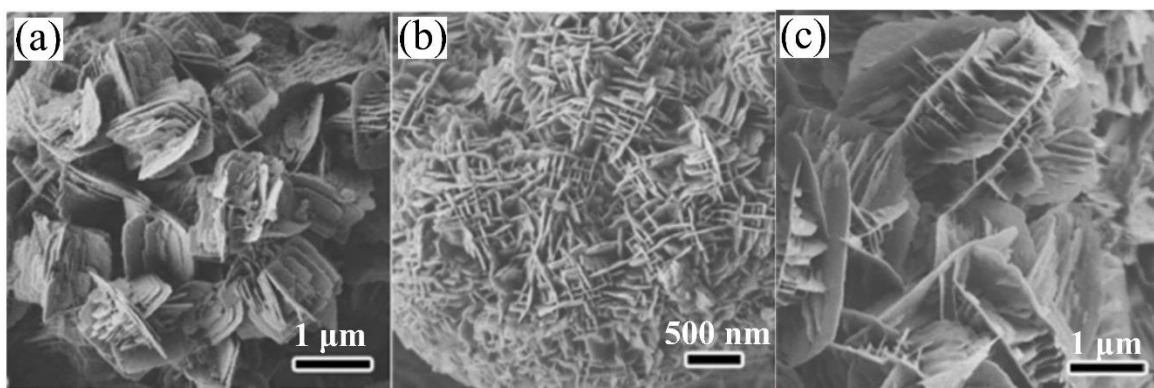
Fig. 1.8 SEM images of zeolite nanosheets using the different tail of structure-directing agents [105]

However, the catalytic pyrolysis of biomass constituents over such zeolite nanosheets has been rarely reported. Xu *et al*. [106] prepared mesoporous ZSM-5 nanosheets using a surfactant with a molecular formula of $[C_{22}H_{45}-N^+ (CH_3)_2-C_6H_{12}-N^+ (CH_3)_2-C_6H_{13}]Br_2$ as a structure-directing agent (SDA).Then, the synthesized catalyst was applied to the catalytic pyrolysis of cellulose. The results showed that although ZSM-5 nanosheets produced similar aromatic hydrocarbon and olefin yields when compared to those of conventional HZSM-5, however, it demonstrated a longer lifetime even though the coke content was also higher than those cases using the HZSM-5 zeolite catalysts since the mesopores enabled better accessibility to active acid sites. Furthermore, because such a nanosheet zeolite has a larger surface area, it could be an outstanding player for loading metal nanoparticles to create a multifunctional zeolite catalyst. With increasing metal loading amounts, the metal nanoparticles could distribute uniformly within zeolite crystals and prevent aggregation during the reaction.

1.5 Motivation and objectives

As is known, biomass is the only renewable energy source and is considered a potential alternative to fossil fuels. Efficient biomass utilization is full of challenges, and among the available technologies, fast pyrolysis is effective in producing bio-oil. However, pyrolysis bio-

oil needs to be upgraded before use as the transport fuels or chemical feedstock due to its low quality as fuels and its low value as the chemicals. Recently, catalytic upgrading of bio-oil derived from fast pyrolysis has been widely studied for converting biomass into aromatics. One of the most widely used catalysts is the ZSM-5 zeolite in the production of renewable oils and chemicals. Although the microporous ZSM-5 was more favorable than other catalysts in applications for catalytic pyrolysis reactions towards olefin and aromatics productions due to its excellent properties including pore size, pore structure and acidity, those compounds in the bio-oil with large molecule sizes inconveniently diffuse through small pores due to diffusion limitations and can easily be deposited by coke on the catalyst surface, leading to catalyst deactivation. Therefore, it is of great interest to develop ZSM-5 based catalysts with more excellent performance by solving diffusion limitations to produce more aromatic compounds and reducing coke formation. In this dissertation, the main objectives are to propose strategies to improve the catalysis efficiency of ZSM-5 based catalysts for the *in-situ* catalytic upgrading of bio-oils derived from fast pyrolysis of biomass that mainly focus on the production of aromatic hydrocarbons.

1.6 Scope of this dissertation

Chapter 1 outlines the fundamentals of catalytic bio-oil upgrading procedures, proposed catalytic mechanisms, influencing factors in catalytic fast pyrolysis over ZSM-5 based catalysts, and strategies for improving ZSM-5 based catalyst performance.

Chapter 2 provides a guide for determining the optimal Cu amount loading on the HZSM-5 in the *in-situ* catalytic deoxygenation of bio-oil derived from fast pyrolysis of biomass with a focus on aromatic hydrocarbon production, as well as a study of the reusability and regeneration of spent zeolites.

Chapter 3 presents the preparation of various hierarchically structured HZSM-5 zeolite catalysts by desilication of commercial HZSM-5 with aqueous NaOH-TPAOH mixtures. It focuses on the determination of the optimal condition for the catalyst preparation utilized for

27

the production of aromatic hydrocarbons obtained from the in-situ catalytic upgrading of bio-oil derived from the fast pyrolysis of sunflower stalk. The desilication mechanisms of the hierarchical HZSM-5 using various alkaline solutions were proposed and discussed. Moreover, the metal loading to improve the performance of the hierarchically structured HZSM-5 catalyst was also studied.

Chapter 4 presents how to make innovative hollow HZSM-5 zeolites in one pot using a facile hydrothermal process. The synthesized catalyst was used for the in-situ catalytic upgrading of bio-oils generated from the rapid pyrolysis of cellulose, hemicellulose and lignin. The catalytic performances of hollow HZSM-5 zeolites with various Si/Al ratios, and subsequently treated hollow HZSM-5 zeolite catalysts by TPAOH solution were investigated. It is found that the hollow structure with mesoporous shell greatly enhance the catalysis performance.

Chapter 5 summarizes the principal findings of this dissertation and suggests guidelines for further researches on the development of the ZSM-5 based catalysts for in-situ catalytic upgrading of bio-oil obtained from fast biomass pyrolysis.

References

[1] A.V. Bridgwater, Principles and practice of biomass fast pyrolysis processes for liquids, J. Anal. Appl. Pyrolysis, 51(1) (1999) 3–22.

[2] S.W. Banks, A.V. Bridgwater, Catalytic fast pyrolysis for improved liquid quality, Handbook of Biofuels Production 2016, pp. 391-429.

[3] E.F. Iliopoulou, K.S. Triantafyllidis, A.A. Lappas, Overview of catalytic upgrading of biomass pyrolysis vapors toward the production of fuels and high-value chemicals, Wiley Interdiscip. Rev.: Energy Environ., 8(1) (2019).

[4] L. Li, J.S. Rowbotham, H. Christopher Greenwell, P.W. Dyer, An introduction to pyrolysis and catalytic pyrolysis: Versatile techniques for biomass conversion, new and future developments in catalysis 2013, pp. 173-208.

[5] J.J. Manyà, M. Azuara, J.A. Manso, Biochar production through slow pyrolysis of different

biomass materials: Seeking the best operating conditions, Biomass Bioenergy, 117 (2018) 115-123.

[6] C. Zhang, Z. Zhang, L. Zhang, Q. Li, C. Li, G. Chen, S. Zhang, Q. Liu, X. Hu, Evolution of the functionalities and structures of biochar in pyrolysis of poplar in a wide temperature range, Bioresour. Technol., 304 (2020) 123002.

[7] D. Ayhan, Biomass resource facilities and biomass conversion processing for fuels and chemicals, Energy Convers. Manage. 42 (11) (2001) 1357–1378.

[8] C.M. Lok, J. Van Doorn, G. Aranda Almansa, Promoted ZSM-5 catalysts for the production of bio-aromatics, a review, Renew. Sustain. Energy Rev., 113 (2019).

[9] R. Bagri, P.T. Williams, Catalytic pyrolysis of polyethylene, J. Anal. Appl. Pyrolysis, 63 (1) (2002) 29-41.

[10] J. Fermoso, H. Hernando, P. Jana, I. Moreno, J. Přech, C. Ochoa-Hernández, P. Pizarro, J.M. Coronado, J. Čejka, D.P. Serrano, Lamellar and pillared ZSM-5 zeolites modified with MgO and ZnO for catalytic fast-pyrolysis of eucalyptus woodchips, Catal. Today, 277 (2016) 171-181.

[11] R. Kumar, V. Strezov, E. Lovell, T. Kan, H. Weldekidan, J. He, S. Jahan, B. Dastjerdi, J. Scott, Enhanced bio-oil deoxygenation activity by Cu/zeolite and Ni/zeolite catalysts in combined in-situ and ex-situ biomass pyrolysis, J. Anal. Appl. Pyrolysis, 140 (2019) 148-160.

[12] M.M. Rahman, R. Liu, J. Cai, Catalytic fast pyrolysis of biomass over zeolites for high quality bio-oil – A review, Fuel Process. Technol., 180 (2018) 32-46.

[13] E. de Jong, R.J.A. Gosselink, Lignocellulose-based chemical products, Bioenergy Research: Advances and Application, 2014, pp. 277-313.

[14] A. Bakhtyari, M.A. Makarem, M.R. Rahimpour, Light olefins/bio-gasoline production from biomass, Bioenergy Systems for the Future, 2017, pp. 87-148.

[15] K.C. Kwon, H. Mayfield, T. Marolla, B. Nichols, M. Mashburn, Catalytic deoxygenation of liquid biomass for hydrocarbon fuels, Renew. Energy, 36(3) (2011) 907-915.

[16] R.H. Venderbosch, W. Prins, Fast pyrolysis technology development, Biofuels Bioprod. Biorefining, 4(2) (2010) 178-208.

[17] A. Sanna, T.P. Vispute, G.W. Huber, Hydrodeoxygenation of the aqueous fraction of bio-oil with Ru/C and Pt/C catalysts, Appl. Catal. B: Environ., 165 (2015) 446-456.

[18] A. Gutierrez, R.K. Kaila, M.L. Honkela, R. Slioor, A.O.I. Krause, Hydrodeoxygenation of guaiacol on noble metal catalysts, Catal. Today, 147(3-4) (2009) 239-246.

[19] S. Oh, H. Hwang, H.S. Choi, J.W. Choi, The effects of noble metal catalysts on the bio-oil quality during the hydrodeoxygenative upgrading process, Fuel, 153 (2015) 535-543.

[20] C. Zhao, J. He, A.A. Lemonidou, X. Li, J.A. Lercher, Aqueous-phase hydrodeoxygenation of bio-derived phenols to cycloalkanes, J. Catal., 280(1) (2011) 8-16.

[21] B. Balagurumurthy, R. Singh, T. Bhaskar, Catalysts for thermochemical conversion of biomass, recent advances in thermo-chemical conversion of biomass, 2015, pp. 109-132.

[22] J. Wildschut, F.H. Mahfud, R.H. Venderbosch, H.J. Heeres, Hydrotreatment of fast pyrolysis oil using heterogeneous noble-metal catalysts, Ind. Eng. Chem. Res., 48 (2009) 10324–10334.

[23] P.M. Mortensen, J.D. Grunwaldt, P.A. Jensen, K.G. Knudsen, A.D. Jensen, A review of catalytic upgrading of bio-oil to engine fuels, Appl. Catal. A: Gen., 407(1-2) (2011) 1-19.

[24] T.-S. Nguyen, D. Laurenti, P. Afanasiev, Z. Konuspayeva, L. Piccolo, Titania-supported gold-based nanoparticles efficiently catalyze the hydrodeoxygenation of guaiacol, J. Catal., 344 (2016) 136-140.

[25] Y. Liu, Z. Li, J.J. Leahy, W. Kwapinski, Catalytically upgrading bio-oil via esterification, Energy Fuels, 29(6) (2015) 3691-3698.

[26] M. Milina, S. Mitchell, J. Pérez-Ramírez, Prospectives for bio-oil upgrading via esterification over zeolite catalysts, Cata.Today, 235 (2014) 176-183.

[27] A.R.K. Gollakota, M. Reddy, M.D. Subramanyam, N. Kishore, A review on the upgradation techniques of pyrolysis oil, Renew. Sustain. Energy Rev., 58 (2016) 1543-1568.

[28] I.V. Babich, M. van der Hulst, L. Lefferts, J.A. Moulijn, P. O'Connor, K. Seshan, Catalytic pyrolysis of microalgae to high-quality liquid bio-fuels, Biomass Bioenergy, 35(7) (2011) 3199-3207.

[29] I. Kurnia, S. Karnjanakom, A. Bayu, A. Yoshida, J. Rizkiana, T. Prakoso, A. Abudula, G. Guan, In-situ catalytic upgrading of bio-oil derived from fast pyrolysis of lignin over high aluminum zeolites, Fuel Process. Technol., 167 (2017) 730-737.

[30] A. Aho, N. Kumar, K. Eränen, T. Salmi, M. Hupa, D.Y. Murzin, Catalytic pyrolysis of woody biomass in a fluidized bed reactor: Influence of the zeolite structure, Fuel, 87(12) (2008) 2493-2501.

[31] C. Engtrakul, C. Mukarakate, A.K. Starace, K.A. Magrini, A.K. Rogers, M.M. Yung, Effect of ZSM-5 acidity on aromatic product selectivity during upgrading of pine pyrolysis vapors, Catal. Today, 269 (2016) 175-181.

[32] H. Ben, A.J. Ragauskas, Influence of Si/Al Ratio of ZSM-5 Zeolite on the properties of lignin pyrolysis products, ACS Sustain. Chem. Eng., 1(3) (2013) 316-324.

[33] A. Silva, L. Miranda, M. Nele, B. Louis, M. Pereira, Insights to achieve a better control of silicon-aluminum ratio and ZSM-5 zeolite crystal morphology through the assistance of biomass, Catalysts, 6(2) (2016).

[34] P. Magnoux, A. Rabeharitsara, H.S. Cerqueira, Influence of reaction temperature and crystallite size on HBEA zeolite deactivation by coke, Appl. Catal. A: Gen., 304 (2006) 142-151.

[35] Nishu, R. Liu, M.M. Rahman, M. Sarker, M. Chai, C. Li, J. Cai, A review on the catalytic pyrolysis of biomass for the bio-oil production with ZSM-5: Focus on structure, Fuel Process. Technol., 199 (2020) 106301.

[36] J. Li, H. Liu, T. An, Y. Yue, X. Bao, Carboxylic acids to butyl esters over dealuminated–realuminated beta zeolites for removing organic acids from bio-oils, RSC Adv., 7(54) (2017) 33714-33725.

[37] Q. Cao, L.e. Jin, W. Bao, Y. Lv, Investigations into the characteristics of oils produced from co-pyrolysis of biomass and tire, Fuel Process. Technol., 90(3) (2009) 337-342.

[38] X. Zhu, L. Wu, P.C.M.M. Magusin, B. Mezari, E.J.M. Hensen, On the synthesis of highly acidic nanolayered ZSM-5, J. Catal., 327 (2015) 10-21.

[39] Y. Zhang, K. Zhu, X. Zhou, W. Yuan, Synthesis of hierarchically porous ZSM-5 zeolites by steam-assisted crystallization of dry gels silanized with short-chain organosilanes, New J. Chem., 38(12) (2014) 5808-5816.

[40] X.-Y. Ren, J.-P. Cao, X.-Y. Zhao, W.-Z. Shen, X.-Y. Wei, Increasing light aromatic products during upgrading of lignite pyrolysis vapor over Co-modified HZSM-5, J. Anal. Appl. Pyrolysis, 130 (2018) 190-197.

[41] Q. Che, M. Yang, X. Wang, Q. Yang, Y. Chen, X. Chen, W. Chen, J. Hu, K. Zeng, H. Yang, H. Chen, Preparation of mesoporous ZSM-5 catalysts using green templates and their performance in biomass catalytic pyrolysis, Bioresour. Technol., 289 (2019) 121729.

[42] H. Chen, X. Shi, J. Liu, K. Jie, Z. Zhang, X. Hu, Y. Zhu, X. Lu, J. Fu, H. Huang, S. Dai, Controlled synthesis of hierarchical ZSM-5 for catalytic fast pyrolysis of cellulose to aromatics, J. Mater. Chem. A, 6(42) (2018) 21178-21185.

[43] K. Wang, J. Zhang, B. H. Shanks, R.C. Brown, Catalytic conversion of carbohydrate-derived oxygenates over HZSM-5 in a tandem micro-reactor system, Green Chem., 17(1) (2015) 557-564.

[44] J. Zhou, Z. Hua, Z. Liu, W. Wu, Y. Zhu, J. Shi, Direct Synthetic strategy of mesoporous ZSM-5 zeolites by using conventional block copolymer templates and the improved catalytic properties, ACS Catal., 1(4) (2011) 287-291.

[45] K. Qiao, X. Shi, F. Zhou, H. Chen, J. Fu, H. Ma, H. Huang, Catalytic fast pyrolysis of cellulose in a microreactor system using hierarchical zsm-5 zeolites treated with various alkalis, Appl. Catal. A: Gen., 547 (2017) 274-282.

[46] A. Galadima, O. Muraza, In situ fast pyrolysis of biomass with zeolite catalysts for

bioaromatics/gasoline production: A review, Energy Convers. Manag., 105 (2015) 338-354.

[47] M. Huang, J. Xu, Z. Ma, Y. Yang, B. Zhou, C. Wu, J. Ye, C. Zhao, X. Liu, D. Chen, W. Zhang, Bio-BTX production from the shape selective catalytic fast pyrolysis of lignin using different zeolite catalysts: Relevance between the chemical structure and the yield of bio-BTX, Fuel Process. Technol., 216 (2021).

[48] Y. Yu, X. Li, L. Su, Y. Zhang, Y. Wang, H. Zhang, The role of shape selectivity in catalytic fast pyrolysis of lignin with zeolite catalysts, Appl. Catal. A: Gen., 447-448 (2012) 115-123.

[49] B. Zhang, Z. Zhong, Q. Xie, P. Chen, R. Ruan, Reducing coke formation in the catalytic fast pyrolysis of bio-derived furan with surface modified HZSM-5 catalysts, RSC Adv., 5(69) (2015) 56286-56292.

[50] B. Gu, J.-P. Cao, Y.-F. Shan, F. Wei, M. Zhao, Y.-P. Zhao, X.-Y. Zhao, X.-Y. Wei, Catalytic fast pyrolysis of sewage sludge over HZSM-5: A study of light aromatics, coke, and nitrogen migration under different atmospheres, Ind. Eng. Chem. Res., 59(39) (2020) 17537-17545.

[51] J.-h. Li, L.-n. Wang, D. Zhang, J.-h. Qian, L. Liu, J.-j. Xing, Effect of ZSM-5 acid modification on aromatization performance of methanol, J. Fuel Chem. Technol., 47(8) (2019) 957-963.

[52] S. Inagaki, S. Shinoda, Y. Kaneko, K. Takechi, R. Komatsu, Y. Tsuboi, H. Yamazaki, J.N. Kondo, Y. Kubota, Facile fabrication of ZSM-5 zeolite catalyst with high durability to coke formation during catalytic cracking of paraffins, ACS Catal., 3(1) (2012) 74-78.

[53] S. Kumar, A.K. Sinha, S.G. Hegde, S. Sivasanker, Influence of mild dealumination on physicochemical, acidic and catalytic properties of H-ZSM-5, J. Mol. Catal. A: Chem. 154 (2000) 115.

[54] J.-X. Wang, J.-P. Cao, X.-Y. Zhao, S.-N. Liu, X.-Y. Ren, L.-Y. Zhang, X.-B. Feng, Y.-P. Zhao, X.-Y. Wei, In Situ upgrading of cellulose pyrolysis volatiles using hydrofluorinated and platinum-loaded HZSM-5 for high selectivity production of light aromatics, Ind. Eng. Chem. Res., 58(49) (2019) 22193-22201.

[55] L.H. Chen, M.H. Sun, Z. Wang, W. Yang, Z. Xie, B.L. Su, Hierarchically structured zeolites: from design to application, Chem. Rev., 120(20) (2020) 11194-11294.

[56] Y. Zhao, L. Deng, B. Liao, Y. Fu, Q.-X. Guo, Aromatics production via catalytic pyrolysis of pyrolytic lignins from bio-oil, Energy Fuels, 24(10) (2010) 5735-5740.

[57] S. Wang, G. Dai, H. Yang, Z. Luo, Lignocellulosic biomass pyrolysis mechanism: A state-of-the-art review, Prog. Energy Combust. Sci., 62 (2017) 33-86.

[58] J. Yu, N. Paterson, J. Blamey, M. Millan, Cellulose, xylan and lignin interactions during pyrolysis of lignocellulosic biomass, Fuel, 191 (2017) 140-149.

[59] C. Song, H. Hu, S. Zhu, G. Wang, G. Chen, Nonisothermal catalytic liquefaction of corn stalk in subcritical and supercritical water, Energy Fuels, 18 (2004) 90-96.

[60] S. Al Arni, B. Bosio, E. Arato, Syngas from sugarcane pyrolysis: An experimental study for fuel cell applications, Renew. Energy, 35(1) (2010) 29-35.

[61] A.M. Azeez, D. Meier, J. Odermatt, T. Willner, Fast pyrolysis of african and European lignocellulosic biomasses using Py-GC/MS and fluidized bed reactor, Energy Fuels, 24(3) (2010) 2078-2085.

[62] Y.-K. Chih, W.-H. Chen, H.C. Ong, P.L. Show, Product characteristics of torrefied wood sawdust in normal and vacuum environments, Energies, 12(20) (2019).

[63] H. Rabemanolontsoa, S. Saka, Comparative study on chemical composition of various biomass species, RSC Adv., 3(12) (2013).

[64] S. Naik, V.V. Goud, P.K. Rout, K. Jacobson, A.K. Dalai, Characterization of canadian biomass for alternative renewable biofuel, Renew. Energy, 35(8) (2010) 1624-1631.

[65] K. Raveendran, A. Ganesh, K.C. Khilar, Influence of mineral matter on biomass pyrolysis characteristics, Fuel, (1995) 1812-1822.

[66] A.K. Varma, L.S. Thakur, R. Shankar, P. Mondal, Pyrolysis of wood sawdust: Effects of process parameters on products yield and characterization of products, Waste Manag., 89 (2019) 224-235.

[67] A.A. Lappas, E.F. Iliopoulou, K. Kalogiannis, Chapter 10. Catalysts in biomass pyrolysis, thermochemical conversion of biomass to liquid fuels and chemicals 2010, pp. 263-287.

[68] Y. Zheng, F. Wang, X. Yang, Y. Huang, C. Liu, Z. Zheng, J. Gu, Study on aromatics production via the catalytic pyrolysis vapor upgrading of biomass using metal-loaded modified H-ZSM-5, J. Anal. Appl. Pyrolysis, 126 (2017) 169-179.

[69] E.F. Iliopoulou, S.D. Stefanidis, K.G. Kalogiannis, A. Delimitis, A.A. Lappas, K.S. Triantafyllidis, Catalytic upgrading of biomass pyrolysis vapors using transition metal-modified ZSM-5 zeolite, Appl. Catal. B: Environ., 127 (2012) 281-290.

[70] Q. Che, M. Yang, X. Wang, Q. Yang, L. Rose Williams, H. Yang, J. Zou, K. Zeng, Y. Zhu, Y. Chen, H. Chen, Influence of physicochemical properties of metal modified ZSM-5 catalyst on benzene, toluene and xylene production from biomass catalytic pyrolysis, Bioresour. Technol., 278 (2019) 248-254.

[71] M. Razzaq, M. Zeeshan, S. Qaisar, H. Iftikhar, B. Muneer, Investigating use of metal-modified HZSM-5 catalyst to upgrade liquid yield in co-pyrolysis of wheat straw and polystyrene, Fuel, 257 (2019).

[72] L. Sun, X. Zhang, L. Chen, B. Zhao, S. Yang, X. Xie, Comparision of catalytic fast pyrolysis of biomass to aromatic hydrocarbons over ZSM-5 and Fe/ZSM-5 catalysts, J. Anal. Appl. Pyrolysis, 121 (2016) 342-346.

[73] M.M. Yung, A.R. Stanton, K. Iisa, R.J. French, K.A. Orton, K.A. Magrini, Multiscale evaluation of catalytic upgrading of biomass pyrolysis vapors on Ni- and Ga-modified ZSM-5, Energy Fuels, 30(11) (2016) 9471-9479.

[74] Balasundram V, Ibrahim N, Kasmani RM, Isha R, Abd Hamid MK, H. H., Catalytic pyrolysis of sugarcane bagasse using molybdenum modified HZSM-5 zeolite, Energy Procedia., 142 (2017) 793-800.

[75] S. Thangalazhy-Gopakumar, S. Adhikari, R.B. Gupta, Catalytic pyrolysis of biomass over H+ZSM-5 under hydrogen pressure, Energy Fuels, 26(8) (2012) 5300-5306.

[76] P.T. Williams, P.A. Horne, The influence of catalyst type on the composition of upgraded biomass pyrolysis oils, J. Anal. Appl. Pyrolysis 31 (1995) 39-61.

[77] E. Marceau, X. Carrier, M. Che, Synthesis of Solid Catalysts in: K.P. De Jong (Ed.), Wiley-VCH, Germany (2010) 59-82.

[78] P. Munnik, P.E. de Jongh, K.P. de Jong, Recent developments in the synthesis of supported catalysts, Chem Rev 115(14) (2015) 6687-718.

[79] K.P. De Jong, Synthesis of Solid Catalysts, in: K.P. De Jong (Ed.), Wiley-VCH, Germany (2010) 111-132.

[80] W. Schwieger, A.G. Machoke, T. Weissenberger, A. Inayat, T. Selvam, M. Klumpp, A. Inayat, Hierarchy concepts: classification and preparation strategies for zeolite containing materials with hierarchical porosity, Chem. Soc. Rev., 45(12) (2016) 3353-76.

[81] L. Xu, F. Wang, Z. Feng, Z. Liu, J. Guan, Hierarchical ZSM-5 zeolite with enhanced catalytic activity for alkylation of phenol with tert-butanol, Catalysts 9(2) (2019).

[82] T. Ge, Z. Hua, X. He, Y. Zhu, W. Ren, L. Chen, L. Zhang, H. Chen, C. Lin, H. Yao, J. Shi, One-pot synthesis of hierarchically structured ZSM-5 zeolites using single micropore-template, Chin. J. Catal., 36(6) (2015) 866-873.

[83] K. Miyake, Y. Hirota, Y. Uchida, N. Nishiyama, Synthesis of mesoporous MFI zeolite using PVA as a secondary template, J. Porous Mater., 23(5) (2016) 1395-1399.

[84] G. Song, W. Chen, P. Dang, S. Yang, Y. Zhang, Y. Wang, R. Xiao, R. Ma, F. Li, Synthesis and characterization of hierarchical ZSM-5 zeolites with outstanding mesoporosity and excellent catalytic properties, Nanoscale Res. Lett., 13(1) (2018) 364.

[85] C.J.H. Jacobsen, C. Madsen, J. Houzvicka, I. Schmidt, A. Carlsson, Mesoporous zeolite single crystals, J. Am. Chem. Soc., 122 (2000) 7116.

[86] D.P. Serrano, J.M. Escola, R. Sanz, R.A. Garcia, A. Peral, I. Moreno, M. Linares, Hierarchical ZSM-5 zeolite with uniform mesopores and improved catalytic properties, New J. Chem., 40(5) (2016) 4206-4216.

[87] X. Li, X. Zhang, S. Shao, L. Dong, J. Zhang, C. Hu, Y. Cai, Catalytic upgrading of pyrolysis vapor from rape straw in a vacuum pyrolysis system over La/HZSM-5 with hierarchical structure, Bioresour. Technol., 259 (2018) 191-197.

[88] Y. Ji, H. Yang, W. Yan, Strategies to enhance the catalytic performance of ZSM-5 zeolite in hydrocarbon cracking: A Review, Catalysts, 7(12) (2017).

[89] S. Abelló, A. Bonilla, J. Pérez-Ramírez, Mesoporous ZSM-5 zeolite catalysts prepared by desilication with organic hydroxides and comparison with NaOH leaching, Appl. Catal. A: Gen., 364(1-2) (2009) 191-198.

[90] D. Wang, L. Zhang, L. Chen, H. Wu, P. Wu, Postsynthesis of mesoporous ZSM-5 zeolite by piperidine-assisted desilication and its superior catalytic properties in hydrocarbon cracking, J. Mater. Chem. A, 3(7) (2015) 3511-3521.

[91] F. Meng, X. Wang, S. Wang, Y. Wang, Fluoride-treated HZSM-5 as a highly stable catalyst for the reaction of methanol to gasoline, Catal. Today, 298 (2017) 226-233.

[92] Q. Ma, T. Fu, H. Li, L. Cui, Z. Li, Insight into the selection of the post-treatment strategy for ZSM-5 zeolites for the improvement of catalytic stability in the conversion of methanol to hydrocarbons, Ind. Eng. Chem. Res., 59(24) (2020) 11125-11138.

[93] Y. Fan, X. Bao, X. Lin, G. Shi, H. Liu, Acidity adjustment of HZSM-5 zeolites by dealumination and realumination with steaming and citric acid treatments, J. Phys. Chem. B, 110 (2006) 15411-15416.

[94] T. Sano, Y. Uno, Z.B. Wang, C.-H. Ahn, K. Soga, Realumination of dealuminated HZSM-5 zeolites by acid treatment and their catalytic properties, Microporous Mesoporous Mater., 31 (1999) 89-95.

[95] S. Kumar, A.K. Sinha, S.G. Hegde, S. Sivasanker, Influence of mild dealumination on physicochemical, acidic and catalytic properties of H-ZSM-5, J. Mol. Catal. A Chem., 154 (2000) 115-120.

[96] J.-P. Zhao, J.-P. Cao, F. Wei, Z.-M. He, N.-Y. Yao, X.-B. Feng, T.-L. Liu, Z.-Y. Wang, X.-

Y. Zhao, X.-Y. Wei, Catalytic upgrading of lignite pyrolysis volatiles over AlF3-Modified HZSM-5 to light aromatics: Synergistic effects of one-step dealumination and realumination, Energy Fuels, 35(15) (2021) 12056-12064.

[97] Z. Qin, L. Lakiss, J.P. Gilson, K. Thomas, J.M. Goupil, C. Fernandez, V. Valtchev, Chemical equilibrium controlled etching of MFI-type zeolite and its influence on zeolite structure, acidity, and catalytic activity, Chem. Mater., 25(14) (2013) 2759-2766.

[98] C. Pagis, A.R. Morgado Prates, D. Farrusseng, N. Bats, A. Tuel, Hollow zeolite structures: An overview of synthesis methods, Chem. Mater., 28(15) (2016) 5205-5223.

[99] Z. Wang, Y. Liu, J.-g. Jiang, M. He, P. Wu, Synthesis of ZSM-5 zeolite hollow spheres with a core/shell structure, J. Mater. Chem., 20(45) (2010).

[100] C. Dai, A. Zhang, M. Liu, X. Guo, C. Song, Hollow ZSM-5 with silicon-rich surface, double shells, and functionalized interior with metallic nanoparticles and carbon nanotubes, Adv. Funct. Mater., 25(48) (2015) 7479-7487.

[101] M. Li, Y. Hu, Y. Fang, T. Tan, Coating mesoporous ZSM-5 by thin microporous silicalite-1 shell: Formation of core/shell structure, improved hydrothermal stability and outstanding catalytic performance, Catal. Today, 339 (2020) 312-320.

[102] L. Yu, A. Farinmade, O. Ajumobi, Y. Su, V.T. John, J.A. Valla, MCM-41/ZSM-5 composite particles for the catalytic fast pyrolysis of biomass, Appl. Catal. A: Gen., 602 (2020).

[103] J.D. Na, G.Z. Liu, M.L. Ji, X.S. Ma, S.L. Hu, L. Wang, Synthesis and properties of ZSM-5/MCM-41 composite zeolite with a core-shell structure for cracking of supercritical *n*-dodecane, Adv. Mater. Res., 528 (2012) 267-271.

[104] R. Kore, R. Srivastava, B. Satpati, ZSM-5 zeolite nanosheets with improved catalytic activity synthesized using a new class of structure-directing agents, Chem. Eur. J., 20(36) (2014) 11511-21.

[105] D. Xu, Y. Ma, Z. Jing, L. Han, B. Singh, J. Feng, X. Shen, F. Cao, P. Oleynikov, H. Sun, O. Terasaki, S. Che, pi-pi interaction of aromatic groups in amphiphilic molecules directing

for single-crystalline mesostructured zeolite nanosheets, Nat. Commun., 5 (2014) 4262.

[106] M. Xu, C. Mukarakate, K. Iisa, S. Budhi, M. Menart, M. Davidson, D.J. Robichaud, M.R. Nimlos, B.G. Trewyn, R.M. Richards, Deactivation of multilayered MFI nanosheet zeolite during upgrading of biomass pyrolysis vapors, ACS Sustain. Chem. Eng., 5(6) (2017) 5477-5484.

Chapter 2 In-situ catalytic upgrading of bio-oil derived from fast pyrolysis of sunflower stalk to aromatic hydrocarbons over bifunctional Cu-loaded HZSM-5

2.1 Introduction

As fossil fuel resources continue to decline and the high production of carbon dioxide and other pollutants are always generated from them, it becomes more and more important to find alternative energy to replace the traditional ones. Biomass energy is one of the attractive and promising options for countries with abundant agriculture and forest resources [1]. Biomass can be converted into various gaseous, liquid and solid fuels and considered to be a zero-net-CO_2 emission energy with high sustainability [2, 3]. Combustion, pyrolysis, gasification and liquefaction are the general methods for converting biomass into convenient energy. Among them, fast pyrolysis could maximize the bio-oil yield from biomass resources (even more than 60%) under the absence of oxygen using a high heating rate with a short residence time of volatile [4, 5]. Although the fast pyrolysis process is capable of producing a high amount of bio-oil with other products such as fuel gases and char, the obtained bio-oil usually includes abundant oxygenated compounds, resulting in the fast pyrolysis oil unstable and corrosive in storage with a low heating value [6]. In addition, the high H_2O concentration hinders the spontaneous blending of the bio-oil with the petroleum. Thus, it cannot be directly applied as a liquid transportation fuel and various catalysts have been developed for the bio-oil upgrading [7-10]. In particular, high aromatic components in the upgrading bio-oil have been achieved by applying zeolites to crack heavy oxygenated compounds to light aromatic hydrocarbons (AHs) like benzene, toluene, ethylbenzene, xylene and naphthalene (BTEXN).

Zeolites are extensively used in the refinery plants. Among them, ZSM-5 with shape selection activity, ion-exchange ability and large surface area is an active catalyst for various reactions such as cracking, alkylation, aromatization and isomerization of hydrocarbons [11-14]. Especially, HZSM-5 exhibits good performance in effective converting of oxygenated compounds to aromatics during catalytic fast pyrolysis of biomass residues [15-17] since it has suitable acid sites and appropriate pore diameter for the shape selectivity toward aromatics production [18]. In our previous study [19], it was found that the HZSM-5 with Si/Al =24 catalytically upgraded the bio-oil from the fast biomass pyrolysis to produce more aromatic hydrocarbons when compared with other zeolites. Meanwhile, sunflower stalk was proven to be a potential biomass as the feedstock for bio-oil production with high aromatic hydrocarbons production. However, the performance of such a kind of catalyst could be further improved by adjusting the acidity and texture properties for the catalytic bio-oil upgrading. Various metals (e.g., Ni, Ga, Zn, Fe, Co and Pd) have been applied for the modification of zeolite catalysts to adjust the acidic and textural characteristics for the bio-oil upgrading [20-28]. Particularly, non-noble transition metals are gaining much more attentions due to their low cost in large-scale industrial applications. Li *et al.* investigated the Cu-modified ZSM-5 catalysts for the upgrading of oil and found that it increased the hydrocarbon yield in the upgrading bio-oils and also showed the acceptable reusability. However, they mainly focused on the use of high metal doping amount (>5 wt.%) and did not report the H_2O concentration in the upgrading bio-oil and the actual aromatic hydrocarbons yield [29]. Widayatno *et al.* found that the introduction of Cu with a low loading amount (0.25-3wt.%) on the β zeolite promoted the selectivity towards hydrocarbons in the bio-oil significantly owing to the moderate acidity property [30]. Although this Cu doped beta zeolite exhibited excellent performance, a catalyst to biomass weight ratio as high as 3.3 to 1 was also needed. It still remains a challenge for the pyrolysis bio-oil upgrading with less amount of the catalyst. On the other hand, the fast pyrolysis in a short period of time (several seconds) is a general way for the high-yield bio-oil

production. Herein, the in-situ fast pyrolysis bio-oil upgrading is also full of challenge since only a short residence time (0.5-10 s) is for the bio-oil vapor passing through the catalyst layer [31]. Thus, high-performance catalysts are required in the in-situ fast pyrolysis bio-oil upgrading. The key factors of the catalyst that cause the oxygen-containing compounds to be converted into aromatic compounds include the acidity, pore size and pore shape of catalysts. For the ZSM-5 based catalysts, as summarized in **Table 2.1**, metal loading on the ZSM-5 could improve the catalytic upgrading performance. The upgraded oil yield and the selectivity to the aromatic hydrocarbons are two important parameters for the evaluating the upgrading performance of the prepared catalysts. From **Table 2.1**, one can see that most of metal loaded ZSM-5 catalysts had upgraded oil yields lower than 30% and/or the selectivities to the aromatic hydrocarbons lower than 60%.

Table 2.1 Reported results on the catalytic upgrading of pyrolysis bio-oil over ZSM-5 and metal-loaded HZSM-5 zeolite.

Catalyst	Feedstock	Bio-oil yield (%)	Aromatics selectivity %	Other key results	Ref.
HZSM-5	Rice husk	3.4-7.2%	2.24%	HZSM-5 exhibited the highest activity for aromatics production when compared with other catalysts.	[14]
HZSM-5, H-USY, H-Beta	Sunflower stalk, Cedar, Knotweed, Apple stem	27-36%	56-100%	HZSM-5 resulted in higher yields of specific aromatic hydrocarbons, especially naphthalene, p-xylene and toluene for all biomass feedstocks.	[19]
Ni/HZSM-5, Co/HZSM-5	Lignocellulo-sic biomass	14-17%	8%	Ni/HZSM-5 and Co/HZSM-5 enhanced the production of aromatics and phenols. In the case using the catalysts, the total liquid yield decreased while the gaseous products and coke increased.	[20]

Co/ HZSM-5	Beech wood	44%	54%	Co-promoted HZSM-5 catalysts enhanced the production of aromatics and phenols	[21]
Fe/ZSM-5	Rice husk	28%	-	4%Fe/ZSM-5 increased the production of hydrocarbons and further increased the selectivity towards BTX (benzene, toluene and xylenes)	[22]
Fe/ZSM-5	Beech sawdust	25%	21%	Fe/ZSM-5 catalyst decreased oxygenated compounds and increased the production of desirable products such as phenolics and aromatics	[23]
Zn/ZSM-5	Douglas fir	33%	50.7%	Zn/ZSM-5 catalysts decreased the bio-oil yield and coke while increased the syngas yield.	[24]
Ga/HZSM -5	Pine sawdust	45.9% (includin g water)	43%	Ga/HZSM-5 showed high selectivity for highly valuable aromatics, such as benzene, toluene, and xylenes (BTX)	[25]
Pd/HZS M-5, Ga/HZSM -5, Co/ HZSM-5, Ni/HZSM -5	Jatropha waste	-	91-97%	The metal/HZSM-5 catalysts improved the aromatic selectivity.	[26]
Mg/HZS M-5, Cu/HZSM -5, Zn/ HZSM-5, Ga/HZSM -5, Ni/HZSM -5, Co/HZSM -5	Yunnan pine particle	15%(Mg), 14%(Cu) , 23%(Zn) , 26%(Ga) , 20%(Ni) , 22%(Co)	-	The metal/HZSM-5 catalysts affected the selectivity of the single-ring aromatic hydrocarbons, such as C7 and C8. The Zn-ZSM-5 catalysts produced the highest content of the single-ring aromatics whereas the Ni-ZSM-5 catalysts produced the highest polycyclic aromatic hydrocarbons	[27]
Ni/HZSM	Pine wood	-	39.8-46.4%	The metal/HZSM-5 catalysts improved the	[28]

				aromatic selectivity.	
-5, Mo/HZSM-5, Co/ HZSM-5, Pt/HZSM-5					
Cu/HZSM-5	Sunflower stalk	30%	73.2%	Cu/HZSM-5 with low Cu loading amount exhibited the best catalytic performance with relative amounts of aromatic hydrocarbons	This work

Based on the previous study [19], this research focused on the use of HZSM-5 modified with low Cu species doping amounts (0-5 wt.%) and the appropriate Cu doping amount was expected to further improve catalytic upgrading performance for the bio-oil from the fast sunflower stalk pyrolysis with a low catalyst to biomass weight ratio of 1:1. The chemical composition in the upgraded bio-oil, the actual aromatics yield and the total mass balance (char, gas, bio-oil, water, coke) were analyzed. Furthermore, the deoxygenation routes were discussed based on the lignin, cellulose and hemicellulose components in the sunflower stalk. Furthermore, the reusability and regeneration property of the catalysts were investigated for the catalysts with the best performance.

2.2 Experimental

2.2.1 Biomass feedstock

Sunflower stalk was the agricultural residue in Aomori city, Japan, which was dried overnight at 110 °C at first, and then ground and sieved to a 0.5-1 mm particle size. Proximate analyses of moisture and ash were carried out following the ASTM D7582 standard, and ultimate analysis was conducted with a Vario EL cube elemental analyzer and the results were reported in our previous study as shown in **Table 2.2** [19].

Table 2.2 Proximate, ultimate and ash composition of sunflower stalk

Biomass	Proximate analysis (%wt.)[a]		Ultimate analysis (%wt)[c]				
	Moisture	ash	C	H	N	S	O[b]
Sunflower stalk	9.6	11.4	39.57	5.39	1.18	0.25	53.61

[a]Dry basis, [b]Mass difference and [c]Dry and ash-free.

2.2.2 Preparation of Catalysts

The commercial HZSM-5 zeolite (Si/Al=24) was purchased from TOSOH Corp. and calcined for 2 h at 650 ℃ in the air to remove impurities. The calcined zeolite was pressed into pellet shapes and ground through a sieve to obtain particle sizes in the range of 0.5-1.0 mm. The zeolite samples were modified with Cu species by the wet impregnation method, where the zeolite powders were immersed in 25 mL of $Cu(NO_3)_2 \cdot 3H_2O$ solutions with different concentrations for the loading of 0.25, 0.5, 1, 3 and 5 wt.% of Cu respectively on the zeolites, and stirred at room temperature for 8 h. After that, the solution was evaporated overnight at 100 ℃ and finally the sample was calcined at 650 ℃ for 4 h. The as-prepared samples were called as the parent zeolite and x wt.%Cu/HZSM-5 (x = 0.25, 0.5, 1, 3 and 5), respectively.

2.2.3 In-situ catalytic upgrading

In-situ catalytic bio-oil upgrading was carried out in a quartz fixed-bed reactor, where biomass (0.5 g) and catalyst (0.5 g) were separated by a quartz wool layer in the center of the reactor, and the carrier gas was passed in the reactor from the biomass to catalyst bed. The quartz fixed-bed reactor was then put in an infrared furnace. The underside of the reactor was connected to a bottle containing cold acetone, which was used for the condensation of upgraded bio-oil. The collected bio-oil was further evaluated offline by a GC-MS. The

schematic diagram of the experimental setup is shown in **Scheme 2.1**
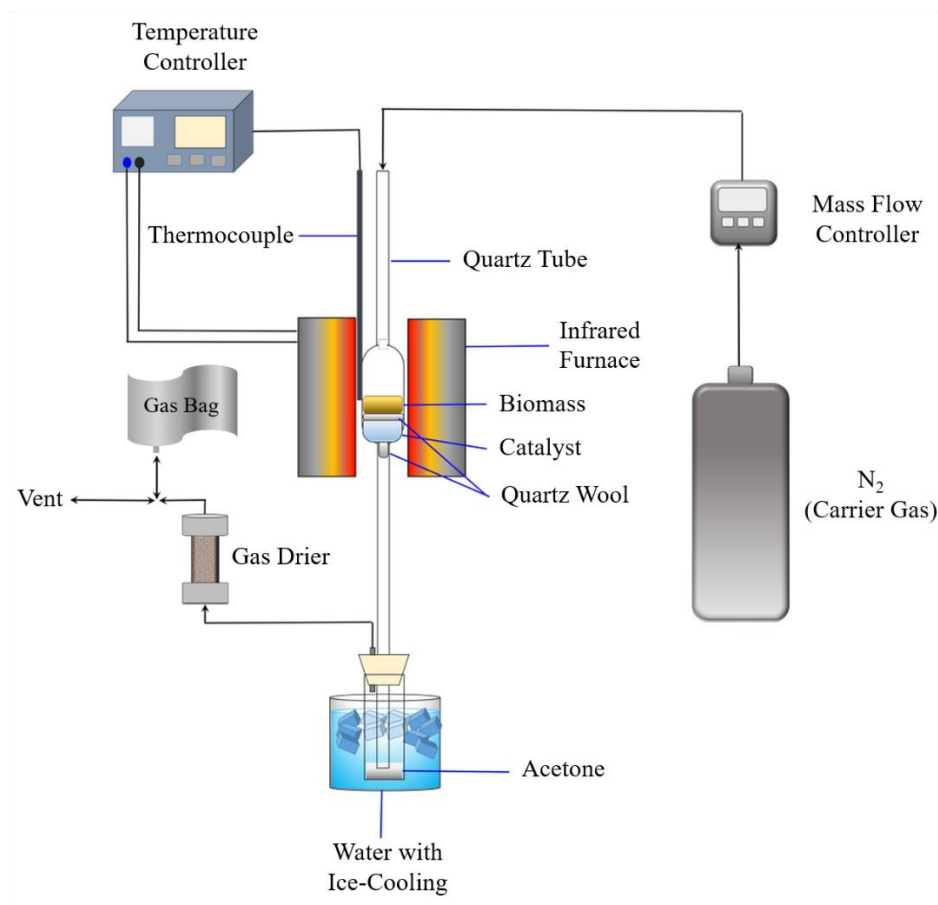
Scheme 2.1 The diagram of fixed bed reactor for in situ-catalytic upgrading of bio-oil

In order to start the reaction under oxygen-free environment, a nitrogen flow (100 cm^3/min) was used to purge the inside of reactor for 10 minutes. Then, the reaction was performed by heating to 500 ºC rapidly from room temperature with a 100 ºC/s heating rate and maintaining at 500ºC for 5 min. The gas product was also collected using the gasbag. Each run was carried out repeatedly for 3 times at the same condition to ensure reproducibility, and the average value was used for the discussion in the following.

The bio-oil was measured by a GC/MS instrument (GCMS-QP2020, Shimadzu, Japan). As soon as the automatic injection of the sample into the column, the oven was heated to 300 ºC from 50 ºC (heating rate: 10 ºC/min) and held at 300ºC for 10 min. Chromatographic peaks were confirmed by using the data of the NIST mass spectrum library. The quantitative analysis of specific aromatic hydrocarbons including benzene, toluene, o-xylenes, p-xylenes,

ethylbenzenes, naphthalenes (e.g., 2,6-dimethyl-naphthalene, 6-methyl-1,2-dihydronaphthalene, 2-ethyl-naphthalene, 2-methyl-naphthalene and so on) and other aromatics (mainly included indene and other alkylbenzenes (e.g., mesitylene, styrene, Benzene, 1-ethyl-2-methyl-benzene, 1-ethenyl-3-methyl-benzene, 1,3,5-trimethyl- benzene) were carried out using an external standard method. The detected bio-oil main components in this study were the light bio-oil compounds only since the quantitative analysis using the present GC/MS was performed at an oven temperature of 300 °C.

Off-line analysis of the non-condensable gases was performed using an Agilent 7890A GC system (USA), where He carrier gas was used for the CO, CH_4 and CO_2 analysis and Ar carrier gas was for H_2 detection. The quantification of those gases was measured by comparing to the calibration curve of each standard gas using an external standard method. The H_2O concentration in the bio-oil was analyzed with an MKS-500 Karl-Fisher instrument (Japan). The solids remaining in the biomass layer were considered as the char, which was directly measured by weight difference. The amounts of coke on the catalysts during the reaction were determined by analyzing 10 mg of the catalyst after the reaction with a DTG-60H thermogravimetric analyzer (Shimadzu, Japan), where the oven temperature was started from a room temperature and ended at 900 °C (heating rate:10 °C/min) under airflow. The coke amount was estimated by the weight difference.

2.2.4 Catalyst characterizations

Powder XRD profiles of the parent HZSM-5 and metal loaded HZSM-5 zeolites were measured on a Rigaku Smartlab XRD instrument (Japan) using a CuKα radiation (λ = 0.1542 nm) with a step of 0.02º in the 2θ range of 10–80º. The surface area and pore size distributions were determined with a NOVA 4200e Quantachrome instrument (USA). Prior to N_2 adsorption (77 K), zeolite powders were treated under vacuum for degassing for 8 h at 473 K. Herein, the Brunauer-Emmett-Teller (BET) method was used to determine the specific surface area. Pore size distribution and average pore size were determined based on the desorption branch. The

t-plot method was used to determine the micropore surface area (S_{micro}) and microporous volumes (V_{micro}). The morphologies of the samples were examined by a SU8010 SEM machine (Hitachi, Japan) and the Cu distribution on the catalyst was confirmed by an EDX detector (Horiba). The acidity was measured by using NH_3-TPD method (BELCAT, Japan). Herein, about 0.1 g of sample was pretreated for 1 h at 700 °C and then NH_3 gas was flowed into the catalyst cell for 1 h at 120 °C. Finally, the desorption of NH_3 was carried out from 120 °C to 800 °C under helium gas flow.

2.3 Results and discussion

2.3.1 Zeolite characteristics before the reaction

The diffraction peaks of the parent HZSM-5 and various Cu/HZSM-5 catalysts were examined by XRD analysis. As shown in **Fig. 2.1**, the HZSM-5 zeolite crystalline structures were preserved even in the case up to 5% of the metal doping. The peaks at 2θ of 23.1°, 23.8° and 24.4° belonged to HZSM-5 [32, 33] whereas the peaks at 2θ of 35.55° and 38.70° corresponded to the Cu species [34]. One can see that Cu modification of HZSM-5 did not alter the zeolite crystalline structure. However, it is mentioned that no obvious peaks relating to Cu species were observed for any percentage doping of Cu, implying that Cu species were dispersed well on the HZSM-5 and the low content of the Cu doping effectively reduced the agglomeration of Cu particles on the surface of HZSM-5, which could occur during the calcination [30].
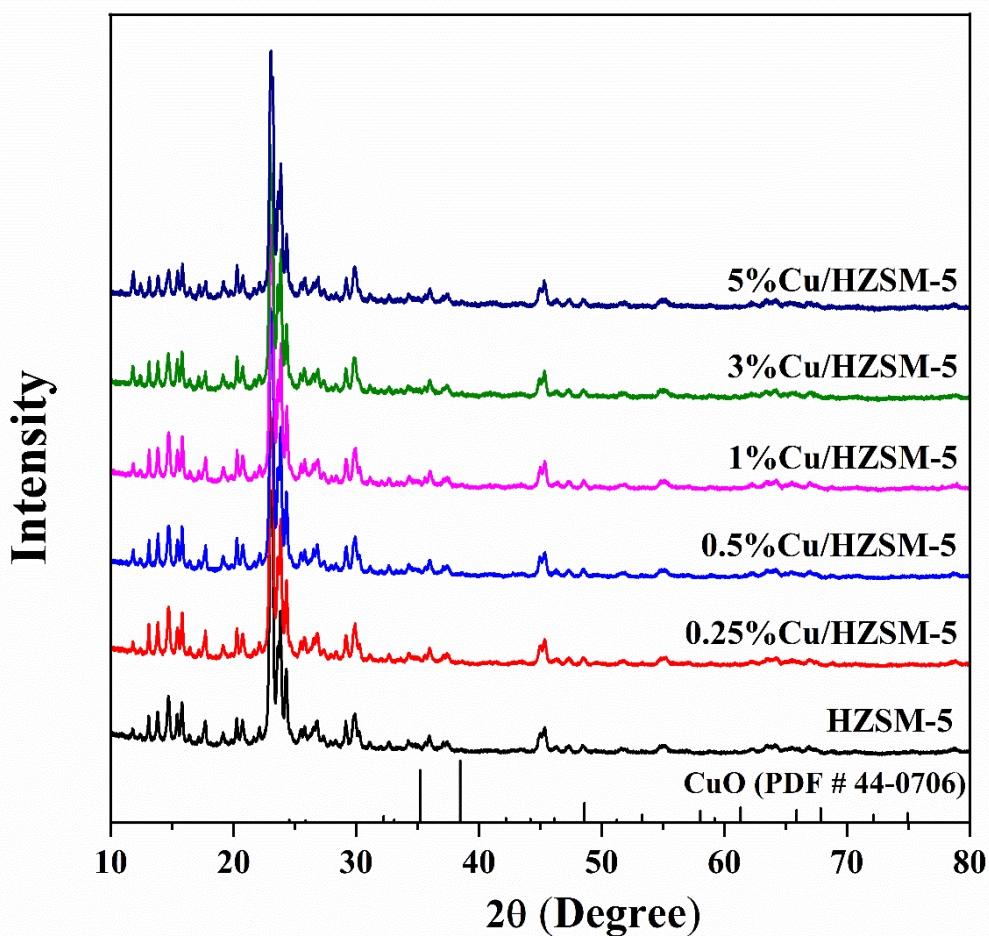
Fig. 2.1 XRD patterns of the parent HZSM-5 and the obtained Cu/HZSM-5catalysts

Fig. 2.2 shows NH_3-TPD curves of the HZSM-5 and Cu/HZSM-5 catalysts. The acidity amounts evaluated based on the peak areas are listed in **Table 2.3**. Two typical peaks appeared at the two temperature ranges of 115-325 ºC and 325-700 ºC represented the weak and the strong acid sites, separately. The desorption temperature of ammonia on weak acid sites slightly shifted to low temperature as the Cu doping amount was raised from 0.25 to 0.5wt.%. Herein, after the Cu was doped on HZSM-5, some of the H^+ cations on the zeolite were replaced by Cu^{2+} cations, and the Cu species could be in the forms of the isolated Cu^{2+} cation or CuO cluster, which caused the shift of the weak acid to lower temperatures with an increased amount of strong acid sites [35]. However, further increasing Cu doping amount from 0.5wt.% caused a weak acid site peak shift to higher temperature, and as the Cu doping amount was increased to 3 wt.% and more, the weak acid site peak shift to the higher temperature became

49
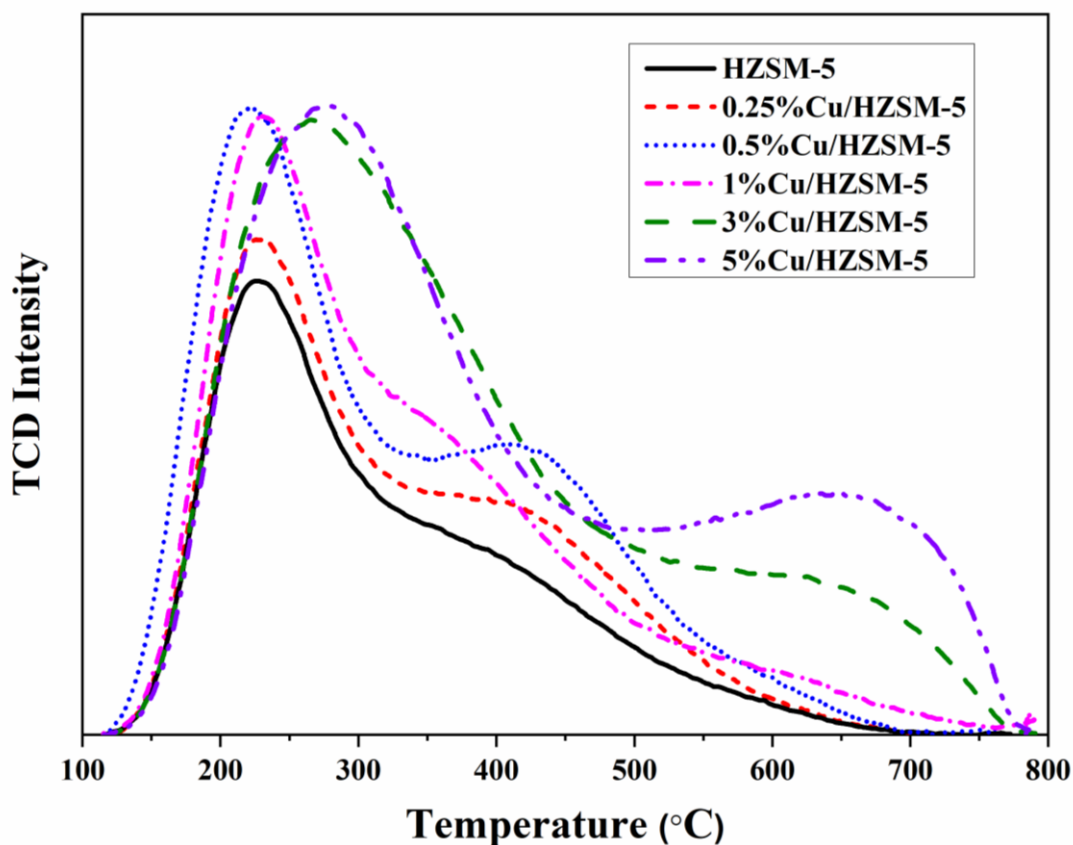
Fig. 2.2 NH$_3$-TPD profiles of the parent HZSM-5 and the obtained Cu/HZSM-5catalysts

more obvious, which could promote the coke formation. In general, the increase of acid amount presents that more active sites can be provided for pyrolytic vapor decomposition, promoting the catalytic deoxygenation [3, 36]. However, it also leads to the formation of coke on the active sites due to the polymerization and condensation, resulting in the deactivation [37-39]. Thus, an optimum Cu doping amount should exist.

Table 2.4 shows the specific BET surface area and porous properties of the catalysts and **Fig. 2.3** shows the related isotherms and pore distributions. The parent HZSM-5 had a 332 m^2/g of surface area with a combined characteristic IUPAC types I and IV isotherms as the nitrogen was adsorbed at low relative pressures (P/P$_0$ < 0.1) with a hysteresis loop as P/P$_0$ > 0.4, indicating the presence of microporous and mesoporous structures [40]. With the introduction of Cu species, the total pore volume and the surface area were remarkably

decreased since Cu species could enter into the meso- and micropores of HZSM-5 [41].

Table 2.3 Acidity of the parent HZSM-5 catalysts and the obtained Cu/HZSM-5 catalysts

Catalyst	Acidity (mmol/g, low temp)	Acidity (mmol/g, high temp)	Total acidity (mmol/g)
HZSM-5	0.47	0.40	0.87
0.25%Cu/HZSM-5	0.41	0.32	0.73
0.5%Cu/HZSM-5	0.60	0.52	1.12
1%Cu/HZSM-5	0.55	0.49	1.04
3%Cu/HZSM-5	1.02	0.37	1.39
5%Cu/HZSM-5	1.01	0.53	1.54

Table 2.4 Textural properties of the parent HZSM-5 and the obtained Cu/HZSM-5 catalysts

Catalyst	S_{BET} (m^2/g)	S_{micro} (m^2/g)	V_{total} (cm^3/g)	V_{micro} (cm^3/g)	Average pore size (nm)
HZSM-5	332.1	365.1	0.28	0.134	3.15
0.25%Cu/HZSM-5	322.7	258.5	0.27	0.130	3.56
0.5%Cu/HZSM-5	316.8	254.9	0.27	0.128	3.53
1%Cu/HZSM-5	310.5	236.5	0.27	0.130	3.50
3%Cu/HZSM-5	306.6	249.0	0.25	0.126	3.25
5%Cu/HZSM-5	280.6	212.8	0.26	0.107	3.35

Figs. 2.4(a) and (b) show morphologies of HZSM-5 and 0.5%Cu/HZSM-5 samples prepared by the wet impregnation method, and Fig. 2.4(d) shows EDX mapping of 0.5%Cu/HZSM-5 catalyst. Multi-particle agglomerations were observed for the HZSM-5 powder due to the interconnection of small particles with a fractured cubic-like shape [27]. The morphology of Cu/HZSM-5 was similar to that of the parent HZSM-5 catalyst, but it was difficult to observe the particles related to Cu species on the surface of HZSM-5. However, based on the Cu EDX mapping (Fig. 2.4(d)), it was found that the Cu elements were evenly distributed on the HZSM-5 surface.
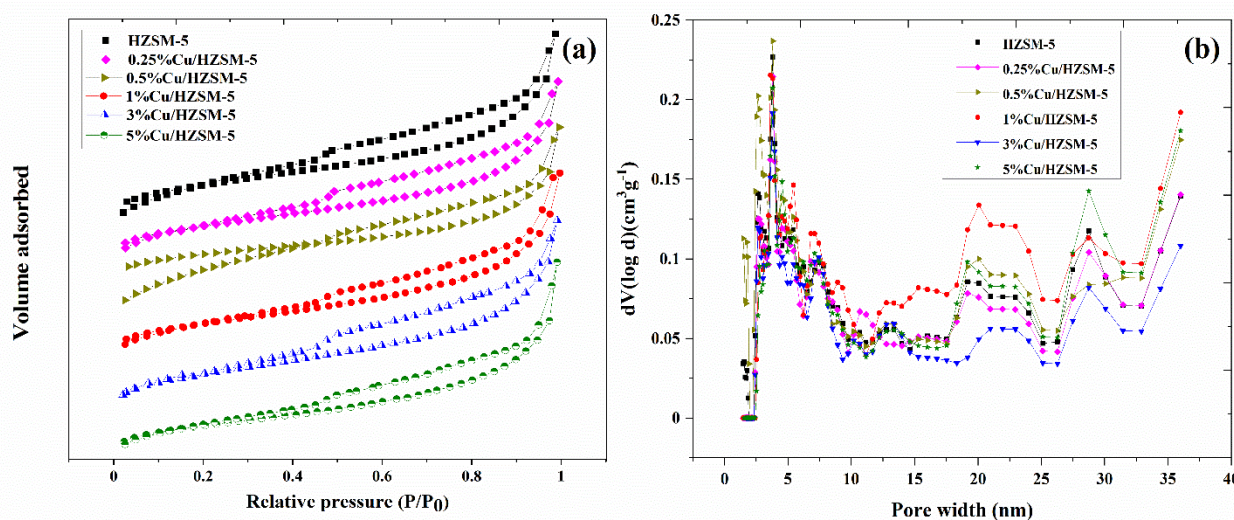
Fig. 2.3 N$_2$ adsorption/desorption isotherms and DFT pore size distributions of the parent HZSM-5 and the obtained Cu/HZSM-5catalysts
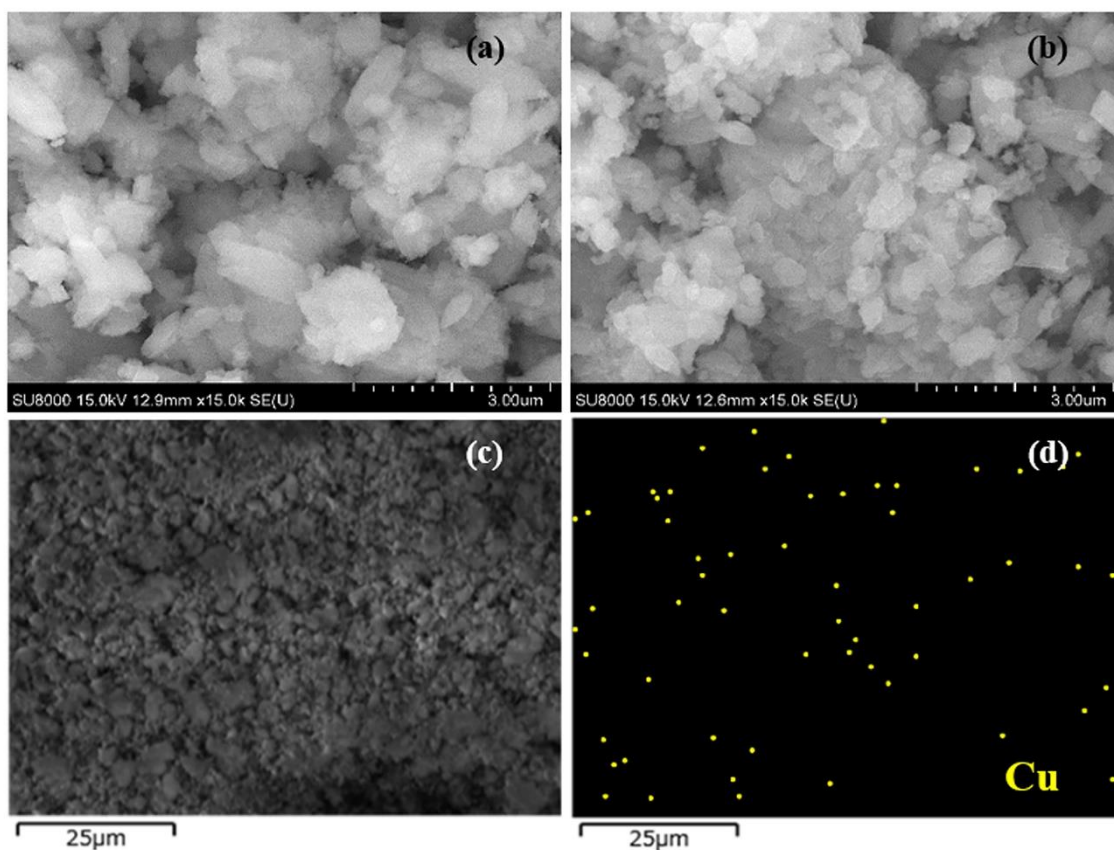
Fig. 2.4 SEM images of (a) parent HZSM-5 and (b-c) 0.5 wt.%Cu/HZSM-5, and EDX mapping image (d) of 0.5 wt.%Cu/HZSM-5

2.3.2 Catalytic bio-oil upgrading

Fig. 2.5(a) displays the percentages of various chemical compositions in the all chemicals (hereafter, it was called as "relative amount") determined by the peak areas in the GC-MS spectrum, which are considered as the key indicator to evaluate the upgraded bio-oil quality and catalyst performance. The relative amounts on the GC-MS spectra related to the upgraded bio-oil compositions from the *in-situ* upgrading of fast pyrolysis oils over the parent HZSM-5 and the various Cu modified HZSM-5 catalysts, which were categorized into 7 groups: (1) aromatic hydrocarbons; (2) aliphatic hydrocarbons; (3) phenols, (4) ketones, (5) acids, (6) aldehydes, and (7) other oxygenated compounds consisted of alcohol, esters and amines. For the parent HZSM-5, deoxygenation could take place on the Brønsted acid sites on either the external surface or internal surface and as a result, the main compounds were aromatic

hydrocarbons (55.0%) followed by acids (13.5%) mainly including acetic acid, and other oxygenated compounds (7.9%). After the Cu doping, the relative aromatic hydrocarbon amount was raised to 59.8% for 0.25 wt.% Cu and reached a maximum of 73.2% for 0.5 wt.% Cu while the acids, phenols and ketones were mainly reduced. However, with the further increasing Cu doping amounts to 1, 3 and 5 wt.%, the relative amounts of the aromatic hydrocarbons were decreased to 67.7%, 59.6% and 53.7%, respectively. Thus, the low content of Cu doping could enhance the efficiency of deoxygenation (dehydration, decarboxylation, decarbonylation), thereby increasing the selectivity towards aromatic hydrocarbons. Herein, it should be noted that 0.5%Cu/HZSM-5 exhibited the best selectivity towards aromatic hydrocarbons. **Fig. 2.5(b)** displays the specific aromatic hydrocarbons yields in the upgrading bio-oils based on dried ash-free (d.a.f) biomass. Herein, those aromatic hydrocarbons with large molecules were not determined, and only the yields of specific aromatic hydrocarbons which can be determined by calibration using the standard chemicals were obtained. It is obvious that the specific aromatic hydrocarbons in the upgrading bio-oil based on all Cu loaded HZSM-5 catalysts showed higher aromatics yield than that from the parent HZSM-5.
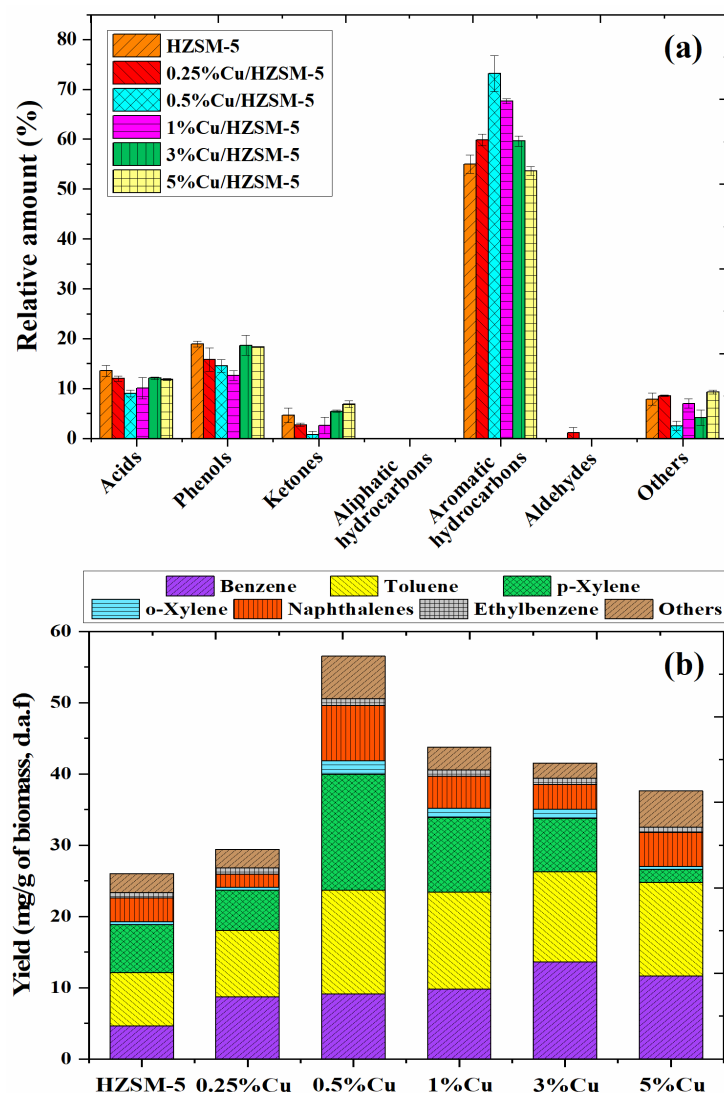
Fig. 2.5 Chemical compositions in the upgraded bio-oils with various Cu/HZSM-5 catalysts (a) and the yields of specific aromatic hydrocarbons based biomass (d.a.f) (b)

Especially, the use of 0.5%Cu/HZSM-5 also gave a maximum specific aromatic hydrocarbon yield of 56.5 mg/g-biomass (d.a.f). This amount is much more than that from the parent HZSM-5 (26.0 mg/g-biomass (d.a.f)). These results indicated that 0.5 wt.% should be the optimum Cu doping amount. Herein, the doping of Cu on HZSM-5 changed the acid properties including acid amount and acid strength, which could effectively influence the catalytic deoxygenation activity and product selectivity. However, the excessive Cu loading could result in excessive acidity and simultaneously the covering of the active sites on the zeolite and the

blockage of zeolite channels with the decrease in surface area, thereby reducing the catalyst activity [42].

Figs. 2.6(a) and **(b)** show product percentage distributions and the yield of gases during the upgrading of fast pyrolysis oils on the parent HZSM-5 and the various Cu modified HZSM-5 catalysts at 500 °C. Herein, the results were also based on the biomass (d.a.f). Obviously, the highest upgraded bio-oil yield of 37.3% with a gas yield of 14.1% and a coke yield of 5.6% was obtained when using the parent HZSM-5, and the bio-oil yield decreased when the Cu/HZSM-5 zeolites with the different Cu doping contents were used, where the upgraded bio-oil yields decreased to 33.4%, 29.8%, 32.2%, 32.9% and 28.5% for 0.25, 0.5, 1, 3 and 5 wt.% Cu doping amounts, respectively, and meanwhile, the yields of gas, water and coke were greater than those using the parent HZSM-5. These differences should be attributed to the changes of the acidity and the physical properties of the Cu modified catalyst as observed by NH_3-TPD and BET results. Herein, the increase in the yields of gases, water, and coke was related to the deoxygenation of those oxygenated compounds. In the case of using 5%Cu/HZSM-5, which had the strongest acidity as detected by NH_3-TPD, the upgraded bio-oil yield decreased to a higher extent while the gas and coke yields increased to 21.5% and 6.3% respectively as shown in **Table 2.5**. Herein, the excessive acid amount could promote not only the deoxygenation but also some secondary reactions (e.g., polycondensation, condensation, cyclization) of primary products like aromatics, phenols and ketones to form coke on the catalyst, resulting in the lower aromatics selectivity and yield. In addition, the blockage of micropores of HZSM-5 by the excessive Cu species resulted in the decrease in the surface area, thereby limiting the diffusions of the reagent as well as the products. It should be noted that the char yields of all experiments were the same since the biomass layer and the catalysts layer were separately located in the reactor. For the gas yields, as can be seen from **Fig. 2.6(b)**, the use of HZSM-5 resulted in lower gas yield than those cases using Cu/HZSM-5 catalysts. The increase in the gas products including CO, CO_2 and H_2 in the cases using the

Cu/HZSM-5 was related to dehydrogenation, dehydration, oligomerization, decarbonylation, and decarboxylation accompanying the increase in the aromatic hydrocarbon yields and the reduction of the oxygen content in the upgrading bio-oils [3, 43]. In addition, it should be noted that the yield of gas increased with the increasing of Cu loading amount, which should be resulted from the gradual enhancement of the secondary cracking reactions of pyrolysis vapor as well as the further pyrolysis of the coke intermediates on the catalyst [9]. Moreover, the increase of acid amount by the modifying by Cu may be more conducive to the improvement of catalytic activity toward gas production as observed in the case using 5%Cu/HZSM-5, which led to the highest gas yield.

Table 2.5 Coke amounts on the spent

Catalyst	Coke deposition (wt.%)
HZSM-5	5.6 ± 0.2
0.25%Cu/HZSM-5	4.6 ± 0.0
0.5%Cu/HZSM-5	6.3 ± 0.2
1%Cu/HZSM-5	5.9 ± 0.1
3%Cu/HZSM-5	4.7 ± 0.0
5%Cu/HZSM-5	6.3 ± 0.2
1st Reuse	8.4 ± 0.1
2nd Reuse	9.3 ± 0.0
3rd Reuse	9.7 ± 0.1
4th Regen	5.6 ± 0.1
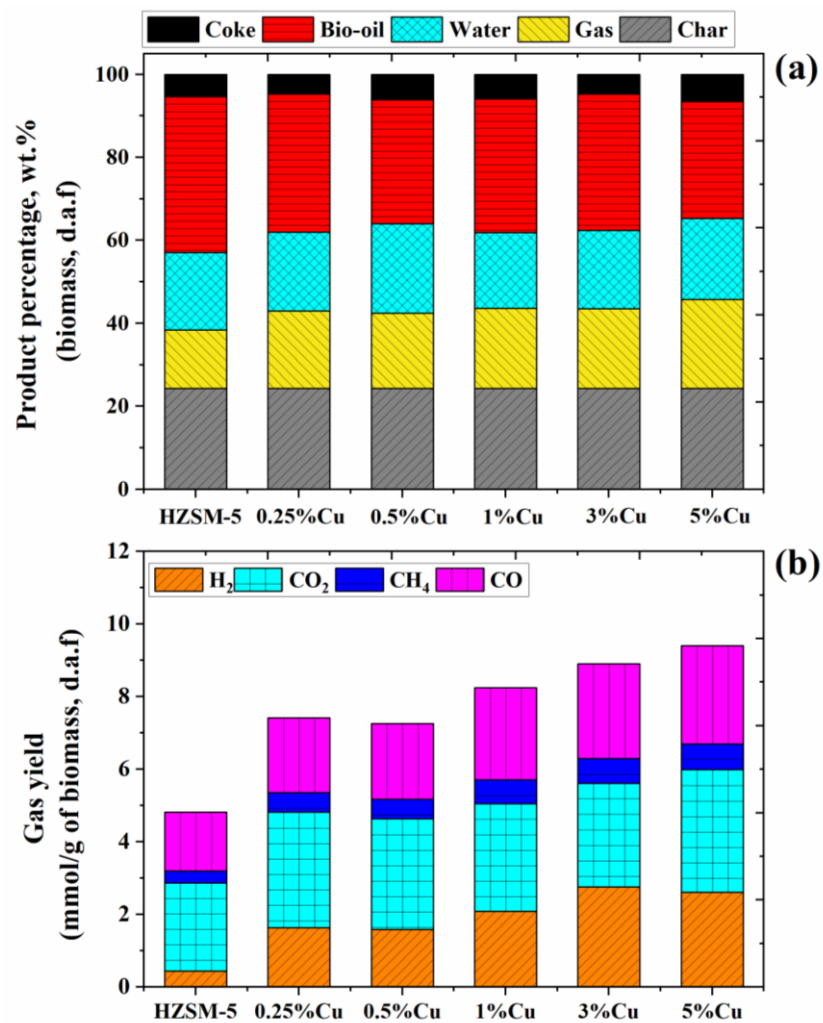
Fig. 2.6 The product distributions (a) and gas yields (b) obtained from the in-situ catalytic upgrading of bio-oil derived from fast pyrolysis of sunflower stalk over the parent HZSM-5 and various Cu/HZSM-5 catalysts
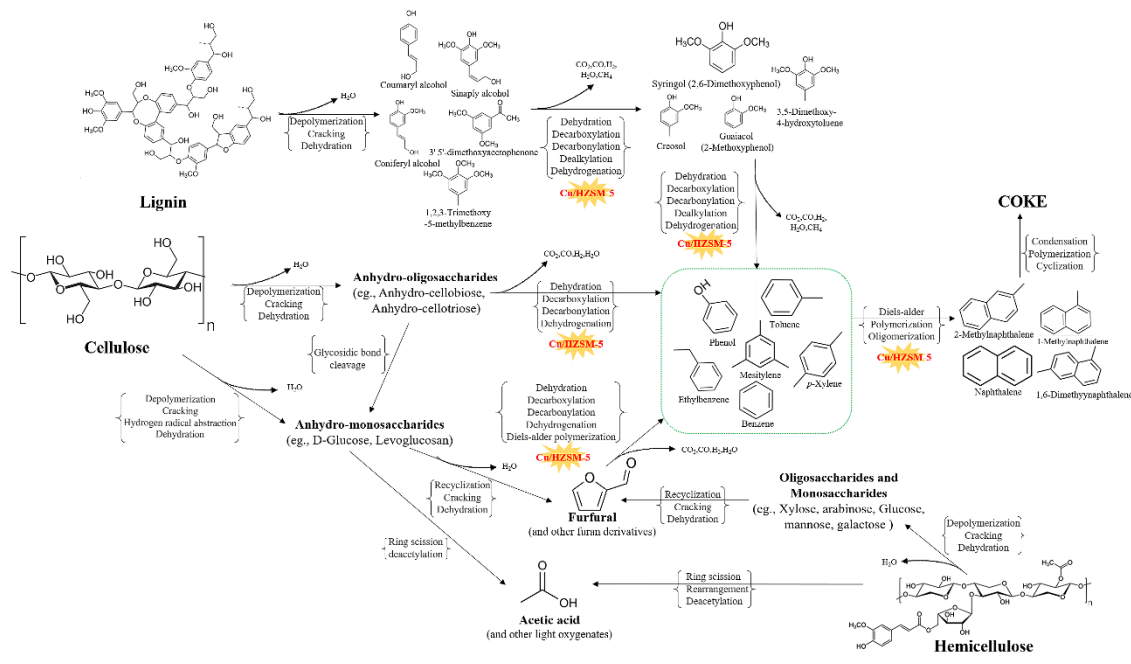
Fig. 2.7 Reaction pathways for the aromatic productions from catalytic upgrading of bio-oil derived from fast pyrolysis of sunflower stalk over Cu/H-ZSM-5 catalysts.

The reaction routes of the *in-situ* upgrading of fast pyrolysis oils over the parent HZSM-5 and the various Cu modified HZSM-5 catalysts is illustrated in **Fig. 2.7**. Generally, lignocellulose biomass with a polymeric structure mainly consists of 3 main constituents, i.e., lignin, cellulose and hemicellulose. The biomass pyrolysis can be classified based on the lignin, cellulose and hemicellulose components. In the cellulose pyrolysis process, anhydro-monosaccharides (e.g., D-glucose and levoglucosan) and anhydro-oligosaccharides will be generated through depolymerization and thermal cracking at first and then, anhydro-monosaccharides are further converted to monoaromatic via diel-alder polymerization on the Brønsted acid sites on either the outer surface or internal surface of zeolite and could continuously convert to polyaromatics such as naphthalene and 2-methylnaphthalene via Diel-alder polymerization [3, 44-46]. While, some polyaromatics could be condensed and polymerized to larger polyaromatics and even coke on those Brønsted acid sites. Herein, the

acidity of zeolite will play the key role for the coking since the coking often occurs at high acidity condition. Similarly, the anhydro-oligosaccharides can be also converted to the monoaromatic via dehydration, decarboxylation and decarbonylation on the Brønsted acid sites and some could change to coke via further condensation and polymerization. In this study, no Anhydro-monosaccharides, as well as anhydro-oligosaccharides, were detected in the final product, suggesting that the components from the thermal pyrolysis of cellulose were effectively converted to aromatic compounds with some acetic acid and ketone compounds. Hemicellulose is more easily decomposed at lower temperatures when compared to cellulose and lignin. It is significantly decomposed into the furfural and acetic acid at first, and then the generated products could be deoxygenated via dehydration, decarboxylation, decarbonylation and dehydrogenation on those Brønsted acid sites. The detected acetic acid in the final upgraded oil should be also mainly driven from the hemicellulose in the sunflower stalk [47]. Lignin consists of numerous branched aromatic rings, which can be divided into three basic units: sinapyl alcohol, coniferyl alcohol, and p-coumaryl alcohol. During the pyrolysis process, lignin could be converted to the compounds based on these three basic units and other heavy compounds at first [48], and subsequently, the secondary products like 3,5-dimethoxy-4-hydroxytoluene, guaiacol (2-Methoxyphenol), and creosol and syringol (2,6-Dimethoxyphenol) are further generated, which were also observed in the final upgraded bio-oil (**Figs. 2.8-2.17**). Thereafter, various reactions like dehydrogenation, dehydration, decarbonylation, dealkylation and decarboxylation could take place on the Brønsted acid sites of catalysts, resulting in the formation of phenol and various monoaromatics as those from the cellulose and hemicellulose [1, 43]. Meanwhile, some of them can be converted into large polyaromatics and coke via further condensation and polymerization in the same way as those species derived from cellulose and hemicellulose.
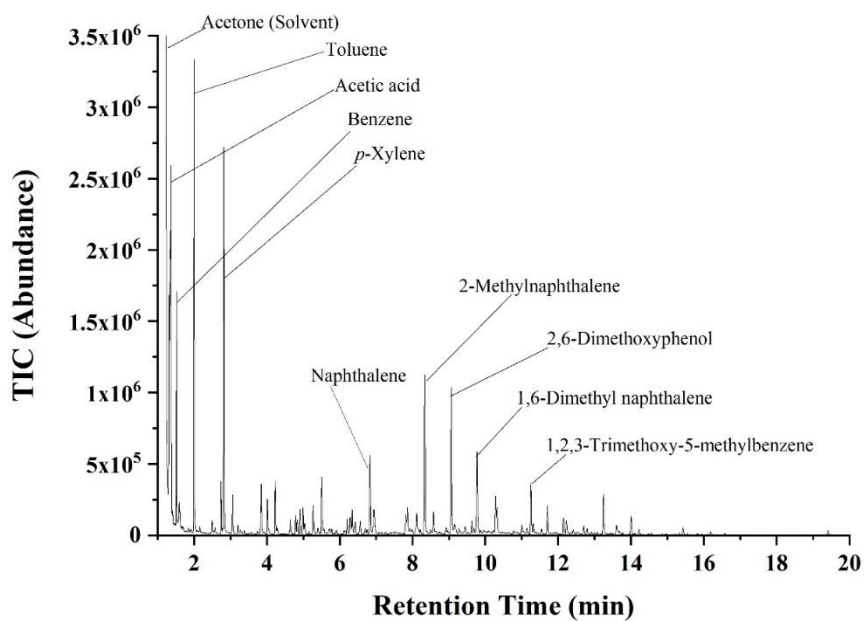
Fig. 2.8 GC/MS chromatogram of the upgraded bio-oils with the parent HZSM-5
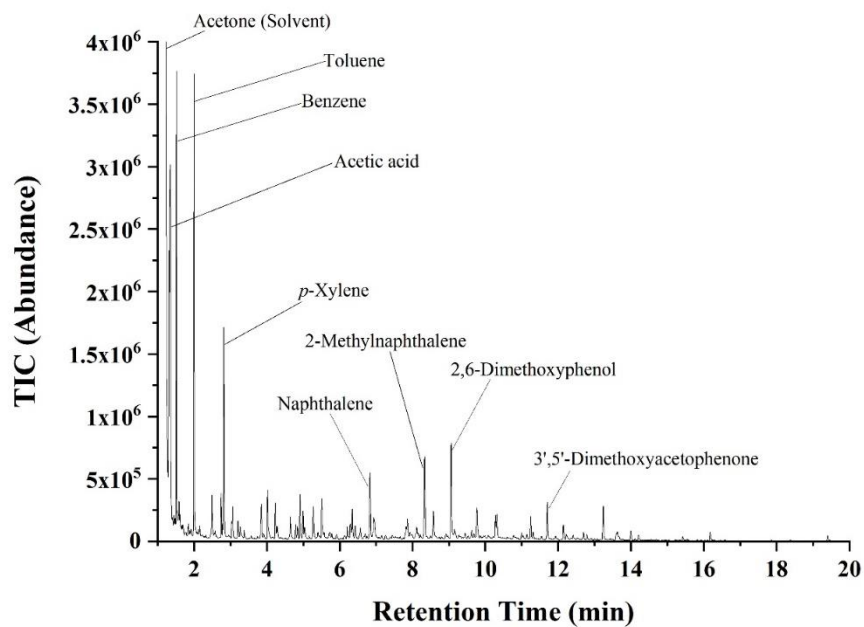
Fig. 2.9 GC/MS chromatogram of the upgraded bio-oils with 0.25wt.%Cu/HZSM-5
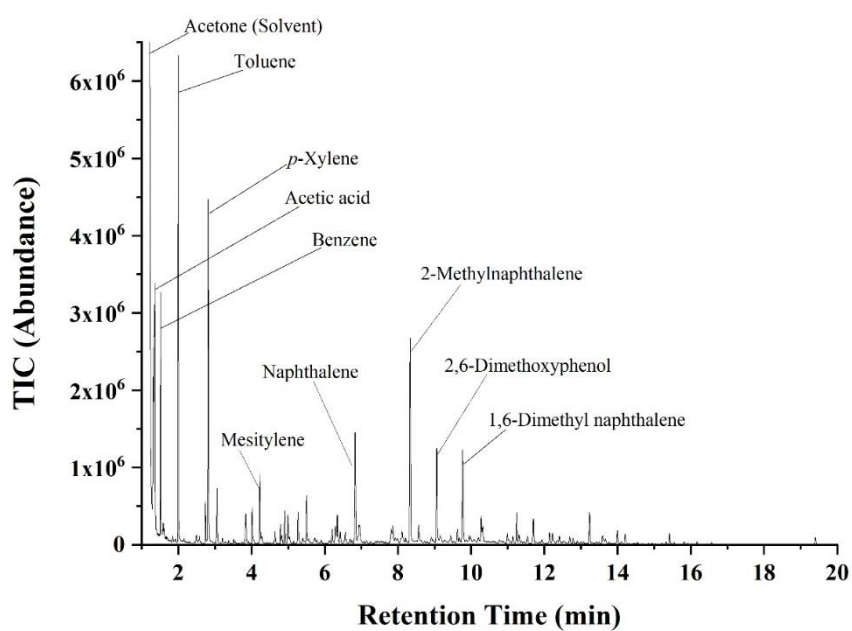
Fig. 2.10 GC/MS chromatogram of the upgraded bio-oils with 0.5wt.%Cu/HZSM-5
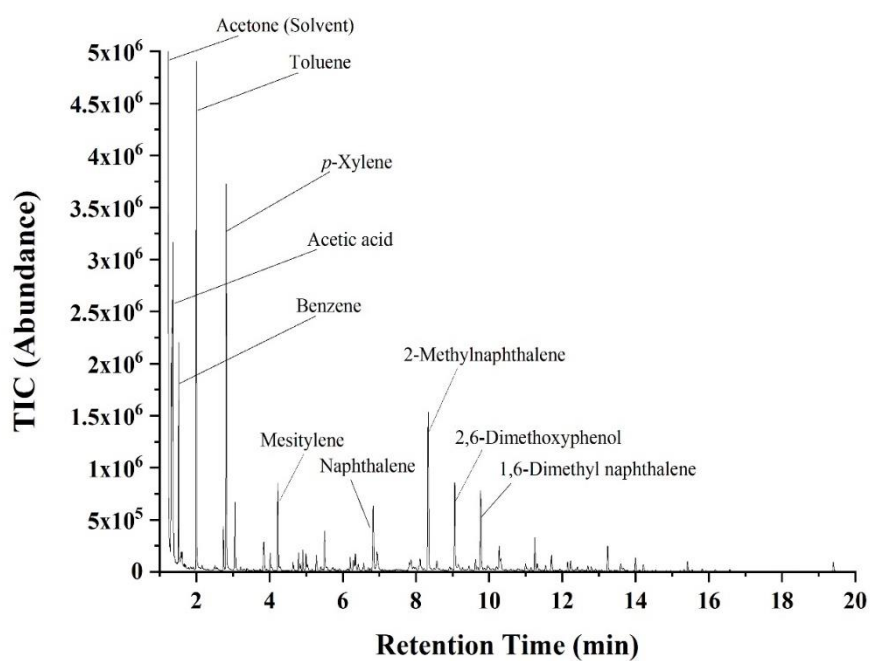
Fig. 2.11 GC/MS chromatogram of the upgraded bio-oils with 1wt.%Cu/HZSM-5
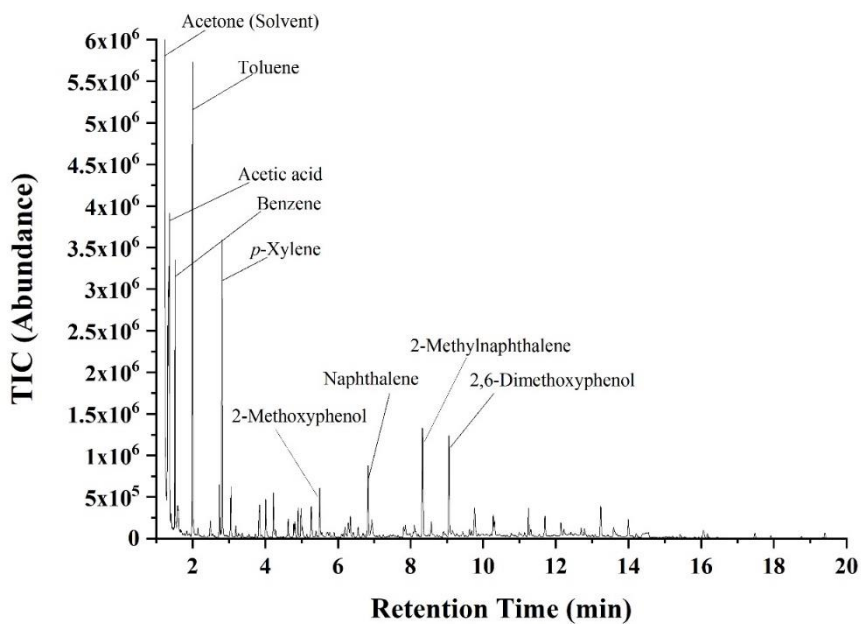
Fig. 2.12 GC/MS chromatogram of the upgraded bio-oils with 3wt.%Cu/HZSM-5
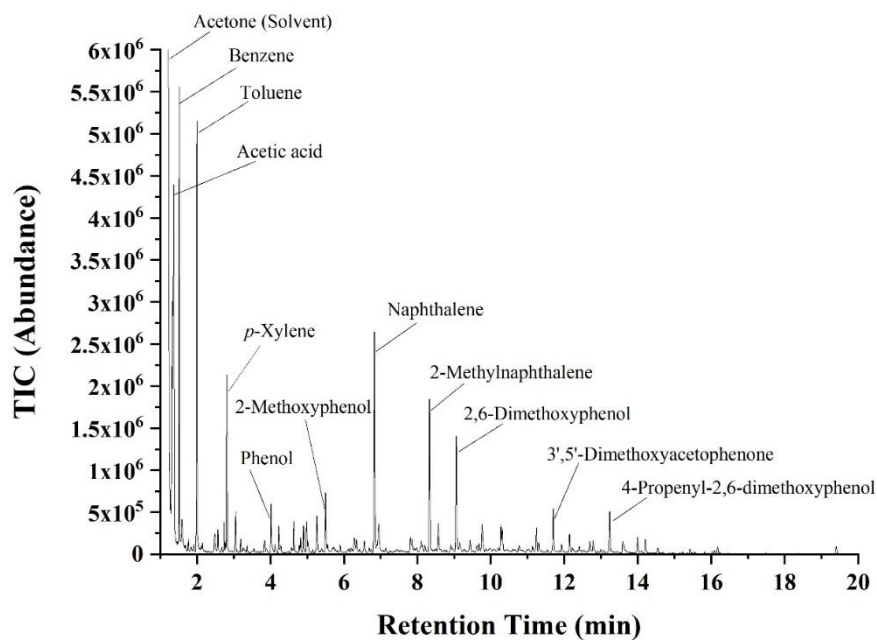
Fig. 2.13 GC/MS chromatogram of the upgraded bio-oils with 5wt.%Cu/HZSM-5
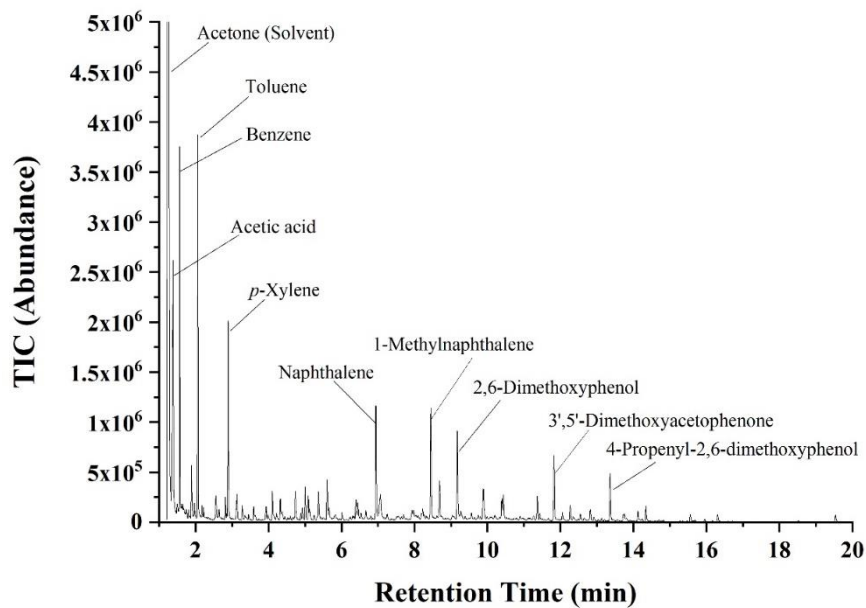
Fig. 2.14 GC/MS chromatogram of the upgraded bio-oil with the 1st reused 0.5wt.%Cu/HZSM-5 without regeneration
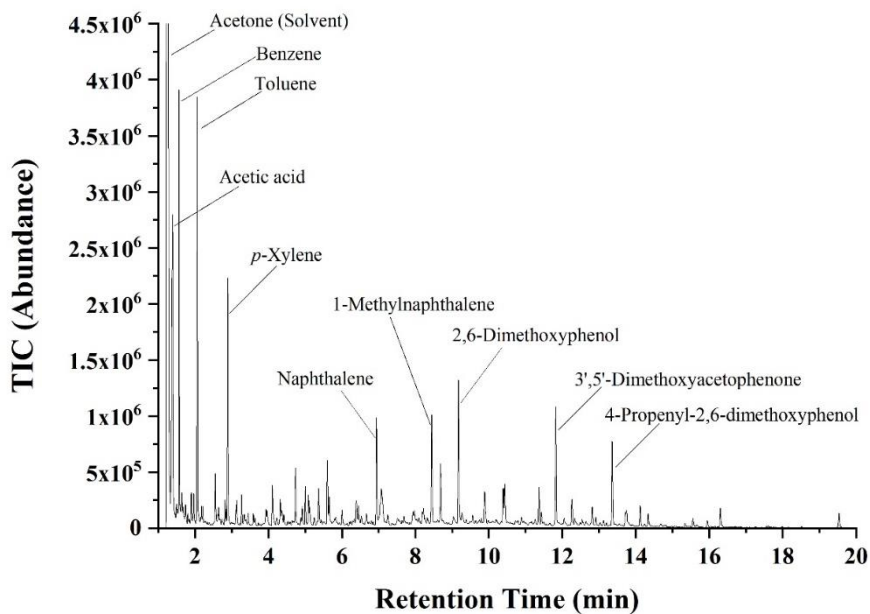
Fig. 2.15 GC/MS chromatogram of the upgraded bio-oils with the 2nd reused 0.5wt.%Cu/HZSM-5 without regeneration
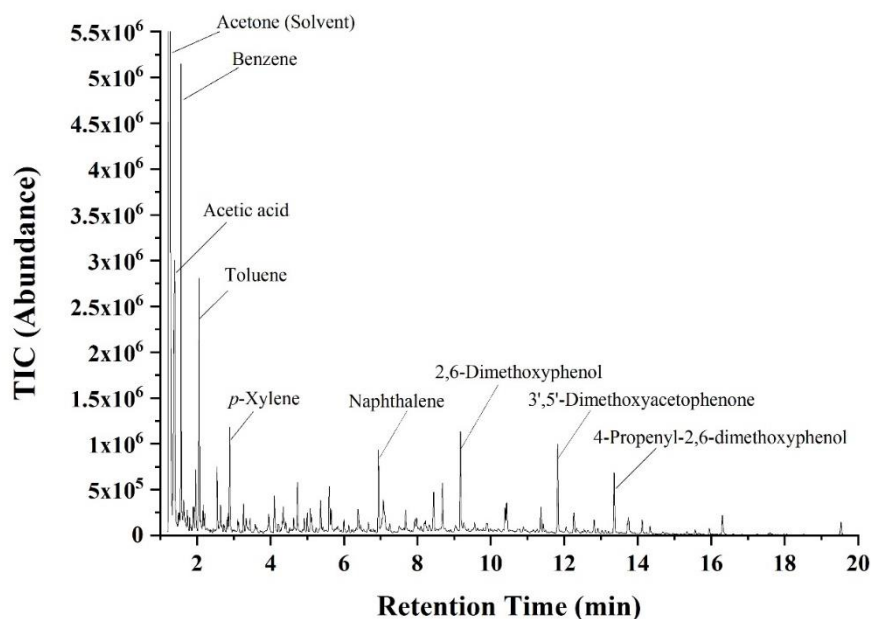
Fig. 2.16 GC/MS chromatogram of the upgraded bio-oil with the 3rd reused 0.5wt.%Cu/HZSM-5 without regeneration
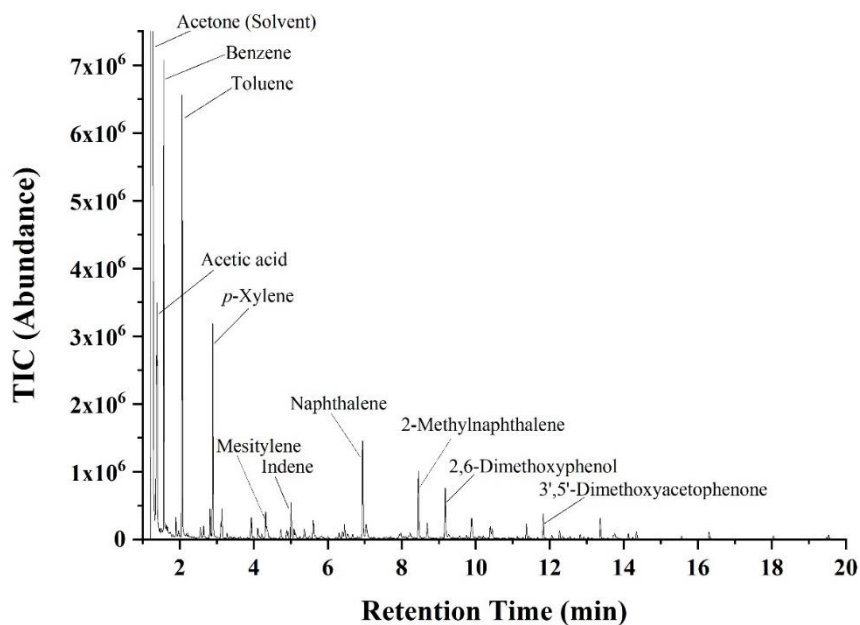
Fig. 2.17 GC/MS chromatogram of the upgraded bio-oils with the 4th reused 0.5wt.%Cu/HZSM-5 with regeneration

2.3.3 Reusability and regeneration of spent zeolites

Figs. 2.18(a) and **(b)** show the reusability and regeneration property of 0.5%Cu/HZSM-5 with the best catalytic performance, which was tested for 4 cycles in the same condition after the testing for the fresh catalyst. The spent catalyst was reused from the first to the third reuse cycle without the regeneration while the catalyst was recovered by a facile calcining at 650 °C for 30 minutes in the air before testing in the fourth cycle. Obviously, after the fresh catalyst was used for the catalytic upgrading reaction without regeneration, a significant decrease in the relative amount of aromatic hydrocarbons from 73.2% (Fresh) to 57.1% (first reuse cycle) was observed and continuously decreased with the increasing number of cycles until 35.3% in the third cycle. Herein, since the coke amount was accumulated in each cycle in the case without the regeneration (**Table 2.5**). It can be seen that the coke increasing extent decreased with the increase on the reuse cycle since some active sites should be covered by the deposited carbon species on the catalyst surface, which decreased the cracking of bio-oil components. The increased accumulation of coke on the catalyst in the reuse cycles decreased should cause the deactivation of the catalyst, thereby decreasing the aromatic selectivity and yield. Besides, compared to the parent HZSM-5, more coke was formed on the 0.5%Cu/HZSM-5 with the increased acidity. However, when the spent catalysts after the third reusing cycle was calcined and tested, the activity was almost recovered to the level of the fresh catalyst with a relative amount for the aromatic hydrocarbons of 73.4% and the high yield of 48.9 mg/g-biomass (d.a.f) for specific aromatic hydrocarbon (**Fig. 2.18(a)**). This indicated that the activity of spent 0.5%Cu/HZSM-5 can be simply recovered by the facile calcination in the air for a short time.
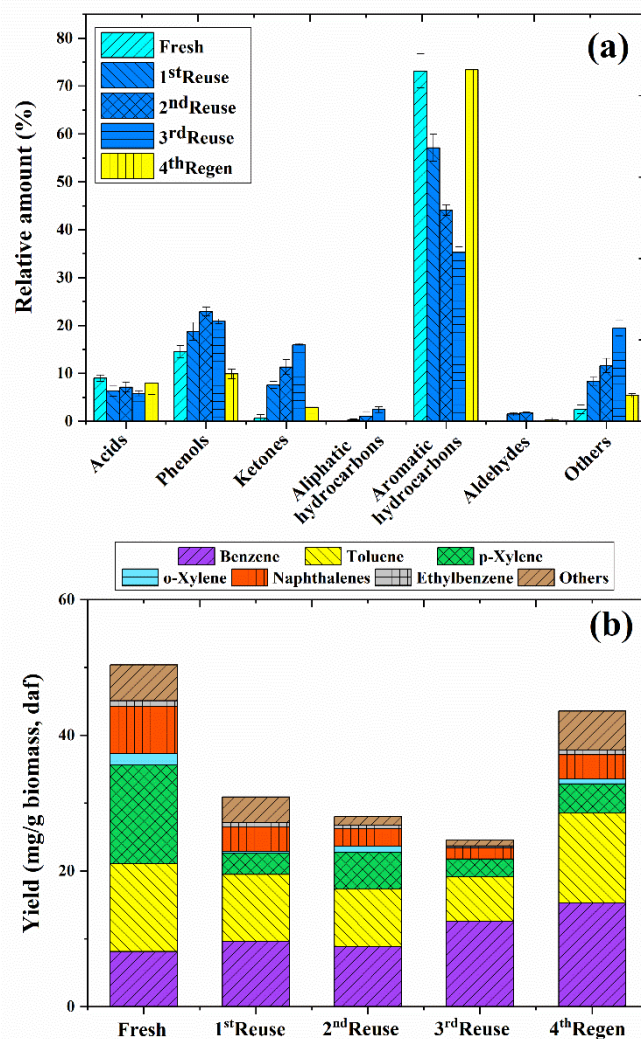
Fig. 2.18 Reusability and regeneration performance of 0.5%Cu/HZSM-5 catalyst

2.4 Conclusions

Cu modified HZSM-5 catalysts with the appropriate Cu loading amount were successfully prepared using the wet impregnation method and applied for the *in-situ* bio-oil upgrading. 0.5wt.% of Cu loading on the HZSM-5 resulted in the highest conversion of pyrolytic vapors to the aromatic hydrocarbons with a relative amount of 73.2% and a yield of specific aromatic hydrocarbons (mainly including BTX) as high as 56.5 mg/g-biomass (d.a.f), which were much higher than those based on the parent HZSM-5 (55.0% and 26.0 mg/g-biomass (d.a.f)). It should be attributed to the most suitable acidity and best textural structure. In addition, although Cu doping resulted in an increased amount of coke during the deoxygenation process

due to the promoting of a series of condensation and polymerization reactions accompanying the deoxygenation, cracking, and aromatization, the deactivated Cu/HZSM-5 catalysts was easily recovered by the simple calcination in the air for a short time.

References

[1] D. Mohan, C.U. Pittman, P.H. Steele, Pyrolysis of wood/biomass for bio-oil a critical review, Energy Fuels, 20 (2006) 848-889.

[2] F. Abnisa, W.M.A. Wan Daud, A review on co-pyrolysis of biomass: an optional technique to obtain a high-grade pyrolysis oil, Energy Convers. Manage., 87 (2014) 71-85.

[3] E.F. Iliopoulou, K.S. Triantafyllidis, A.A. Lappas, Overview of catalytic upgrading of biomass pyrolysis vapors toward the production of fuels and high-value chemicals, Wiley Interdiscip. Rev. Energy Environ, 8 (2019).

[4] T. Kan, V. Strezov, T.J. Evans, Lignocellulosic biomass pyrolysis: a review of product properties and effects of pyrolysis parameters, Renewable Sustainable Energy Rev., 57 (2016) 1126-1140.

[5] T. Bhaskar, A. Pandey, Advances in thermochemical conversion of biomass—introduction, in: recent advances in thermo-chemical conversion of biomass, 2015, pp. 3-30.

[6] G. Lv, S. Wu, G. Yang, J. Chen, Y. Liu, F. Kong, Comparative study of pyrolysis behaviors of corn stalk and its three components, J. Anal. Appl. Pyrolysis, 104 (2013) 185-193.

[7] R. Kumar, V. Strezov, E. Lovell, T. Kan, H. Weldekidan, J. He, S. Jahan, B. Dastjerdi, J. Scott, Enhanced bio-oil deoxygenation activity by Cu/zeolite and Ni/zeolite catalysts in combined in-situ and ex-situ biomass pyrolysis, J. Anal. Appl. Pyrolysis, 140 (2019) 148-160.

[8] J.-P. Zhao, J.-P. Cao, F. Wei, X.-B. Feng, N.-Y. Yao, Y.-P. Zhao, M. Zhao, X.-Y. Zhao, J.-L. Zhang, X.-Y. Wei, Catalytic reforming of lignite pyrolysis volatiles over sulfated HZSM-5: Significance of the introduced extra-framework Al species, Fuel, 273 (2020).

[9] J.-X. Wang, J.-P. Cao, X.-Y. Zhao, T.-L. Liu, F. Wei, X. Fan, Y.-P. Zhao, X.-Y. Wei, Study

on pine sawdust pyrolysis behavior by fast pyrolysis under inert and reductive atmospheres, J. Anal. Appl. Pyrolysis, 125 (2017) 279-288.

[10] J. Adam, E. Antonakou, A. Lappas, M. Stöcker, M.H. Nilsen, A. Bouzga, J.E. Hustad, G. Øye, In situ catalytic upgrading of biomass derived fast pyrolysis vapours in a fixed bed reactor using mesoporous materials, Microporous Mesoporous Mater., 96 (2006) 93-101.

[11] N. Rahimi, R. Karimzadeh, Catalytic cracking of hydrocarbons over modified ZSM-5 zeolites to produce light olefins: a review, Appl. Catal., A, 398 (2011) 1-17.

[12] J.S. Jung, J.W. Park, G. Seo, Catalytic cracking of n-octane over alkali-treated MFI zeolites, Appl. Catal., A, 288 (2005) 149-157.

[13] D.J. Mihalcik, C.A. Mullen, A.A. Boateng, Screening acidic zeolites for catalytic fast pyrolysis of biomass and its components, J. Anal. Appl. Pyrolysis, 92 (2011) 224-232.

[14] M.S. Abu Bakar, J.O. Titiloye, Catalytic pyrolysis of rice husk for bio-oil production, J. Anal. Appl. Pyrolysis, 103 (2013) 362-368.

[15] L. Sun, X. Zhang, L. Chen, B. Zhao, S. Yang, X. Xie, Comparision of catalytic fast pyrolysis of biomass to aromatic hydrocarbons over ZSM-5 and Fe/ZSM-5 catalysts, J. Anal. Appl. Pyrolysis, 121 (2016) 342-346.

[16] C. Lorenzetti, R. Conti, D. Fabbri, J. Yanik, A comparative study on the catalytic effect of H-ZSM5 on upgrading of pyrolysis vapors derived from lignocellulosic and proteinaceous biomass, Fuel, 166 (2016) 446-452.

[17] A. Pattiya, J.O. Titiloye, A.V. Bridgwater, Fast pyrolysis of cassava rhizome in the presence of catalysts, J. Anal. Appl. Pyrolysis, 81 (2008) 72-79.

[18] Y.T. Cheng, J. Jae, J. Shi, W. Fan, G.W. Huber, Production of renewable aromatic compounds by catalytic fast pyrolysis of lignocellulosic biomass with bifunctional Ga/ZSM-5 catalysts, Angew. Chem. Int. Ed. Engl., 124 (2012) 1416-1419.

[19] N. Chaihad, S. Karnjanakom, I. Kurnia, A. Yoshida, A. Abudula, P. Reubroycharoen, G. Guan, Catalytic upgrading of bio-oils over high alumina zeolites, Renew. Energy, 136

(2019) 1304-1310.

[20] E.F. Iliopoulou, S.D. Stefanidis, K.G. Kalogiannis, A. Delimitis, A.A. Lappas, K.S. Triantafyllidis, Catalytic upgrading of biomass pyrolysis vapors using transition metal-modified ZSM-5 zeolite, Appl. Catal. B: Environ., 127 (2012) 281-290.

[21] E.F. Iliopoulou, S. Stefanidis, K. Kalogiannis, A.C. Psarras, A. Delimitis, K.S. Triantafyllidis, A.A. Lappas, Pilot-scale validation of Co-ZSM-5 catalyst performance in the catalytic upgrading of biomass pyrolysis vapours, Green Chem., 16 (2014) 662-674.

[22] S. Zhang, H. Zhang, X. Liu, S. Zhu, L. Hu, Q. Zhang, Upgrading of bio-oil from catalytic pyrolysis of pretreated rice husk over Fe-modified ZSM-5 zeolite catalyst, Fuel Process. Technol., 175 (2018) 17-25.

[23] E. Saraçoğlu, B.B. Uzun, E. Apaydın-Varol, Upgrading of fast pyrolysis bio-oil over Fe modified ZSM-5 catalyst to enhance the formation of phenolic compounds, Int. J. Hydrog. Energy, 42 (2017) 21476-21486.

[24] L. Wang, H. Lei, Q. Bu, S. Ren, Y. Wei, L. Zhu, X. Zhang, Y. Liu, G. Yadavalli, J. Lee, S. Chen, J. Tang, Aromatic hydrocarbons production from ex situ catalysis of pyrolysis vapor over Zinc modified ZSM-5 in a packed-bed catalysis coupled with microwave pyrolysis reactor, Fuel, 129 (2014) 78-85.

[25] H.J. Park, H.S. Heo, J.-K. Jeon, J. Kim, R. Ryoo, K.-E. Jeong, Y.-K. Park, Highly valuable chemicals production from catalytic upgrading of radiata pine sawdust-derived pyrolytic vapors over mesoporous MFI zeolites, Appl. Catal. B: Environ., 95 (2010) 365-373.

[26] S. Vichaphund, D. Aht-ong, V. Sricharoenchaikul, D. Atong, Catalytic upgrading pyrolysis vapors of Jatropha waste using metal promoted ZSM-5 catalysts: An analytical PY-GC/MS, Renew. Energy, 65 (2014) 70-77.

[27] Y. Zheng, F. Wang, X. Yang, Y. Huang, C. Liu, Z. Zheng, J. Gu, Study on aromatics production via the catalytic pyrolysis vapor upgrading of biomass using metal-loaded modified H-ZSM-5, J. Anal. Appl. Pyrolysis, 126 (2017) 169-179.

[28] S. Thangalazhy-Gopakumar, S. Adhikari, R.B. Gupta, Catalytic Pyrolysis of Biomass over H+ZSM-5 under Hydrogen Pressure, Energy Fuels, 26 (2012) 5300-5306.

[29] C. Li, J. Ma, Z. Xiao, S.B. Hector, R. Liu, S. Zuo, X. Xie, A. Zhang, H. Wu, Q. Liu, Catalytic cracking of Swida wilsoniana oil for hydrocarbon biofuel over Cu-modified ZSM-5 zeolite, Fuel, 218 (2018) 59-66.

[30] W.B. Widayatno, G. Guan, J. Rizkiana, J. Yang, X. Hao, A. Tsutsumi, A. Abudula, Upgrading of bio-oil from biomass pyrolysis over Cu-modified β-zeolite catalyst with high selectivity and stability, Appl. Catal. B: Environ., 186 (2016) 166-172.

[31] M. Balat, M. Balat, E. Kırtay, H. Balat, Main routes for the thermo-conversion of biomass into fuels and chemicals. Part 1: Pyrolysis systems, Energy Convers. Manag., 50 (2009) 3147-3157.

[32] F. Bin, C. Song, G. Lv, J. Song, S. Wu, X. Li, Selective catalytic reduction of nitric oxide with ammonia over zirconium-doped copper/ZSM-5 catalysts, Appl. Catal. B: Environ., 150-151 (2014) 532-543.

[33] S. Vichaphund, D. Aht-ong, V. Sricharoenchaikul, D. Atong, Catalytic upgrading pyrolysis vapors of Jatropha waste using metal promoted ZSM-5 catalysts: An analytical PY-GC/MS, Renew. Energy, 65 (2014) 70-77.

[34] S. Karnjanakom, A. Bayu, P. Xiaoketi, X. Hao, S. Kongparakul, C. Samart, A. Abudula, G. Guan, Selective production of aromatic hydrocarbons from catalytic pyrolysis of biomass over Cu or Fe loaded mesoporous rod-like alumina, RSC Adv., 6 (2016) 50618-50629.

[35] A. Veses, B. Puértolas, M.S. Callén, T. García, Catalytic upgrading of biomass derived pyrolysis vapors over metal-loaded ZSM-5 zeolites: Effect of different metal cations on the bio-oil final properties, Microporous Mesoporous Mater., 209 (2015) 189-196.

[36] J.D. Adjaye, N.N. Bakhshi, Production of hydrocarbons by catalytic upgrading of a fast pyrolysis bio-oil. Part I: Conversion over various catalysts, Fuel Process. Technol., 45

(1995) 161-183.

[37] H. Persson, I. Duman, S. Wang, L.J. Pettersson, W. Yang, Catalytic pyrolysis over transition metal-modified zeolites: A comparative study between catalyst activity and deactivation, J. Anal. Appl. Pyrolysis, 138 (2019) 54-61.

[38] J.S. Jung, T.J. Kim, G. Seo, Catalytic cracking of n-octane over zeolites with different pore structures and acidities, Korean J. Chem. Eng., 21 (2004) 777-781.

[39] M. Guisnet, P. Magnoux, Organic chemistry of coke formation, Appl. Catal. A Gen., 212 (2001) 83-96.

[40] X.-Y. Ren, J.-P. Cao, X.-Y. Zhao, Z. Yang, Y.-J. Wang, Q. Chen, M. Zhao, X.-Y. Wei, Catalytic conversion of lignite pyrolysis volatiles to light aromatics over ZSM-5: SiO_2/Al_2O_3 ratio effects and mechanism insights, J. Anal. Appl. Pyrolysis, 139 (2019) 22-30.

[41] S. Karnjanakom, G. Guan, B. Asep, X. Hao, S. Kongparakul, C. Samart, A. Abudula, Catalytic upgrading of bio-oil over Cu/MCM-41 and Cu/KIT-6 Prepared by β-cyclodextrin-assisted coimpregnation method, J. Phys. Chem. C, 120 (2016) 3396-3407.

[42] A.N. Kay Lup, F. Abnisa, W.M.A. Wan Daud, M.K. Aroua, A review on reactivity and stability of heterogeneous metal catalysts for deoxygenation of bio-oil model compounds, J. Ind. Eng. Chem., 56 (2017) 1-34.

[43] S. Karnjanakom, G. Guan, B. Asep, X. Du, X. Hao, J. Yang, C. Samart, A. Abudula, A green method to increase yield and quality of bio-oil: ultrasonic pretreatment of biomass and catalytic upgrading of bio-oil over metal (Cu, Fe and/or Zn)/γ-Al_2O_3, RSC Adv., 5 (2015) 83494-83503.

[44] D. Shen, W. Jin, J. Hu, R. Xiao, K. Luo, An overview on fast pyrolysis of the main constituents in lignocellulosic biomass to valued-added chemicals: Structures, pathways and interactions, Renew. Sustain. Energy Rev., 51 (2015) 761-774.

[45] R. French, S. Czernik, Catalytic pyrolysis of biomass for biofuels production, Fuel

Process. Technol., 91 (2010) 25-32.

[46] W. Wang, Y. Shi, Y. Cui, X. Li, Catalytic fast pyrolysis of cellulose for increasing contents of furans and aromatics in biofuel production, J. Anal. Appl. Pyrolysis, 131 (2018) 93-100.

[47] J.-S. Kim, G.-G. Choi, Pyrolysis of Lignocellulosic Biomass for Biochemical Production, in: Waste Biorefinery, 2018, pp. 323-348.

[48] Z. Zhang, L. Liu, B. Shen, C. Wu, Preparation, modification and development of Ni-based catalysts for catalytic reforming of tar produced from biomass gasification, Renew. Sustain. Energy Rev., 94 (2018) 1086-1109.

Chapter 3 Preparation of various hierarchical HZSM-5 based catalysts for *in-situ* fast upgrading of bio-oil

3.1 Introduction

Various aromatic compounds such as benzene, toluene, and xylene (BTX), naphthalene and ethylbenzene are in great demand in the world market [1]. More than 85% of aromatics production traditionally depends on the catalytic reforming of petroleum resources. With a shortage of fossil resources and a continuously growing demand of aromatics, production of aromatics from alternative and environmentally friendly resources has received widespread attention [2]. Biomass is a renewable and abundantly available resource that is considered an attractive feedstock for producing liquid biofuels as well as valuable chemicals such as aromatics [3-5]. Fast pyrolysis is widely used for the production of liquid product (bio-oil) from biomass under the oxygen-free condition, atmospheric pressure and moderate temperatures (450–600 °C) [6,7]. As the crude oil, the bio-oil can be used as an important intermediate feedstock for the chemical and biofuel production. However, different from the crude oil, a high amount of oxygenated compounds are contained in the bio-oil so that it has low calorific value with high viscosity, high density, corrosive nature, thermal instability, extreme ignition delay, and incomplete volatility [8-10]. To improve the quality of bio-oil, catalytic cracking is an effective way since it can deoxygenate to produce valuable compounds suited for fuel through the removal of oxygen [11-13]. Zeolites such as beta, zeolite Y, and ZSM-5 have been used extensively for the catalytic upgrading of bio-oils since their pore structure and acidity can control the composition and distribution of upgraded bio-oil [9,14]. Especially, ZSM-5 has well-defined microporous structure, high hydrothermal stability, and strong acidity, which exhibited high activity and high selectivity towards aromatic hydrocarbons [15-17]. However, the micropores of ZSM-5 zeolite usually lead to slow

diffusion of molecules with different sizes including reactants, intermediates and products, which seriously restrict its catalytic application for the upgrading of bio-oil [18]. In particular, the mass transfer limitations would reduce the access of the pyrolysis vapor to the acid sites, resulting in a low catalyst utilization with less desirable products. In order to overcome the steric limitations in the micropores of ZSM-5, mesopores can be generated in the ZSM-5 to reduce the diffusion path lengths and meanwhile increase the external surface area [18-20]. Recently, hierarchically structured zeolites with the generated mesopores have been widely investigated [21, 22]. The occurrence of mesoporosity facilitates molecular diffusion in the zeolites and allows the reagents to have better accessibility towards the active sites in the zeolite structure, removing steric limitations and shortening the intracrystalline diffusion pathways [21]. Desilication is an effective way to obtain mesopores in the ZSM-5 zeolite, and maintain suitable Brønsted acidity, which can increase the yield of aromatic hydrocarbons when used for the upgrading of bio-oil [23]. To date, alkaline agents such as NaOH, Na_2CO_3, tetrapropylammonium hydroxide (TPAOH) and tetrabutylammonium hydroxide (TBAOH) are widely used for the fabrication of hierarchical zeolites [24-26]. By using NaOH as an alkaline medium, the silicon in the framework can be extracted to create mesopores [27]. However, in this case, the extraction of silicon is too fast and strong, resulting in the uncontrollable formation of mesopores and the loss of a certain amount of micropores and acid sites in the zeolite structure. Meanwhile, some organic quaternary ammonium hydroxides such as TPAOH and TBAOH were also used for the desilication, however, they are less reactive towards silicon dissolution than inorganic hydroxide. Thus, to tailor the degree of mesoporosity, NaOH was combined with the organic base such as the TPAOH and TBAOH for the desilication [18, 19]. Herein, the addition of the organic base can maintain more acid sites and increase the surface area in the final hierarchical zeolites than that using NaOH alone. It should be noted that the acidity and surface area have great influences on the catalytic upgrading process [28]. To date, the hierarchical zeolites with highly mesoporous structure

prepared by using NaOH combined with an organic base have been applied for the conversion of methanol to hydrocarbons and N_2O decomposition [19, 29], however, the *in-situ* catalytic upgrading of bio-oil derived from fast pyrolysis of biomass over such zeolite catalysts has not yet been reported. In this case, the generated bio-oil from the real biomass always passes through the catalyst layer rapidly. It should be important to achieve fast catalytic upgrading of the bio-oil over the hierarchical zeolites. Moreover, the hierarchical zeolites prepared based on different parent zeolites could lead to different properties. Thus, it should be important to achieve fast catalytic upgrading of the bio-oil over various hierarchical zeolites. In addition, it is reported that the hierarchical zeolites modified by metals such as Cu and Mg can enhance the deoxygenation process and lead to an increase in the aromatic hydrocarbon yield and a decrease in the coke formation on the catalysts [30, 31].

In this study, the desilication of HZSM-5 to fabricate hierarchical HZSM-5 was performed by using the fixed concentration of NaOH with the addition of different concentrations of TPAOH, and the obtained hierarchical HZSM-5 catalysts were applied for the catalytic upgrading of bio-oils derived from the fast pyrolysis of sunflower stalk. Physicochemical properties of the obtained catalysts were characterized, and the catalytic upgrading performance related to the yield of aromatic hydrocarbons was investigated. To solve the coking problem and increase the aromatic hydrocarbons production, the hierarchical HZSM-5 was also modified by various metals including Cu, Mg and Ag. It is expected to enhance the basic knowledge of hierarchical zeolite for *in-situ* catalytic upgrading of bio-oil from the fast pyrolysis of biomass.

3.2 Experimental

3.2.1 Material

Sunflower stalk was collected from Aomori, Japan. The collected sample was dried at 110 °C and crushed with a grinder, and then sieved into a particle size of 0.5-1.0 mm. The results on the proximate and ultimate analyses for the samples were shown in our previous work [32].

NaOH, TPAOH, Mg(NO$_3$)$_2$•6H$_2$O, Cu(NO$_3$)$_2$•3H$_2$O and AgNO$_3$ were purchased from Wako, Japan. HZSM-5 (Si/Al of 40) zeolite powder was provided by TOSOH Corp., Japan.

3.2.2 Hierarchical HZSM-5 zeolite preparation

The catalysts were prepared by desilication of commercial HZSM-5 in aqueous base solutions. The conditions were optimized according to the acidity (**Table 3.1**) as well as textural property (**Table 3.2**) and the selectivity and yield of aromatic hydrocarbon as shown in **Fig. 3.1**. The three typical hierarchical HZSM-5 zeolites in **Tables 3.1** and **3.2** were prepared by adding 10 g of HZSM-5 zeolite powders into 100 mL of 0.2 M NaOH solution, 100 mL of mixed solution composed of 50 mL of 0.2 M NaOH and 50 mL of 0.25 M TPAOH, and 100 mL of 0.5 M pure TPAOH, respectively, under stirring at 80 ºC for 1 h. After the treatment, the solids were collected by filtration, washed with distilled water until the neutral pH, and then dried at 110 °C overnight. Thereafter, the alkaline-treated zeolites were dispersed in 200 mL of 1 M NH$_4$NO$_3$ at 80 °C for 4 h, collected by filtration, and finally calcinated at 550 °C for 4 h. Herein, the parent zeolite is denoted as HZ5, the zeolites treated by NaOH, mixture of NaOH and TPAOH, and TPAOH are denoted as HZ5-0.2M, HZ5-(0.2M+ 0.25TP) and HZ5-0.5TP, respectively. The metal-modified hierarchical HZSM-5 zeolites were prepared by the wet impregnation method. Firstly, metal nitrates with the calculated metal-loading amounts (i.e., 0.1, 0.25, 0.5 and 1 wt.%) were dissolved in deionized water and the HZ5-(0.2M+0.25TP) powders with the best catalytic performance were impregnated in it for 10 h with stirring, followed by drying at 110 °C for 12 h and calcined at 550 °C for 4 h. Prior to the performance testing, the obtained catalyst powders were pressed, crushed, and sieved to a particle size in the range of 0.5-1.0 mm. The preparation of each sample was repeated for at least 3 times.

Table 3.1 Acidity of hierarchical HZ5 catalysts

Catalyst	Acidity (mmol/g, low temp)	Acidity (mmol/g, high temp)	Total acidity (mmol/g)
HZ5	0.58	0.67	1.25
HZ5-0.1N	0.48	0.43	0.90
HZ5-0.2N	0.48	0.39	0.87
HZ5-0.35N	0.30	0.23	0.53
HZ5-(0.2N+0.1TP)	0.45	0.56	1.01
HZ5-(0.2N+0.25TP)	0.52	0.43	0.95
HZ5-(0.2N+0.5TP)	0.38	0.39	0.77
HZ5-0.5TP	0.48	0.43	0.91

Table 3.2 Textural properties of hierarchical HZ5 catalysts

Catalyst	Si/Al molar ratio on Surface[a]	S_{BET} (m^2/g)	S_{micro} (m^2/g)	V_{total} (cm^3/g)	V_{micro} (cm^3/g)	Average pore size (nm)
HZ5	22.0	325.9	307.7	0.18	0.15	2.97
HZ5-0.1N	16.0	323.1	296.4	0.19	0.14	3.12
HZ5-0.2N	16.6	319.1	281.5	0.20	0.13	3.95
HZ5-0.35N	12.9	390.5	321.9	0.33	0.16	4.01
HZ5-(0.2N+0.1TP)	21.1	341.4	305.1	0.21	0.15	3.71
HZ5-(0.2N+0.25TP)	21.6	359.9	317.4	0.22	0.15	3.78
HZ5-(0.2N+0.5TP)	17.3	379.8	284.7	0.23	0.14	3.92
HZ5-0.5TP	18.3	292.6	271.7	0.17	0.14	3.14
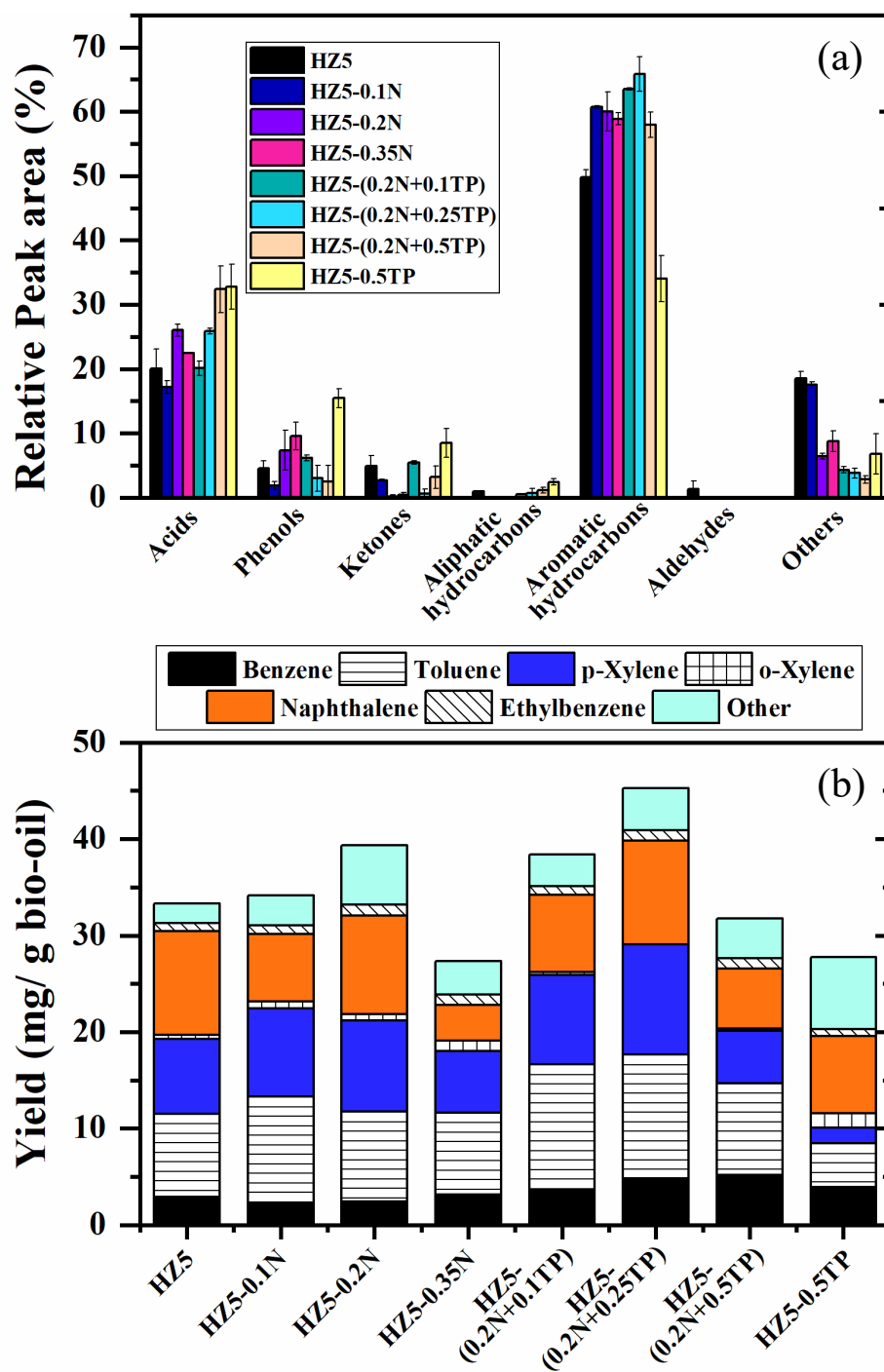
Fig. 3.1 Chemical compositions of the upgraded bio-oils upgraded with hierarchical HZSM-5 catalysts (a) and the selectivity towards specific aromatic hydrocarbons in the upgraded bio-oils (b)

3.2.3 Characterizations

N$_2$-adsorption/desorption isotherms were measured on an automated surface area and pore size analyzer (NOVA 4200e, Quantachrome Instruments, USA) at the liquid nitrogen temperature (77 K). Prior to analysis, the catalysts were vacuum-degassed at 200 °C for 2 h. The multipoint Brunauer–Emmett–Teller method (BET) in a pressure range of 0.05-0.30 P/P$_0$ was used to determine the total specific surface area. The total pore volume was estimated from the N$_2$ amount adsorbed at P/P$_0$=0.99 and converted it to liquid N$_2$ volume. The micropore surface area (S$_{micro}$) and volume (V$_{micro}$) of micropores were calculated using t-plot method while the external specific surface area (S$_{external}$) and the mesopore volume (V$_{meso}$) were calculated by difference. The pore size distribution and the average pore size were determined by density functional theory (DFT) method with the desorption branch.

The acidity and acid site distribution of the catalysts were determined by NH$_3$-Temperature Programmed Desorption method (NH$_3$-TPD) (Belcat, Japan), in which the catalyst was heated from room temperature to 700 °C with a heating rate of 10 °C/min in a 50 cm^3/min of helium flow rate and held at that temperature for 1 h. Then the catalyst was cooled down to 120 °C and stabilized for 10 min. Thereafter, NH$_3$ stream was introduced into the measurement cell for 1 h. To ensure the single layer adsorption of NH$_3$ on the catalyst surface, the catalyst was then flushed with 50 cm^3/ min of helium stream for 1 h to remove the physically adsorbed NH$_3$. After stabilization at 120 °C for 10 min, NH$_3$ desorption was carried out until 800 °C with a heating rate of 10 °C/min in 30 cm^3/min of helium stream and held for 10 min. Herein, the NH$_3$ desorption peak, which expresses the amount of the desorbed ammonia, was detected using a thermal conductivity detector (TCD), and converted using the calibration data and presented as a function of temperature.

XRD measurement of catalysts was conducted by an X-ray Diffractometer (Smartlab, Rigaku, Japan). The scanning angle (2θ) was ranged from 10º to 90º using a filtered Cu-Kα radiation (λ=0.1542) with a scanning step of 0.02º. The relative crystallinity of parent HZ5 was set to

100% and calculated the relative crystallinity of hierarchical HZSM-5 catalysts by comparing the sum of peak intensities between $2\theta = 0\text{-}80^\circ$ from the XRD pattern with that of the parent HZ5. The existence of metal species on the catalysts was investigated using a scanning electron microscopy (SEM, SU8010, Hitachi, Japan) coupled with an energy dispersive X-ray detector (EDX). The effect of alkaline treatment at different conditions on the porous structure of the hierarchical zeolite was investigated by a transmission electron microscopy (TEM).

3.2.4 In-situ catalytic upgrading of bio-oil

In-situ catalytic upgrading of bio-oil was performed in a quartz fixed-bed reactor placed inside an infrared furnace (VHT series, ULVAC, Japan) with a N_2 flow as the carrier gas from the upper to lower side direction, in which 0.5 g of sunflower stalk powder (the upper side) and 0.5 g of catalysts (the lower side) were separately placed in the middle of the reactor with quartz wool. Before heating the reactor, the reactor was purged with a N_2 flow for 10 min. Then, the reactor was rapidly heated to 500 ºC with a heating rate of 1000 ºC/min, and held at that temperature for 5 min. The obtained bio-oil carried by the N_2 flow was condensed with cold acetone and collected for the analysis [32]. The non-condensable gases were collected in a gasbag. The reliability of experimental data was confirmed by repeating the experiments for at least three times. The gas chromatography/mass spectrometry (GC-MS) (GC-2010 Plus for GC, QP-2010 Ultra for MS, Shimadzu Japan) equipped with an Ultra ALLOY+ −5 capillary column was used to determine the composition of bio-oil. Compound identification was carried out using the NIST 05 (National Institute of Standards and Technology) mass spectrum library. In this analysis, only the light components with a boiling point below 300 °C were detected. Specific aromatic hydrocarbons were used as the external standards to determine the yields of main aromatic hydrocarbon products. The amount of coke deposited on the spent catalysts was determined from the difference in the weight of the catalyst before and after the calcination at 650 °C in air for 30 min in a muffle furnace. The gas analysis was implemented on a gas chromatography (Agilent 7890A GC system, USA) equipped with a thermal

conductivity detector (TCD) and 3 packed columns (1 molecular sieve 5A column +1 HayeSep Q column +1 molecular sieve 5A column). A standard gas mixture with constant concentrations of CO_2, CO, N_2, H_2, and CH_4 was used for the calibration of gaseous products. The water content in the bio-oil was determined by a Karl-Fischer titrator (MKS-500, KEM, Japan).

3.3 Results and discussion

3.3.1 Desilication mechanism

Since the desilication of HZSM-5 zeolite is the extraction of Si from the structure. In NaOH solution containing both Na^+ and OH^- ions, Si extraction could begin from the outer surface area of HZSM-5 by the attack of OH^- ions on the Si species at first, then, the Na^+ ions are also absorbed to reach a balance with the negative charge. As such, the desilication occurs continuously without any protection, resulting in mesopores with the further attacking by OH^- ions on the Si species inside the HZSM-5 bulk body so that the mesopores are formed in the interior of HZSM-5 crystals and the pore size becomes larger and larger with the increase in the desilication time. Thus, as illustrated in **Scheme3.1(a)**, the desilication is difficult to be controlled in the case using NaOH solution. In comparison, with the addition of suitable TPAOH into the NaOH solution, the total OH^- ion content in the solution is from both NaOH and TPAOH, but the alkalinity is decreased to some extent. More importantly, this mixed solution has two different Na^+ and TPA^+ cations, and the nature of the organic base is different from that of the inorganic base in the terms of steric hindrance, solvation, and stability [33], which could result in a different desilication pathway. That is, when these two cations are absorbed on the outer surface of the HZSM-5 to balance the negative charge, the extraction of Si from OH^- ion attacking should more easily occur near the Si sites adsorbed with Na^+ cations because Na^+ cation has smaller size and less steric hindrance, which cannot hinder the attacking by the OH^- ions. In contrast, TPA^+ cation has a large size, making it better protect the adsorbed Si sites from the attacking by the OH^- ions. Also, the hydrophobicity of the long

hydrocarbon chain of TPA$^+$ cation is benefit for the propyl groups to protect the hydrophobic silicate [33]. As such, the parts with the absorbed TPA$^+$ cations should be more stable than those absorbed by Na$^+$ cations [33]. Thus, the Si extraction starts from the absorbed Na$^+$ cation areas, and by adjusting the amount of TPAOH in the solution, the formation of suitable mesopores in the HZSM-5 becomes controllable. As illustrated in **Scheme3.1(b)**, when small mesopores are formed on the outer surface by the attacking of OH$^-$ ions, some TPA$^+$ cations will enter the inside with the Na$^+$ cations to balance the negative charge but they can prevent the increasing Si extraction by the OH$^-$ ion attacks, resulting in that the desilication of the HZSM-5 becomes more controllable [19]. In the case of using only TPAOH solution, a large amount of TPA$^+$ cations balance the negative charges on almost all surface areas. This causes excessive protection to inhibit the desilication as well as the formation of large mesopores. As illustrated in **Scheme3.1(c)**, after HZSM-5 is treated by using TPAOH alone, only some mesopores with small sizes could be formed on the outer surface of zeolite crystals, which could decrease the external surface area and mesopore volume [19].

TPA+ ⌇⌇· ● Na+ ▲ OH-

HZ5-0.2N   **HZ5-(0.2N+0.25TP)**   **HZ5-0.5TP**

(a)   **(b)**   **(c)**
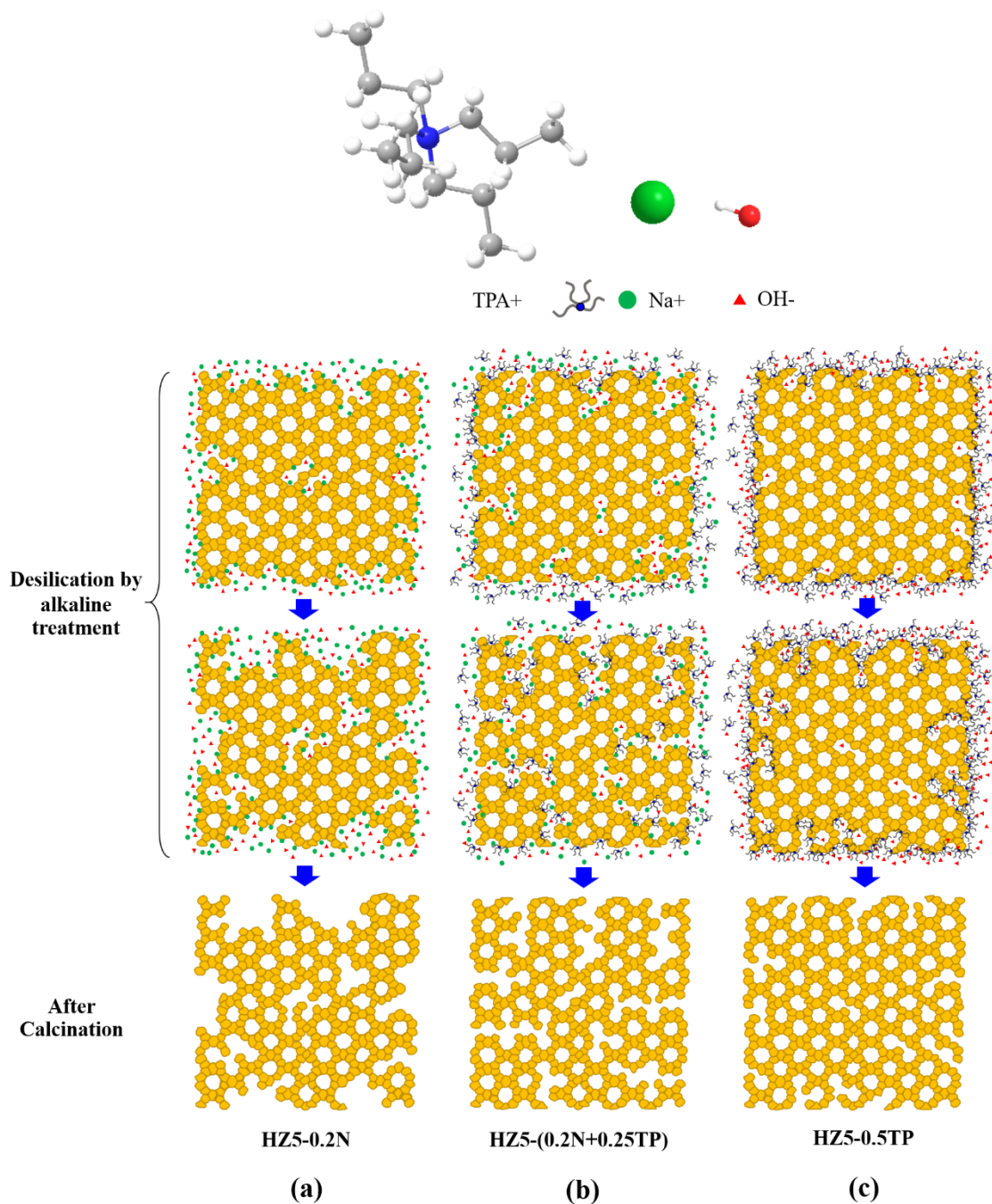
Scheme 3.1 The desilication mechanism of the hierarchical HZSM-5 using various alkaline solutions

3.3.2 Characterizations of catalysts

Fig. 3.2 shows the XRD patterns of the prepared hierarchical HZSM-5 zeolites and the parent HZ5. One can see that all the catalysts retained the typical framework of HZ5 since the characterized diffraction peaks at 2θ of 12-18° and 20-26° remained the same as those of the

HZ5. It suggested that the crystalline structure of HZ5 was maintained after the desilication. However, as shown in **Table 3.3**, the HZ5-0.2M exhibited lower relative crystallinity of 87.2%. It should be attributed to the severe desilication by the strong alkaline solution since it could result in the collapse of zeolite framework. In contrast, with the assistance of TPAOH, the obtained hierarchical HZSM-5 zeolite of HZ5-(0.2M+0.25TP) had higher relative crystallinity, indicating that the existence of TPAOH helped to maintain the framework structure of zeolite [19]. In addition, the HZSM-5 zeolite treated by 0.5 M TPAOH only decreased the crystallinity a little due to the weak alkalinity.

Table 3.3 The relative crystallinity of hierarchical HZSM-5 catalysts to the parent HZSM-5 catalyst

	HZ5	HZ5-0.2N	HZ5-(0.2N+0.25TP)	HZ5-0.5TP
Relative crystallinity (%)	100	87.2	88.6	97.3
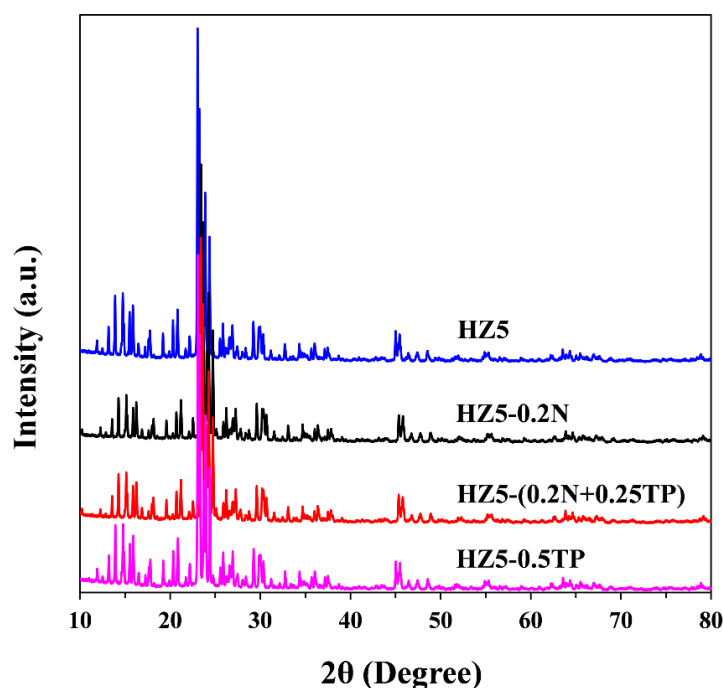
Fig. 3.2 XRD patterns of the prepared hierarchical HZSM-5 catalysts and the parent HZSM-5.

Table 3.4 Textural properties of the prepared hierarchical HZSM-5 catalysts and the parent HZSM-5 catalyst

Catalyst	Si/Al molar ratio on Surface[a]	S_{BET} (m²/g)	S_{micro} (m²/g)	V_{total} (cm³/g)	V_{micro} (cm³/g)	Average pore size (nm)
HZ5	22.0	325.9	307.7	0.18	0.15	2.97
HZ5-0.2N	16.6	319.1	281.5	0.20	0.13	3.95
HZ5-(0.2N+0.25TP)	21.6	359.9	317.4	0.22	0.15	3.78
HZ5-0.5TP	18.3	292.6	271.7	0.17	0.14	3.14

[a] Si/Al ratio were obtained using EDS-SEM.

As shown in **Table 3.4**, the BET surface area (S_{BET})of hierarchical HZSM-5 zeolite of HZ5-(0.2N+0.25TP) increased to some extent (359.9 m²/g) with a little decrease of micropore surface area (S_{micro}=317.4 m²/g) but an increase of total pore volume (V_{total}=0.22 cm³/g) and an enlargement of average pore size (D=3.78 nm) in the case using NaOH with the assistance of TPAOH for the desilication when compared with the parent HZ5 (S_{BET} =325.9 m²/g, S_{micro}=307.7 m²/g, V_{total}=0.18 cm³/g, D=2.97 nm). In contrast, the desilications with either strong NaOH solution or weak TPAOH solution resulted in the decrease of the surface area as well as micropore surface area and volume. Thus, the desilication with a suitable alkaline solution like the solution with 0.2 M NaOH and 0.25 M TPAOH could increase the mesoporosity of the obtained hierarchical HZSM-5 zeolites and simultaneously preserve the microporous structure. Herein, the TPA$^+$ ions tend to interact with hydrophobic silicate generated by the deprotonation of Si-OH groups in the alkaline medium [33], and the
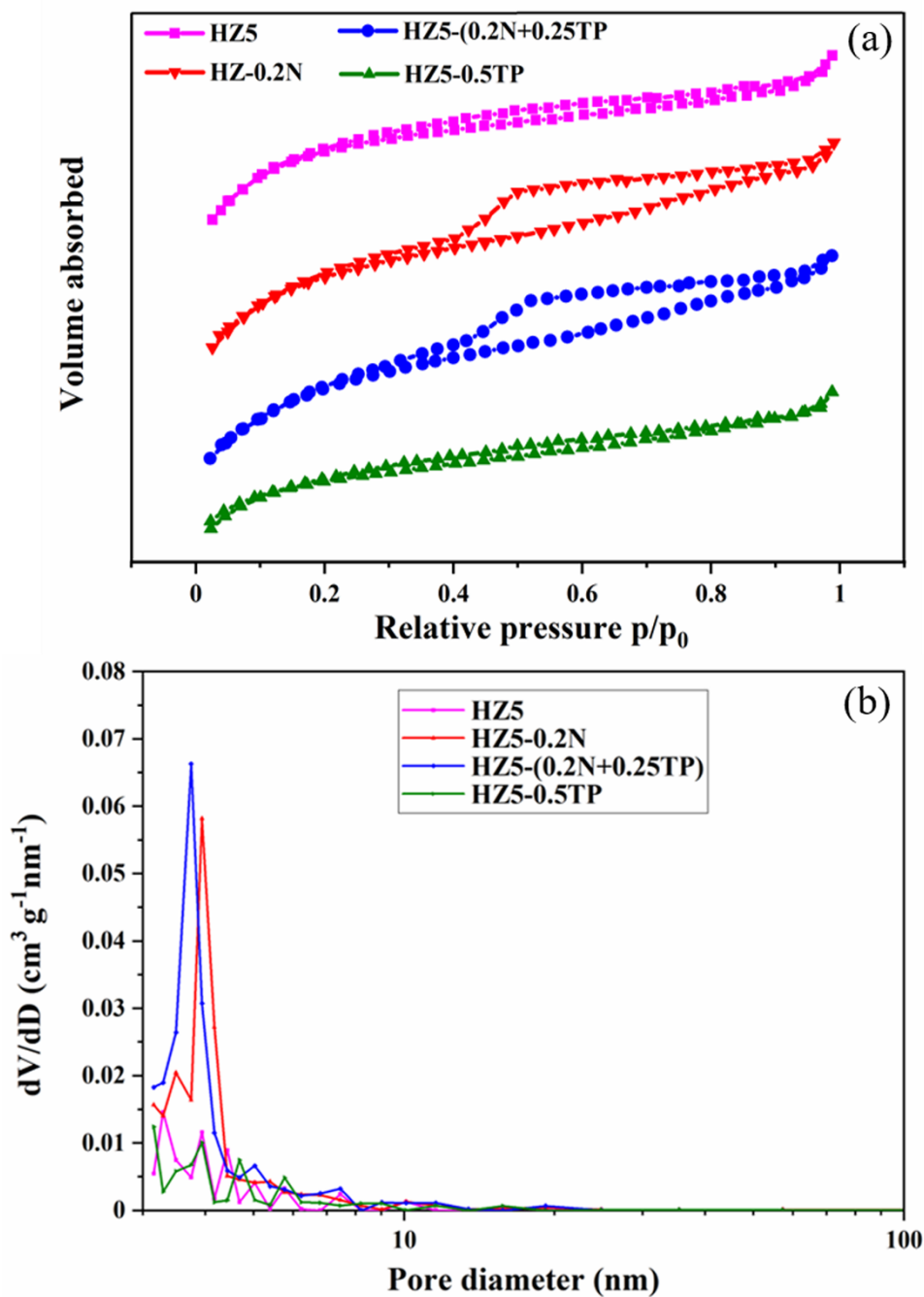
Fig. 3.3 N_2 adsorption/desorption isotherms (a) and DFT pore size distributions (b) for the hierarchical HZSM-5 catalysts.

preferentially attached TPA$^+$ ions would prevent HZSM-5 crystals from further severe desilication, which is beneficial for the formation of good hierarchical structure. In addition, as shown in **Fig. 3.3(a)**, the hysteresis loop of HZ-0.2N and HZ5-(0.2N+0.25TP) exhibited type IV isotherms with H_4 hysteresis loop at P/P_0 above 0.4, also indicating the existence of

mesoporous structures [34-36]. In contrast, the HZ5-0.5TP had a typical type I isotherm, verifying that it had a similar microporous structure as the parent HZ5, but no mesopores were formed under such a pure-TPAOH-solution treatment with relatively weak alkalinity.

Fig. 3.4 shows NH_3-TPD profiles of the hierarchical HZSM-5 zeolites and the parent HZ5 zeolite. The peaks at the lower and higher temperatures were assigned to the desorptions of NH_3 on the weak Lewis acid sites and on the strong Brønsted acid sites, respectively. One can see that the peaks shifted to the higher temperature direction after the desilication and more NH_3 could be adsorbed on the Lewis acid sites for the hierarchical HZ5-(0.2N+0.25TP) zeolite. The acidities of these catalysts were calculated from the related peak areas and summarized in **Table 3.5**. One can see that the acidity of all hierarchical zeolites decreased to great extent at either weak or strong acid sites, which is consistent with the reported results [37]. In addition, the treatment of parent HZ5 in 0.5 M TPAOH alone also decreased the surface Si/Al molar ratio, but the acidities at both weak and strong acid sites were not greatly changed, which is also consistent with the reported results [33].

Table 3.5 Acidity of hierarchical HZSM-5 catalysts and the parent HZSM-5 catalyst

Catalyst	Acidity (mmol/g, low temp)	Acidity (mmol/g, high temp)	Total acidity (mmol/g)
HZ5	0.58	0.67	1.25
HZ5-0.2N	0.48	0.39	0.87
HZ5-(0.2N+0.25TP)	0.52	0.43	0.95
HZ5-0.5TP	0.48	0.43	0.91
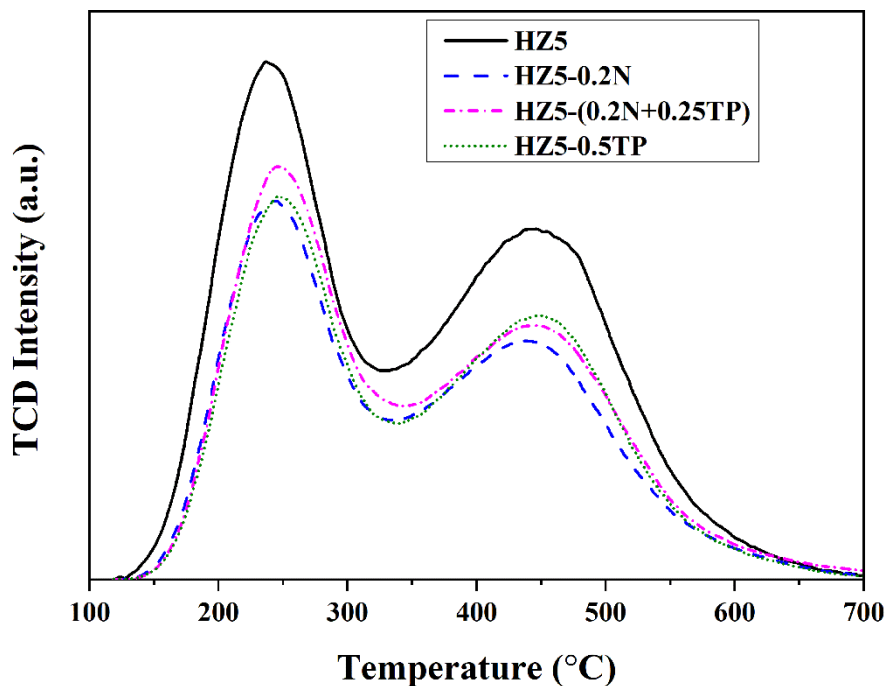
Fig. 3.4 NH$_3$-TPD profiles of the hierarchical HZSM-5 catalysts.

Fig. 3.5 shows SEM images of parent HZ5 and the hierarchical HZSM-5 zeolites derived from HZ5, in which the obvious differences were not observed. However, from the TEM images (**Fig. 3.6**), the edges of hierarchical HZSM-5 zeolites (**Figs.3.6(b-d)**) were completely different from that of the parent HZ5 (**Fig. 3.6(a)**). It is obvious that the HZ5 crystal had a highly dense edge. In comparison, for the hierarchical HZ-0.2N, a large amount of mesopores were generated with some macropores in the edge part of the crystal (**Fig. 3.6(b)**), which is similar as the reported one [19]. Meanwhile, for the hierarchical HZ-(0.2N+0.25TP) zeolite, abundant uniform mesopores appeared in the edge part of the crystal (**Fig. 3.6(c)**) due to the mild desilication with the assistance of a small amount of TPAOH. In addition, no obvious changes on the edge of crystal were observed under the pure-TPAOH-solution treatment even at relatively high concentration. These results are also consistent with the N$_2$ adsorption-desorption isotherms.
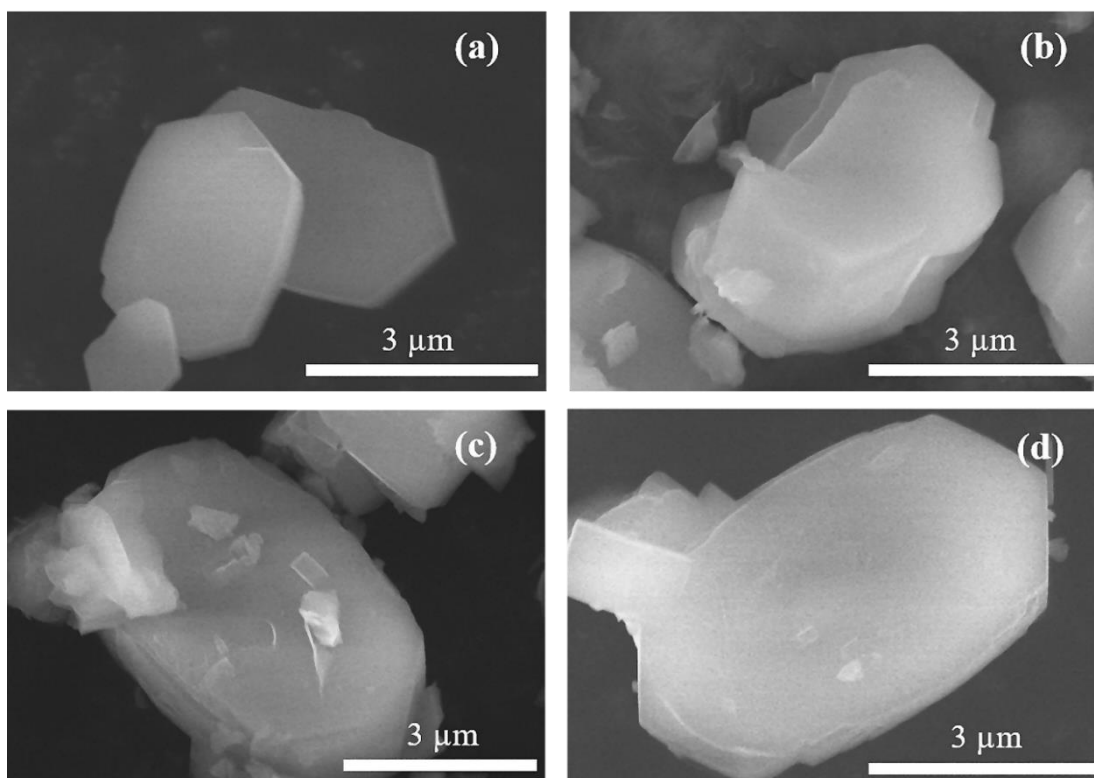
Fig. 3.5 SEM images of (a) HZ5, (b) HZ5-0.2N, (c) HZ5-(0.2N t 0.25TP) and (d) HZ5-0.5TP catalysts.
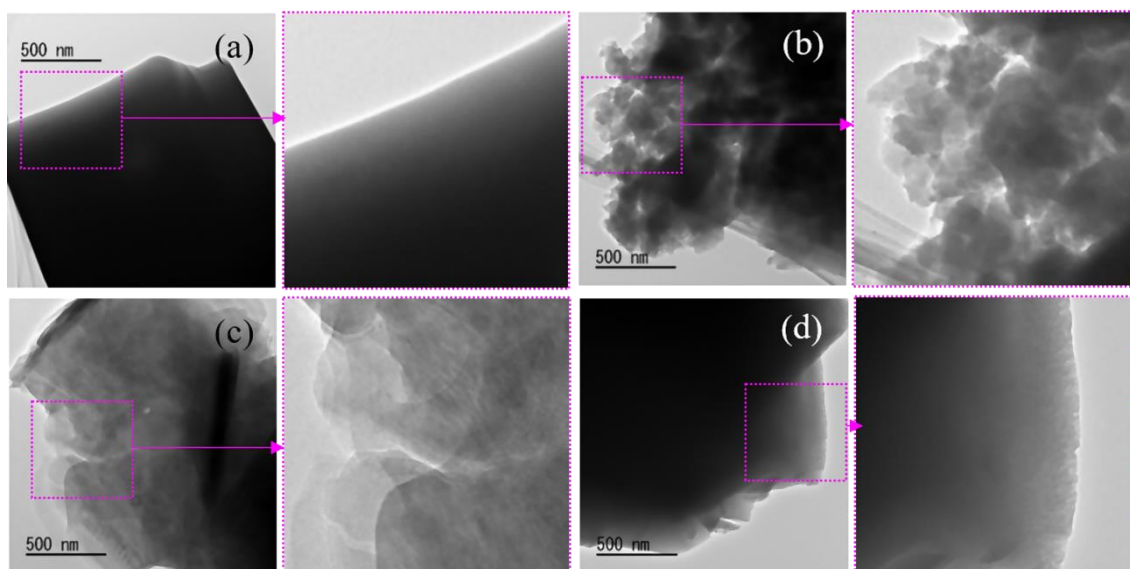
Fig. 3.6 TEM images of (a) HZ5, (b) HZ5-0.2N, (c) HZ5-(0.2N t 0.25TP) and (d) HZ5-0.5TP catalysts.

3.3.3 In-situ catalytic upgrading of bio-oil over hierarchical HZSM-5

In-situ catalytic upgrading of bio-oil derived from the fast pyrolysis of sunflower stalk over

hierarchical HZSM-5 catalysts was performed at a reaction temperature of 500 ºC based on the preliminary experiments. As shown in **Fig. 3.7(a)**, based on the GC-MS analysis results, the chemicals in the upgraded bio-oil can be classified into seven groups, i.e., acids, phenols, ketones, aliphatic hydrocarbons, aromatic hydrocarbons, aldehydes, and others including alcohol, ether, ester, sugar, amide and amine. Herein, the total relative peak area of all detected aromatic hydrocarbons in the upgraded bio-oil was considered as the indicator to determine the upgrading effectivity of the catalysts, which was defined as the ratio of the total peak area related to the aromatic hydrocarbons and the total peak area of all detected chemicals. As a result, the relative peak area of aromatic hydrocarbons from the upgrading over the hierarchical HZ-(0.2N+0.25TP) zeolite increased to 65.8% from 49.8% over the parent HZ5, which was also higher than that over HZ5-0.2N (60.0%) catalyst. Especially, those undesirable compounds such as ethers, amides, and amines, ketones, phenols, and esters were greatly reduced in the upgraded oil by using this hierarchical HZSM-5 catalyst. This result should be attributed to the higher S_{BET} with the preservation of the microporous volume as well as the higher acidity of HZ5-(0.2N+0.25TP). Generally, high acidity could enhance the cracking, dehydrogenation and aromatization of oxygenated compounds to aromatic hydrocarbons [23, 31]. Therefore, it is important to generate suitable acidity on the hierarchical HZSM-5 catalyst for the increasing of aromatization.

The specific aromatic hydrocarbons produced during the *in-situ* catalytic upgrading process can be categorized into seven typical chemicals, i.e., benzene, toluene, o-xylene, p-xylene, ethylbenzene, naphthalenes, and others. Herein, the naphthalenes included naphthalene and alkyl naphthalenes such as 2,6-dimethyl-naphthalene, 1,6-dimethyl-naphthalene, 2,3-dimethyl-naphthalene, 2-methyl-naphthalene, 2-ethyl-naphthalene, 1,7-dimethyl-naphthalene and others included indene, 2-methylidene, other substituted benzenes such as 1-ethyl-2-methyl-benzene, 1-ethyl-3-methyl-benzene, 1,3,5-trimethyl-benzene, and 1,3-dimethyl-benzene. **Fig. 3.7(b)** shows the yields of these specific aromatic hydrocarbons in the upgraded
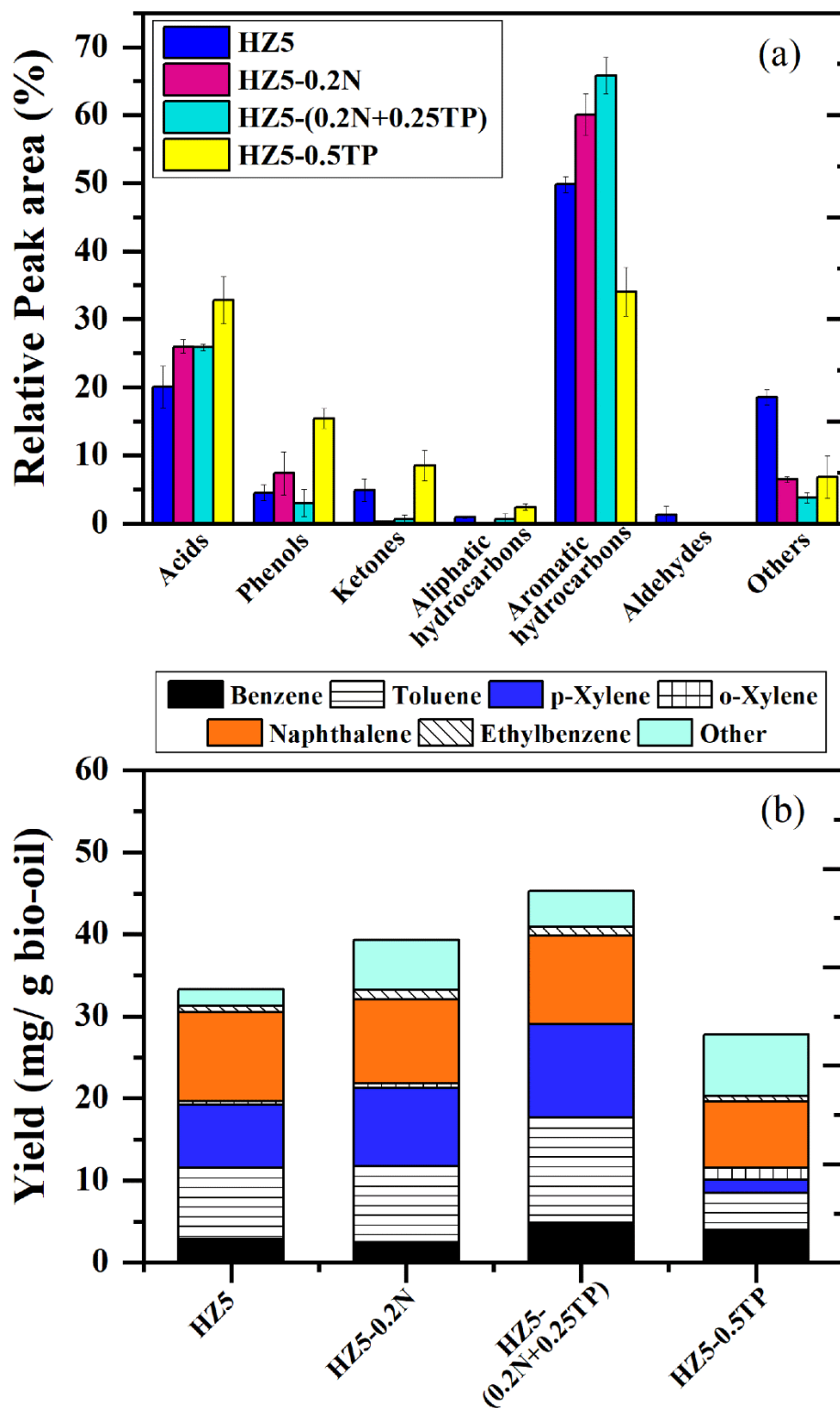
Fig. 3.7 Chemical compositions in the upgraded bio-oils with hierarchical HZSM-5 catalysts (a) and the selectivity towards specific aromatic hydrocarbons in the upgraded bio-oils (b).

bio-oil obtained by using the parent HZ5 and the hierarchical HZSM-5 catalysts. In this study, those large polycyclic aromatic hydrocarbons such as anthracene, phenanthrene, and fluorene were not detected in all samples. As shown in **Fig. 3.7(b)**, the yield of specific aromatic hydrocarbons in the upgraded bio-oil derived from the upgrading over the HZ5-(0.2N+0.25TP) reached to 45.2 mg/g bio-oil, which was much higher than that from the parent HZ5 (33.1 mg/g bio-oil), also higher than that from the HZ5-0.2N (38.8 mg/g bio-oil), indicating that the hierarchical HZ5-(0.2N+0.25TP) catalyst had higher selectivity and activity than other prepared catalysts. Herein, the enlarged channel and pore sizes should be suitable for the large molecules in the bio-oil easily entering the inside of the HZ5-(0.2N+0.25TP) zeolite, whereas the increased surface area provided more active sites for the upgrading reaction, leading to the generation of more monoaromatic hydrocarbons and small polyaromatic hydrocarbons [38].

    Fig. 3.8(a) shows the mass balance in the upgrading of bio-oil over the parent HZ5 and the hierarchical HZSM-5 catalysts. One can see that the water content in the upgraded bio-oil derived from the upgrading over the HZ5-(0.2N+0.25TP) catalyst increased to 25.1wt.% from 22.4 wt.% for the parent HZ5, and simultaneously, the gas yield (**Fig. 3.8(b)**) was also increased from 15.8 wt.% to 20.8 wt.%. Whereas, the bio-oil yield was reduced from 35.1 wt.% for the HZ5 to 26.4 wt.% for the HZ5-(0.2N+0.25TP). It indicated that the deoxygenation by using these catalysts resulted in the formation of H_2O, CO_2 and CO via various reactions such as dehydration, decarboxylation, and decarbonylation [39, 40]. Meanwhile, it is found that the obtained hierarchical zeolites did not inhibit the coke formation on their surface, and the coke yield was even increased to some extent along with the obvious increase in the yield of aromatic hydrocarbons by using the HZ5-(0.2N+0.25TP). Herein, the increase of the acidity of HZ5-(0.2N+0.25TP) on the Lewis acid sites should be the main reason for the more coke formation since the cracking reactions also easily occur on such sites. Thus, to modify the acid sites for reducing the coking, metal doping on the HZ5-

(0.2N+0.25TP) was also performed in the following study
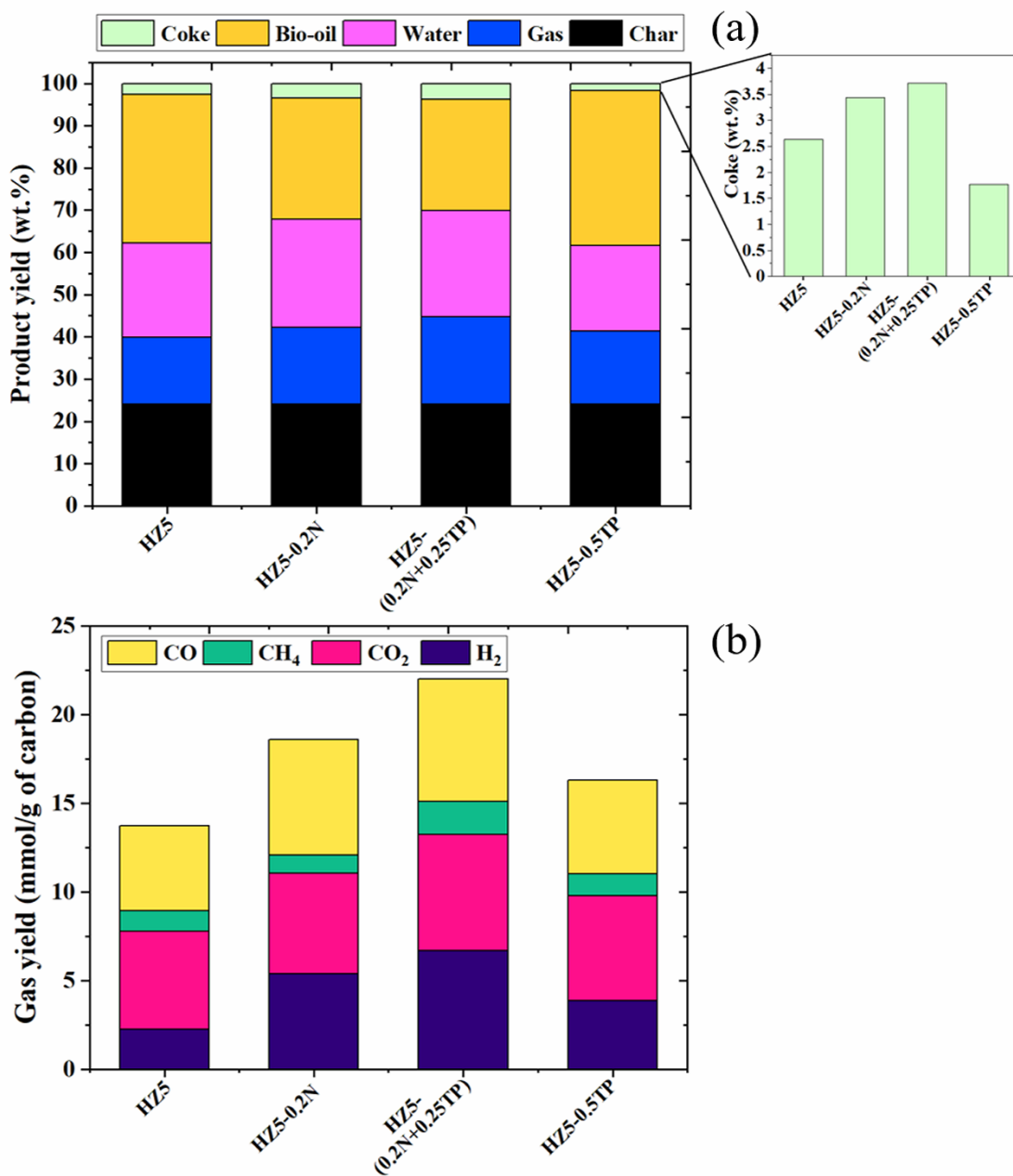
Fig. 3.8 The product distribution (a) and gas yields (b) obtained from of catalytic upgrading of bio-oil derived from fast pyrolysis of sunflower stalk over hierarchical HZSM-5 catalysts and parent HZSM-5 catalyst.

3.3.4 Influence of metal-doping on the performance of hierarchical HZSM-5

In this study, to investigate the influence of metal-doping on the performance of hierarchical HZSM-5 catalyst, Cu, Ag and Mg were separately doped on the hierarchical

HZ5(0.2N+0.25TP) zeolites. **Figs. 3.9(a), (c)** and **(e)** show the relative peak areas of various chemicals in the upgraded bio-oils obtained by using the Cu, Ag and Mg doped catalysts with different doping amounts, respectively. Meanwhile, the related specific aromatic hydrocarbon yields were also determined and shown in **Figs. 3.9(b), (d)** and **(f)**, respectively. One can see that the chemical compositions in the upgraded bio-oil were greatly affected the aromatic hydrocarbon production, and the optimum doping amounts of Cu, Ag and Mg were found to be 0.25 wt.%, 0.25 wt.% and 0.1 wt.%, respectively. In particular, although the relative peak areas related to the aromatic hydrocarbons in the upgraded bio-oil were reduced (**Figs. 3.9(a), (c)** and **(e)**) with the 0.25 wt.% Cu, 0.25 wt.% Ag and 0.1 wt.% Mg doping amounts, the specific aromatic hydrocarbon yields obviously increased to 54.5, 49.1 and 51.9 mg/g-bio-oil from 45.2 mg/g-bio-oil for the undoped hierarchical HZ5(0.2N+0.25TP) zeolite, respectively (**Figs. 3.9(b), (d)** and **(f)**), indicating that the doping with the optimum amount of metal could increase the selectivity of the hierarchical zeolite. Herein, all the metal doped HZ5-(0.2N+0.25TP) zeolites showed high selectivity towards naphthalenes, toluene, p-xylene and a few other types of aromatic hydrocarbons, therefore increasing the overall aromatic hydrocarbons production.
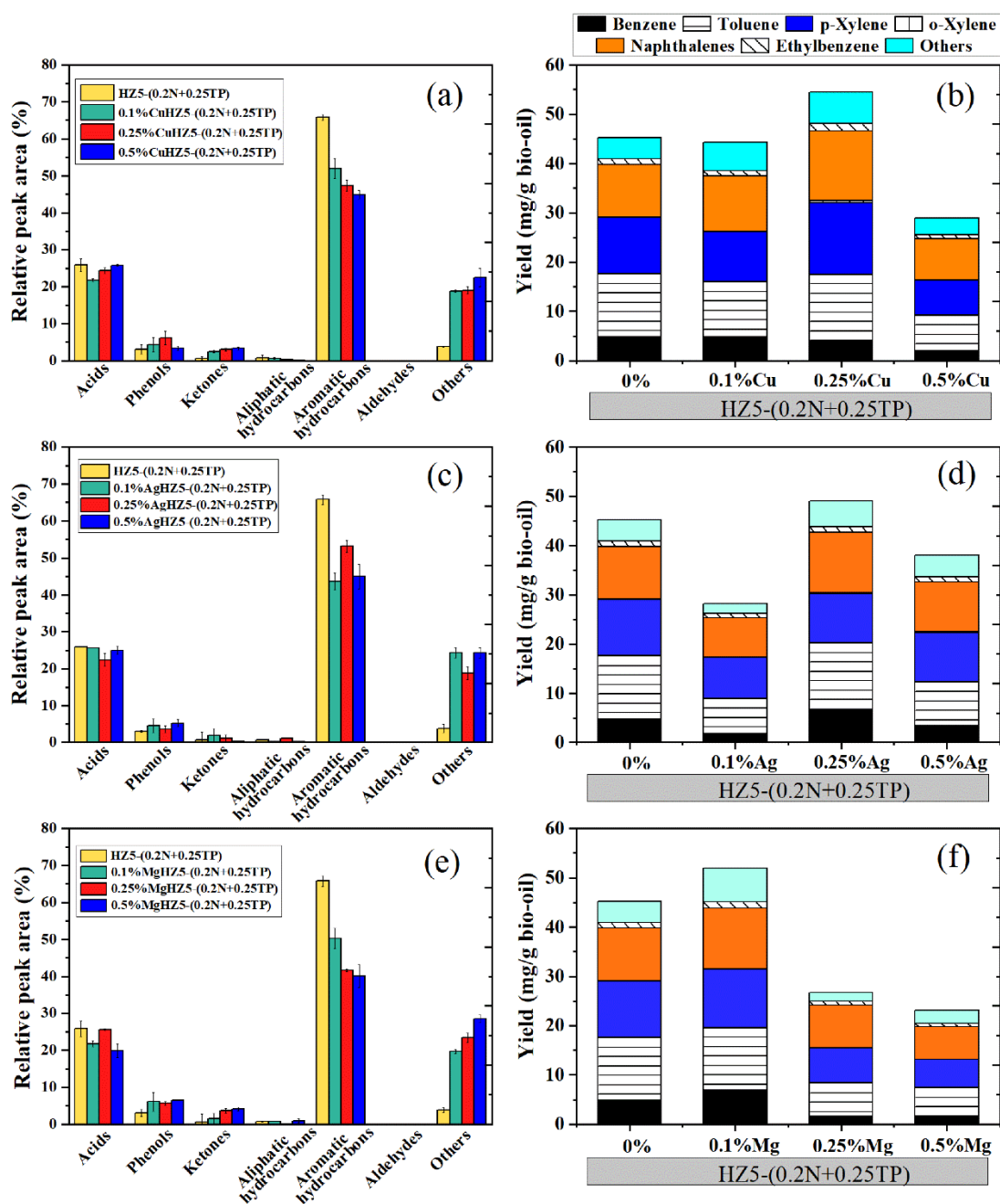
Fig. 3.9 Chemical compositions of the bio-oils upgraded with the metal doped hierarchical HZSM-5 catalysts, Cu (a), Ag (c) and Mg (e) doped ones and the selectivity towards specific aromatic hydrocarbons in the upgraded bio-oils in the cases of Cu (b), Ag (d) and Mg (f) dopings.

Fig. 3.10(a) shows the mass balance in the upgrading of bio-oil over the metal doped hierarchical HZ5-(0.2N+0.25TP) zeolites. One can see that the water contents in the upgraded bio-oil derived from the upgrading over the 0.25% Cu and 0.1% Mg doped HZ5-

(0.2N+0.25TP) catalysts increased to 26.2wt.% and 25.3wt.%, respectively, but decreased to some extent for the 0.25% Ag doping. Meanwhile, Gas yields (**Fig. 3.10(b)**) slightly decreased to 20.4% and 19.7% for 0.25wt.% Cu and 0.25wt.% Ag dopings, respectively, whereas increased to 21.1% for the 0.1 wt.% Mg doping when compared with that for the non-doped HZ5-(0.2N+0.25TP) catalyst (20.8%). It is reported that Mg doping could promote the formation of gaseous products by cracking, reforming, and other reactions [41]. Furthermore, as shown in **Fig. 3.10(b)**, the coke yields decreased after the metal doping when compared with that in the case using the undoped HZ5-(0.2N+0.25TP) zeolite catalyst. Herein, the replacement of H^+ on the surface of hierarchical HZ5-(0.2N+0.25TP) zeolite by the metal species, resulting in the decrease of acidity (**Fig. 3.11** and **Table 3.6**). which could reduce the coke formation on the acid sites [31]. In addition, as shown in **Fig. 3.12**, due to the very low doping amount and/or well dispersion of the doping species on the surface of the catalysts, after Cu, Mg and Ag were doped on the surface of hierarchical HZ5-(0.2N+0.25TP) catalysts, the catalyst framework had no any changes and meanwhile no characteristic peaks corresponding to the doped metal species were observed [8, 30, 42]. However, the S_{BET} and total pore volume (**Table 3.7**) decreased to some extent after the metal doping on the HZ5-(0.2N+0.25TP), which should be related to the blocking of some micropores by the metal species and/or the presence of metal oxide aggregates on the external surface [43,44].
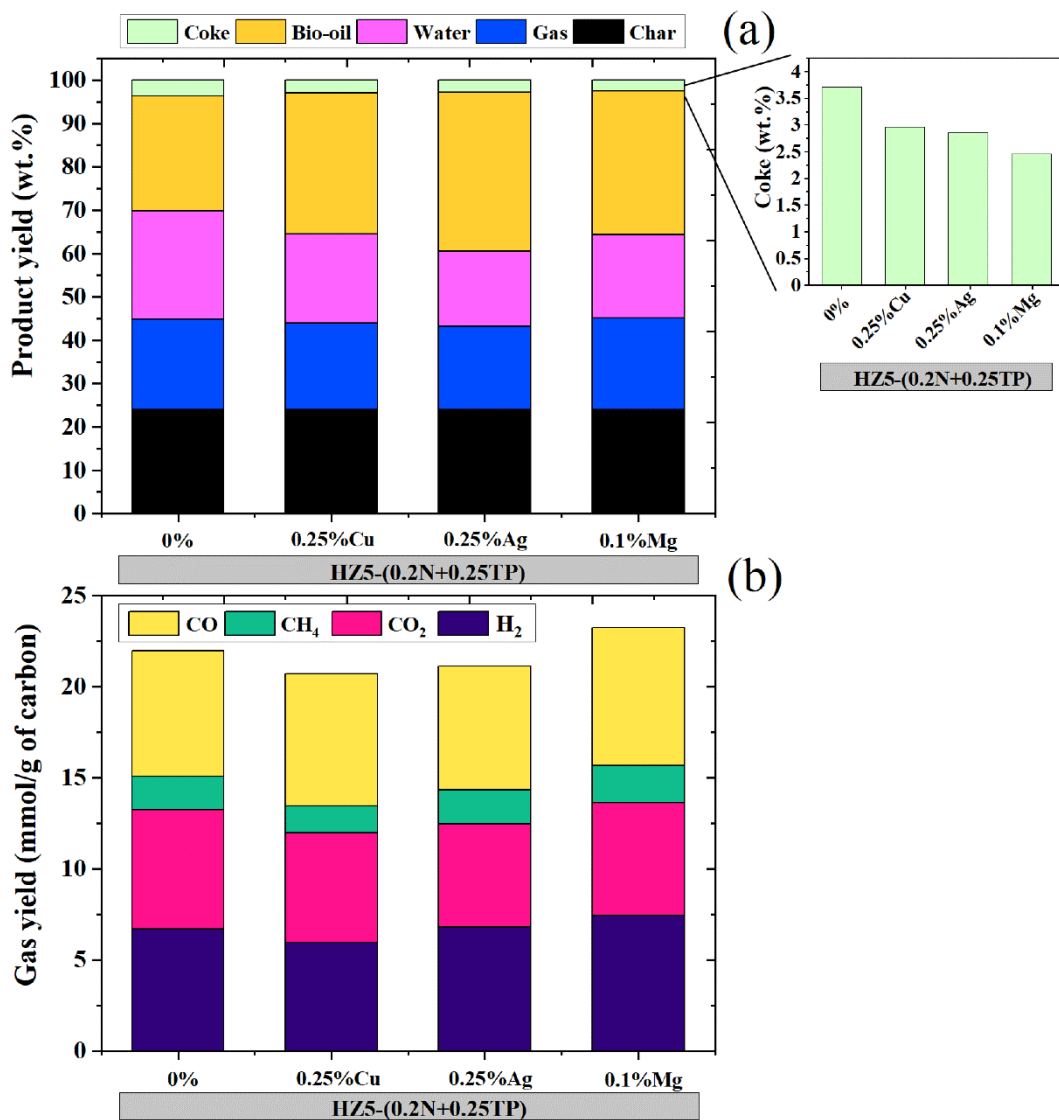
Fig. 3.10 The product distribution (a) and gas yield (b) obtained from the in-situ catalytic upgrading of bio-oil derived from fast pyrolysis of sunflower stalk over metal doped hierarchical HZ5-(0.2N t 0.25TP) catalysts.

Table 3.6 Acidity of metal doped hierarchical HZ5(0.2M+0.25TP) catalysts

Catalyst	Acid amount (mmol/g, low temp)	Acid amount (mmol/g, high temp)	Total acid amount (mmol/g)
0.25%CuHZ5-(0.2N+0.25TP)	0.44	0.35	0.79
0.25%AgHZ5-(0.2N+0.25TP)	0.45	0.37	0.82
0.1%MgHZ5-(0.2N+0.25TP)	0.47	0.36	0.83

Table 3.7 Textural properties of metal doped hierarchical HZ5(0.2M+0.25TP) catalysts

Catalyst	S_{BET} (m^2/g)	S_{micro} (m^2/g)	V_{total} (cm^3/g)	V_{micro} (cm^3/g)	Average pore size (nm)
0.25%CuHZ5-(0.2N+0.25TP)	316.5	283.6	0.20	0.14	3.75
0.25%AgHZ5-(0.2N+0.25TP)	326.7	290.2	0.18	0.15	3.74
0.1%MgHZ5-(0.2N+0.25TP)	314.5	297.2	0.18	0.15	3.73
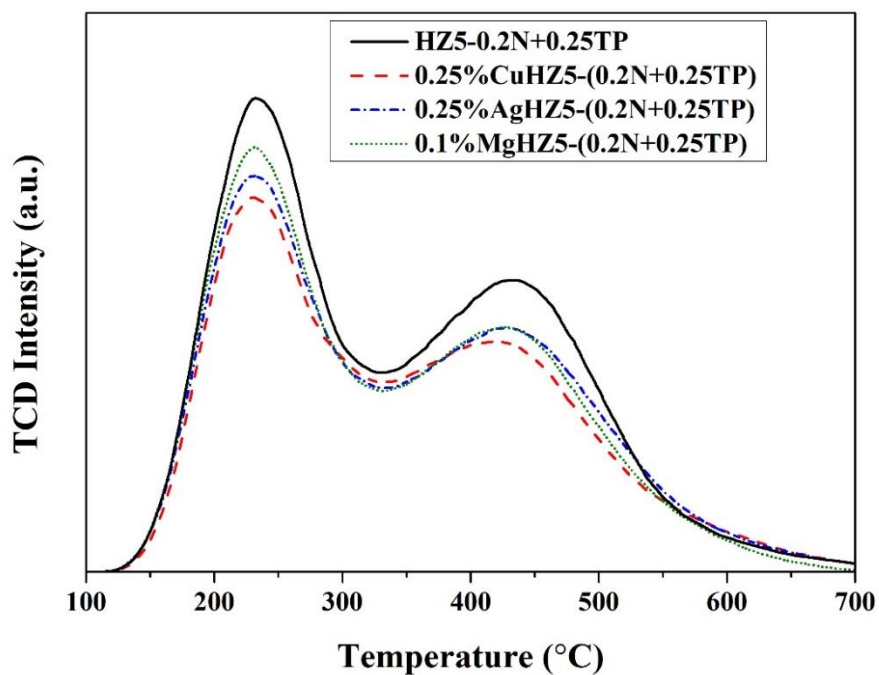
Fig. 3.11 NH₃-TPD profiles of the metal doped hierarchical HZ5(0.2M+0.25TP) catalysts
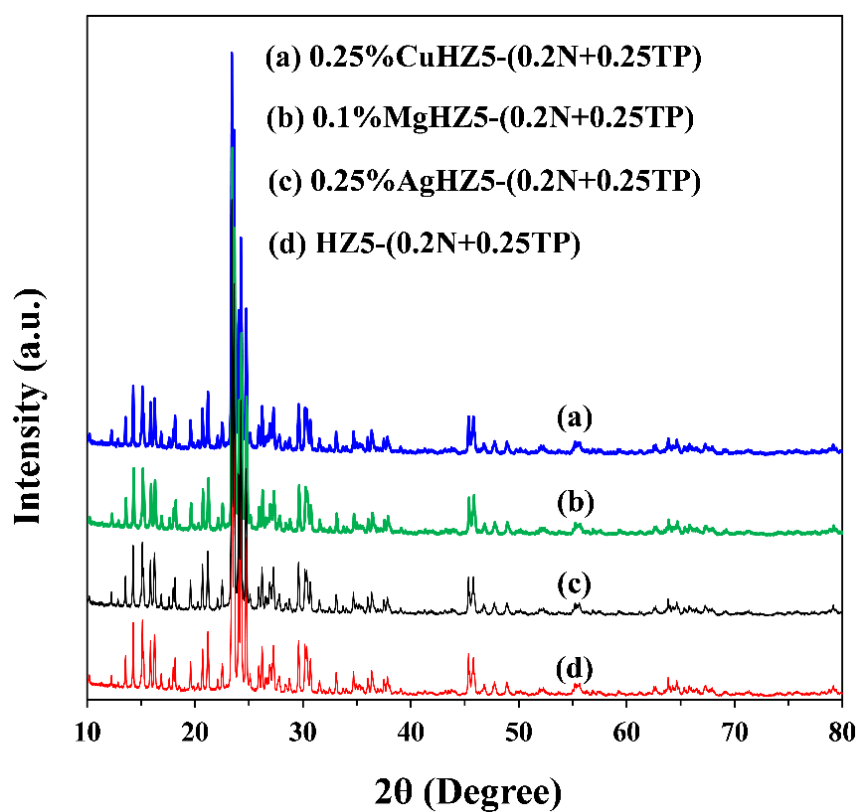
Fig. 3.12 XRD patterns of metal-doped hierarchical HZ5(0.2M+0.25TP) catalysts

4. Conclusions

Hierarchical HZSM-5 zeolites were prepared by desilication of commercial HZSM-5 with aqueous NaOH-TPAOH mixture, and successfully applied for the *in-situ* catalytic upgrading of bio-oil derived from the fast pyrolysis of sunflower stalk powders. The obtained hierarchical HZSM-5 by using a mixture of 0.2 M NaOH with 0.25 M TPAOH for the desilication showed the best catalytic performance. It is found that the relative total peak area related to the detected aromatic hydrocarbons reached 65.8% with a yield of aromatic hydrocarbons up to 45.2 mg/g-bio-oil. However, the coking on the surface of catalyst was not hindered. To solve the coking problem and increase the aromatic hydrocarbons production, the hierarchical HZSM-5 zeolites were modified by Cu, Ag, and Mg. It is found that the doping amount had a great effect on the catalytic performance, and with the optimum doping amounts, i.e., 0.25 wt.% Cu, 0.25 wt.% Ag and 0.1 wt.% Mg doping amounts, the specific aromatic hydrocarbon yields were obviously increased to 54.5, 49.1 and 51.9 mg/g-bio-oil from 45.2 mg/g-bio-oil for the undoped hierarchical HZSM-5 zeolite, respectively. Also, the coking formation was hindered by the metal doping.

References

[1] S. Al-Khattaf, S.A. Ali, A.M. Aitani, N. Žilková, D. Kubička, J. Čejka, Recent Advances in reactions of alkylbenzenes over novel zeolites: The effects of zeolite structure and morphology, Catal. rev., 56 (2014) 333-402.

[2] K. Qiao, X. Shi, F. Zhou, H. Chen, J. Fu, H. Ma, H. Huang, Catalytic fast pyrolysis of cellulose in a microreactor system using hierarchical zsm-5 zeolites treated with various alkalis, Appl. Catal. A Gen., 547 (2017) 274-282.

[3] S. Cheng, L. Wei, J. Julson, K. Muthukumarappan, P.R. Kharel, Upgrading pyrolysis bio-oil to biofuel over bifunctional Co-Zn/HZSM-5 catalyst in supercritical methanol, Energy Convers. Manag., 147 (2017) 19-28.

[4] E. David, J. Kopač, Upgrading the characteristics of the bio-oil obtained from rapeseed oil

cake pyrolysis through the catalytic treatment of its vapors, J. Anal. Appl. Pyrolysis, 141 (2019).

[5] S. Ahmadi, E. Reyhanitash, Z. Yuan, S. Rohani, C. Xu, Upgrading of fast pyrolysis oil via catalytic hydrodeoxygenation: Effects of type of solvents, Renew. Energy, 114 (2017) 376-382.

[6] H. Hernando, I. Moreno, J. Fermoso, C. Ochoa-Hernández, P. Pizarro, J.M. Coronado, J. Čejka, D.P. Serrano, Biomass catalytic fast pyrolysis over hierarchical ZSM-5 and Beta zeolites modified with Mg and Zn oxides, Biomass Convers. Biorefin., 7 (2017) 289-304.

[7] Y. Makkawi, Y. El Sayed, M. Salih, P. Nancarrow, S. Banks, T. Bridgwater, Fast pyrolysis of date palm (Phoenix dactylifera) waste in a bubbling fluidized bed reactor, Renew. Energy, 143 (2019) 719-730.

[8] M. Razzaq, M. Zeeshan, S. Qaisar, H. Iftikhar, B. Muneer, Investigating use of metal-modified HZSM-5 catalyst to upgrade liquid yield in co-pyrolysis of wheat straw and polystyrene, Fuel, 257 (2019).

[9] R. French, S. Czernik, Catalytic pyrolysis of biomass for biofuels production, Fuel Process. Technol., 91 (2010) 25-32.

[10] S. Czernik, A.V. Bridgwater, Overview of Applications of Biomass Fast Pyrolysis Oil, Energy Fuels, 18 (2004) 590-598.

[11] B. Zhang, Z. Zhong, K. Ding, Y. Cao, Z. Liu, Catalytic Upgrading of corn stalk fast pyrolysis vapors with fresh and hydrothermally treated HZSM-5 catalysts using Py-GC/MS, Ind. Eng. Chem. Res., 53 (2014) 9979-9984.

[12] A. Palizdar, S.M. Sadrameli, Catalytic upgrading of beech wood pyrolysis oil over iron- and zinc-promoted hierarchical MFI zeolites, Fuel, 264 (2020).

[13] B.B. Uzun, N. Sarioğlu, Rapid and catalytic pyrolysis of corn stalks, Fuel Process. Technol., 90 (2009) 705-716.

[14] Y. Yu, X. Li, L. Su, Y. Zhang, Y. Wang, H. Zhang, The role of shape selectivity in catalytic

fast pyrolysis of lignin with zeolite catalysts, Appl. Catal. A Gen., 447-448 (2012) 115-123.

[15] Y. Xu, J. Wang, G. Ma, J. Lin, M. Ding, Designing of hollow ZSM-5 with controlled mesopore sizes to boost gasoline production from syngas, ACS Sustain. Chem. Eng., 7 (2019) 18125-18132.

[16] E.F. Iliopoulou, S.D. Stefanidis, K.G. Kalogiannis, A. Delimitis, A.A. Lappas, K.S. Triantafyllidis, Catalytic upgrading of biomass pyrolysis vapors using transition metal-modified ZSM-5 zeolite, Appl.Catal. B Environ., 127 (2012) 281-290.

[17] Y.-K. Park, M.L. Yoo, S.H. Jin, S.H. Park, Catalytic fast pyrolysis of waste pepper stems over HZSM-5, Renew. Energy, 79 (2015) 20-27.

[18] D. Wang, L. Zhang, L. Chen, H. Wu, P. Wu, Postsynthesis of mesoporous ZSM-5 zeolite by piperidine-assisted desilication and its superior catalytic properties in hydrocarbon cracking, J. Mater. Chem. A, 3 (2015) 3511-3521.

[19] W. Wan, T. Fu, R. Qi, J. Shao, Z. Li, Coeffect of Na+ and tetrapropylammonium (TPA+) in alkali treatment on the fabrication of mesoporous ZSM-5 catalyst for methanol-to-hydrocarbons reactions, Ind. Eng. Chem. Res., 55 (2016) 13040-13049.

[20] Y. Tao, H. Kanoh, L. Abrams, K. Kaneko, Mesopore-modified zeolites: Preparation, characterization, and applications., Chem. Rev., 106 (2006) 896-910.

[21] D.P. Serrano, J.M. Escola, R. Sanz, R.A. Garcia, A. Peral, I. Moreno, M. Linares, Hierarchical ZSM-5 zeolite with uniform mesopores and improved catalytic properties, New J. Chem., 40 (2016) 4206-4216.

[22] F. Wang, M.-x. Zhou, X.-h. Yang, L.-j. Gao, G.-m. Xiao, The effect of hierarchical pore architecture on one-step catalytic aromatization of glycerol: Reaction routes and catalytic performances, Mol. Catal., 432 (2017) 144-154.

[23] J. Li, X. Li, G. Zhou, W. Wang, C. Wang, S. Komarneni, Y. Wang, Catalytic fast pyrolysis of biomass with mesoporous ZSM-5 zeolites prepared by desilication with NaOH

solutions, Appl. Catal. A Gen., 470 (2014) 115-122.

[24] X. Li, X. Zhang, S. Shao, L. Dong, J. Zhang, C. Hu, Y. Cai, Catalytic upgrading of pyrolysis vapor from rape straw in a vacuum pyrolysis system over La/HZSM-5 with hierarchical structure, Bioresour. Technol., 259 (2018) 191-197.

[25] B. Puertolas, A. Veses, M.S. Callen, S. Mitchell, T. Garcia, J. Perez-Ramirez, Porosity-acidity interplay in hierarchical ZSM-5 zeolites for pyrolysis oil valorization to aromatics, Chem. Sus. Chem., 8 (2015) 3283-3293.

[26] A. Palizdar, S.M. Sadrameli, Catalytic upgrading of biomass pyrolysis oil over tailored hierarchical MFI zeolite: Effect of porosity enhancement and porosity-acidity interaction on deoxygenation reactions, Renew. Energy, 148 (2020) 674-688.

[27] J. Pérez-Ramírez, D. Verboekend, A. Bonilla, S. Abello, Zeolite catalysts with tunable hierarchy factor by pore-growth moderators, Adv. Funct. Mater., 19 (2009) 3972-3979.

[28] I. Kurnia, S. Karnjanakom, A. Bayu, A. Yoshida, J. Rizkiana, T. Prakoso, A. Abudula, G. Guan, In-situ catalytic upgrading of bio-oil derived from fast pyrolysis of lignin over high aluminum zeolites, Fuel Process. Technol., 167 (2017) 730-737.

[29] Q. Shen, L. Zhang, M. Wu, C. He, W. Wei, N. Sun, Y. Sun, Postsynthesis of mesoporous ZSM-5 zeolites with TPAOH-assisted desilication and determination of activity performance in N2O decomposition, J. Porous Mater., 24 (2016) 759-767.

[30] A. Veses, B. Puértolas, J.M. López, M.S. Callén, B. Solsona, T. García, Promoting deoxygenation of bio-oil by metal-loaded hierarchical ZSM-5 zeolites, ACS Sustain. Chem. Eng., 4 (2016) 1653-1660.

[31] H. Chen, H. Cheng, F. Zhou, K. Chen, K. Qiao, X. Lu, P. Ouyang, J. Fu, Catalytic fast pyrolysis of rice straw to aromatic compounds over hierarchical HZSM-5 produced by alkali treatment and metal-modification, J. Anal. Appl. Pyrolysis, 131 (2018) 76-84.

[32] N. Chaihad, S. Karnjanakom, I. Kurnia, A. Yoshida, A. Abudula, P. Reubroycharoen, G. Guan, Catalytic upgrading of bio-oils over high alumina zeolites, Renew. Energy, 136

(2019) 1304-1310.

[33] S. Abelló, A. Bonilla, J. Pérez-Ramírez, Mesoporous ZSM-5 zeolite catalysts prepared by desilication with organic hydroxides and comparison with NaOH leaching, Appl. Catal. A Gen., 364 (2009) 191-198.

[34] G. Song, D. Xue, J. Xue, F. Li, Synthesis and catalytic characterization of ZSM-5 zeolite with uniform mesopores prepared in the presence of a novel organosiloxane, Microporous Mesoporous Mater., 248 (2017) 192-203.

[35] Y. Jia, J. Wang, K. Zhang, G. Chen, Y. Yang, S. Liu, C. Ding, Y. Meng, P. Liu, Hierarchical ZSM-5 zeolite synthesized via dry gel conversion-steam assisted crystallization process and its application in aromatization of methanol, Powder Technol., 328 (2018) 415-429.

[36] L. Meng, B. Mezari, M.G. Goesten, E.J.M. Hensen, One-step synthesis of hierarchical ZSM-5 using cetyltrimethylammonium as mesoporogen and structure-directing Agent, Chem. Mater., 29 (2017) 4091-4096.

[37] Y. Gao, B. Zheng, G. Wu, F. Ma, C. Liu, Effect of the Si/Al ratio on the performance of hierarchical ZSM-5 zeolites for methanol aromatization, RSC Adv., 6 (2016) 83581-83588.

[38] Z. Zhang, H. Cheng, H. Chen, J. Li, K. Chen, X. Lu, P. Ouyang, J. Fu, Catalytic fast pyrolysis of rice straw to aromatics over hierarchical HZSM-5 treated with different organosilanes, Energy Fuels, 33 (2018) 307-312.

[39] X. Li, W. Dong, J. Zhang, S. Shao, Y. Cai, Preparation of bio-oil derived from catalytic upgrading of biomass vacuum pyrolysis vapor over metal-loaded HZSM-5 zeolites, J. Energy Inst., 93 (2020) 605-613.

[40] S. Karnjanakom, A. Bayu, P. Xiaoketi, X. Hao, S. Kongparakul, C. Samart, A. Abudula, G. Guan, Selective production of aromatic hydrocarbons from catalytic pyrolysis of biomass over Cu or Fe loaded mesoporous rod-like alumina, RSC Adv., 6 (2016) 50618-50629.

[41] X.-Y. Ren, J.-P. Cao, X.-Y. Zhao, Z. Yang, S.-N. Liu, X.-Y. Wei, Enhancement of aromatic products from catalytic fast pyrolysis of lignite over hierarchical HZSM-5 by piperidine-assisted desilication, ACS Sustain. Chem. Eng., 6 (2017) 1792-1802.

[42] G. Dai, S. Wang, Q. Zou, S. Huang, Improvement of aromatics production from catalytic pyrolysis of cellulose over metal-modified hierarchical HZSM-5, Fuel Process. Technol., 179 (2018) 319-323.

[43] X.-Y. Ren, J.-P. Cao, X.-Y. Zhao, Z. Yang, T.-L. Liu, X. Fan, Y.-P. Zhao, X.-Y. Wei, Catalytic upgrading of pyrolysis vapors from lignite over mono/bimetal-loaded mesoporous HZSM-5, Fuel, 218 (2018) 33-40.

[44] G. Chen, J. Liu, X. Li, J. Zhang, H. Yin, Z. Su, Investigation on catalytic hydrodeoxygenation of eugenol blend with light fraction in bio-oil over Ni-based catalysts, Renew. Energy, 157 (2020) 456-465.

Chapter 4 In-situ catalytic upgrading of bio-oil from rapid pyrolysis of biomass over hollow HZSM-5 with mesoporous shell

4.1 Introduction

With the growing environmental concerns and the ongoing shortage of petroleum resources, the importance of applying renewable resources as the alternatives is becoming more and more obvious [1,2]. Lignocellulosic biomass is an abundantly renewable feedstock that can be utilized to produce bio-oil containing various aromatic hydrocarbons via a fast pyrolysis process. However, the obtained bio-oil always has undesirable properties like low calorific value, corrosiveness, high viscosity, and thermal instability since it is a complicated mixture containing acids, phenols and aldehydes which therefore makes it impossible using as the transportation fuel [3,4]. Thus, the bio-oil generated from the biomass pyrolysis must firstly undergo a catalytic upgrading process with the assistance of efficient catalysts so that the pyrolysis oil has a high quality with low oxygen content and other undesired properties [5, 6].

Zeolites have been widely used as catalysts or support of catalysts for the petroleum oil upgrading based on their high surface area, good shape selectivity and excellent hydrothermal stability [7]. In particular, they have appropriate acidity, which are suitable to be used as isomerization/alkylation catalysts or cracking catalysts [8, 9]. Among various zeolites, ZSM-5 is the most active deoxygenation catalyst with high selectivity to produce aromatic hydrocarbons like BTXN (benzene, toluene, xylene and naphthalene) [10, 11]. Although the unique micropore structure of ZSM-5 is favorable for the aromatics production, its pore channels limit the diffusion of various large molecules and finally limit the catalysis performance [12]. Therefore, how to increase the accessibility to the active sites by modifying

pore structure of ZSM-5 zeolite, thereby enhancing the catalytic activity and obtaining higher aromatics yield, becomes the important issue [13, 14]. In addition, the acidity of zeolite is also an important factor in enhancing the catalysis performance [15, 16]. Many efforts have been made in the synthesis of zeolites by generation of shortened porous structures to reduce diffusion length for the further improving the catalytic activity [17,18]. One popular way is to introduce mesoporous structure by a direct synthesis way or by post-treatment with a base solution such as NaOH, tetrabutylammonium hydroxide (TPAOH), Na2CO3 and their mixture to remove silicon species from zeolite framework [19-21]. Recently, hollow structured ZSM-5 zeolites with short diffusion pathway length and high adsorption capacity have been received great attention [22, 23], which have been applied in various reactions such as Fischer−Trøpsch reaction [24], methanol to aromatics [25] and catalytic oxidation of cyclohexane [26]. There are two general techniques for the preparation of hollow zeolites. One is direct growth of zeolite crystals along with the interface by using some suspension or emulsion precursor, which often generates micrometer-scale hollow zeolite crystals with a polycrystalline shell [23]. The other one is to synthesize zeolite crystal at first and then use a base solution to leach it for the creating of internal hollows with higher surface area [27]. In this study, various nanosized hollow HZSM-5 zeolite catalysts with different Si/Al molar ratios were prepared and applied for in-situ catalytic upgrading of bio-oils generated from the rapid pyrolysis of biomass components (i.e., cellulose, hemicellulose and lignin) using a Py/GC–MS instrument at first. Then, the best hollow HZSM-5 zeolite was further treated with tetrapropylammonium hydroxide (TPAOH) solution to obtain hollow HZSM-5 catalyst with a mesoporous shell, and applied for the in-situ catalytic upgrading of bio-oils. To fully understand the effect of biomass to catalyst ratio on the aromatics yield and verify the results obtained from Py-GC/MS analysis, a fixed bed reactor was also used. It is expected to obtained a novel zeolite structure for more effective upgrading of the bio-oils.

4.2 Experimental

4.2.1 Materials

Cellulose and dealkaline lignin were provided by Wako, Japan and Tokyo Chemical Industry Co. Ltd., Japan, respectively. Xylan, a representative of hemicellulose, was purchased from Nacalai Tesque, Inc. (NTI, Japan). The samples were dried overnight to ensure the removal of water content. The ultimate analysis of cedar wood revealed that it is composed of 48.2 wt% C, 6.0 wt% H, 45.8 wt% O, and 0 wt% S. The chemicals used for the synthesis of zeolite, i.e., tetraethyl orthosilicate (TEOS, 95%), NaOH and $Al(NO_3)_3 \cdot 9H_2O$ were purchased from Wako, and tetrapropylammonium hydroxide (TPAOH, 25 wt% in water) was purchased from TCI, Japan.

4.2.2 Preparation of Catalysts

Hollow ZSM-5 zeolites were synthesized by a hydrothermal way with molar compositions of $xTEOS: 1.3Al_2O_3: 14TPAOH: 6.5Na_2O: 285H_2O$, where x was varied to obtain the zeolites with different initial Si/Al molar ratios of 30, 40, and 60 in the precursors, respectively. In a typical synthesis, TEOS as Si source and TPAOH as template were mixed and stirred vigorously for 1 h at 80°C before dropwise adding of the mixture of aluminum nitrate as Al source, NaOH and H_2O, and finally the mixed solution was stirred for 5 h at ambient temperature. Thereafter, the mixed solution was heated at 80ºC for 1 h to get the precursor gel, which was then introduced into a stainless-steel autoclave with Teflon-coating layer inside and reacted at 170ºC for 72 h. The zeolite product was recovered by centrifugation, rinsed with distilled water until neutral, dried overnight, and calcined at 550ºC for 6 h. In order to get H-form zeolite, the obtained catalyst was ion-exchanged with 1 M NH_4NO_3 twice and then calcined at 550 ºC for 6 h. Herein, the product is named as Hollow(X), where "X" is Si/Al molar ratio in the precursor. Furthermore, the catalyst with the highest catalysis performance, i.e, the hollow HZSM-5(30) as described in the following section, was treated with TPAOH again in order to get a mesoporous shell in the hollow zeolite. In brief, 1 g of hollow HZSM-

5(30) was introduced into 5 ml of 1M TPAOH solution and then, the mixed solution was introduced into a stainless-steel autoclave with Teflon-coating layer inside and reacted at 170ºC for 24 h. Finally, this post-treated catalyst was separated by centrifugation, rinsed with distilled water until neutral pH state, dried overnight, and calcined at 550ºC for 6 h. Herein, the as-prepared sample was denoted as Hollow(30)-TP. In comparison to the hollow HZSM-5 samples, conventional HZSM-5 catalyst with a Si/Al molar ratio of 30 was also synthesized by the one-step hydrothermal method without NaOH addition and the preparation step was similar to that for the synthesis of hollow HZSM-5 zeolite as described previously. The final sample was named as Solid HZSM-5.

4.2.3 Characterizations

X-ray diffraction (XRD) patterns were determined on an XRD instrument (Smart lab, Rigaku, Japan) equipped with a Cu Kα radiation ($\lambda= 1.542$ Å) at 40 kV and 40 mA in the 2θ range of 10º-80º. The specific BET surface area was measured by Brunauer–Emmet–Teller (BET) analysis in a Quantachrome device (NOVA 4200e, USA), in which the sample was degassed under vacuum at 300 ºC overnight for removing any moisture and then cooled by immersing in a liquid nitrogen bath at -196 ºC for physisorption analysis. The pore size distribution was obtained based on the desorption branch of the isotherm. While, the total pore volume was determined by the absorbed N_2 volume at a relative pressure P/P_0 of 0.99, whereas the micropore volume and surface area were obtained based on the t-plot method. In addition, the $S_{external}$ (external specific surface area) and V_{meso} (mesopore volume) were determined by difference. The acidic properties were determined by an ammonia-temperature-programmed desorption (NH_3-TPD) method using a Belcat catalyst evaluation apparatus (Japan) with a TCD (thermal conductivity detector). The fresh catalyst was pretreated by heating from room temperature to 700 ºC in the helium gas flow and maintaining at 700 ºC for 1 h, and then cooled down to 120 ºC. Thereafter, NH_3 adsorption was performed in a 10 % NH_3/He gas flow for 60 min at 120 °C, followed by flushing with He, and then the NH_3 desorption was realized

at 120-800 ºC temperature range with 10 °C/min heating rate. The morphology and nanostructure of catalyst were checked using a SEM (scanning electron microscope) equipment (SU8010, Hitachi, Japan) and a TEM (transmission electron microscope) apparatus, respectively.

2.4 Py-GC/MS analysis

Hollow HZSM-5 catalysts with various initial Si/Al molar ratios were screened using the Py/GC–MS instrument to determine the relative ability for in-situ raw bio-oil deoxygenation, in which a pyroprobe pyrolyzer (PY-3030D, Frontier Lab) coupled with an auto-shot sampler AS-1020E is connected to a Shimadzu GC-MS (gas chromatography/mass spectrometry, GC-2010 Plus/QP-2010 Ultra) so that the pyrolysis product generated in the Py can be rapidly analyzed. 0.5 mg of commercial cellulose, hemicellulose or lignin with a catalyst to biomass weight ratio of 1:2 for each reaction was used, where the biomass was placed under the catalyst layer in a small stainless-steel cell. Herein, quartz wool was used to separate the biomass and catalyst layers and also protect catalyst at the top side from being blown by the gas flow. The catalytic upgrading experiment in the Py/GC–MS instrument was carried out at 500 ºC for 3 min based on the preliminary experiments. It should be noted that the complex chemicals in the pyrolysis products cannot be all determined by the GC/MS accurately, and thus the signal peak area was used to reflect the relative yields of those detected pyrolysis products.

2.5 In-situ catalytic bio-oil upgrading in a fixed bed reactor

The catalytic upgrading experiments using the screened best catalyst by the Py/GC–MS analysis were further carried out in a quartz-glass-made fixed-bed reactor system. Typically, 0.25 g biomass sample and 0.25 g catalyst (B/C wight ratio = 1:1) were put separately at the reactor centre, which was heated by an ULVAC infrared furnace (VHT series, Japan) purged by N_2 gas with a flow rate of 100 cm^3/min for 10 min at ambient temperature for 10 min. The fixed-bed reactor was then heated rapidly to 500ºC with 1000 ºC/min heating rate and held at 500ºC for 3 min. During this period, a gas bag was used to collect the gas product. After the

reaction reached 3 min, the reactor was cooled to room temperature by a cooling water coil while the gas product was analyzed offline by a TCD-type GC system (Agilent 7890A, USA). The liquid product was condensed into cold acetone and analyzed using a Shimadzu Model GC 2010-Plus system equipped with a QP-2010 Ultra MS detector (MS), in which a 30 m×0.25 mm I.D.×0.25 μm HP-5MS column was utilized for determining the bio-oil composition with a boiling point below 300 ℃ based on NIST mass spectrum library. In this analysis. Generally, all compounds should be quantified using the calibration curves obtained from external standards. However, the complexity of the products made it impossible to find all available pure chemicals for making the standard curve. Therefore, in this research, the percentage of the relative peak area corresponding to each compound was applied to reflect the selectivity of product compounds whereas the peak area was used for the product quantification. The solids (catalyst and char) amounts were determined by directly weighting. Coke formed on the catalyst surface was analyzed via a Shimadzu TGA analysis instrument (DTG-60H, Japan), in which 10 mg of sample was heated from room temperature to 900 ℃ with 10℃/min heating rate in the air. All the experiments were repeated two or three times to confirm the results. The amount of coke on the catalyst was calculated from the decomposition temperature greater than 200 ℃ because the mass loss below 200 ℃ was attributed to the water evaporation and weakly absorbed organic compounds. For comparison, the B/C ratios of 1:2 and 1:4 were also used.

4.3 Results and discussion

4.3.1 Characterizations of Catalysts

Fig. 4.1 displays the morphologies of those synthesized hollow HZSM-5 samples with different initial Si/Al molar ratios of 30, 40 and 60. All catalysts had a quasi-rectangular shape with a particle size range of 150-350 nm. The cavity in each particle was obviously observed. With the increasing of the initial Si/Al molar ratio, the resulting crystal size slightly increased with a larger hollow cavity. These results are also consistence with the TEM analysis results

as displayed in **Fig.4.2**. In comparison, the Solid HZSM-5 had a uniform solid morphology. As shown in **Fig. 4.2(b-c)**, the zeolites with larger hollow cavities were obtained in the cases with the initial Si/Al molar ratios of 40 and 60, which had thinner zeolite shell. These results indicated that the hollow HZSM-5 nanoparticles can be simply synthesized by the present facile method. Furthermore, when the Hollow(30) zeolite was further treated with TPAOH (Hollow(30)-TP), the hollow cavity became larger but the overall size had almost no change. More interestingly, many mesopores were formed on the shell of Hollow(30)-TP due to the mild desilication by the TPAOH solution [22], which should be benefit for the providing more active sites and diffusion channels for the upgrading of the bio-oil.
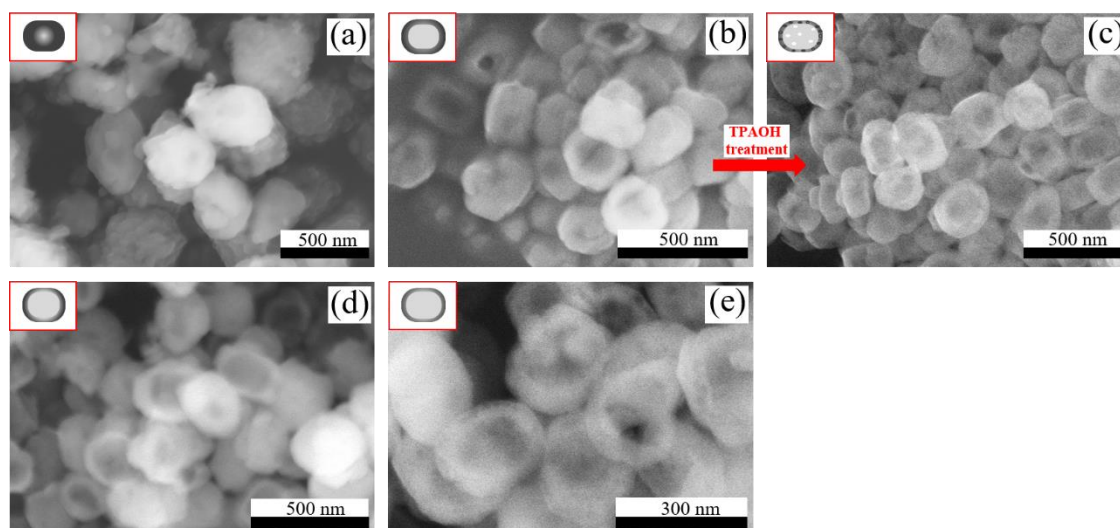
Fig. 4.1 SEM images of (a) Solid HZSM-5; (b) Hollow(30); (c) Hollow(30)-TP; (d) Hollow(40) and (e) Hollow(60).
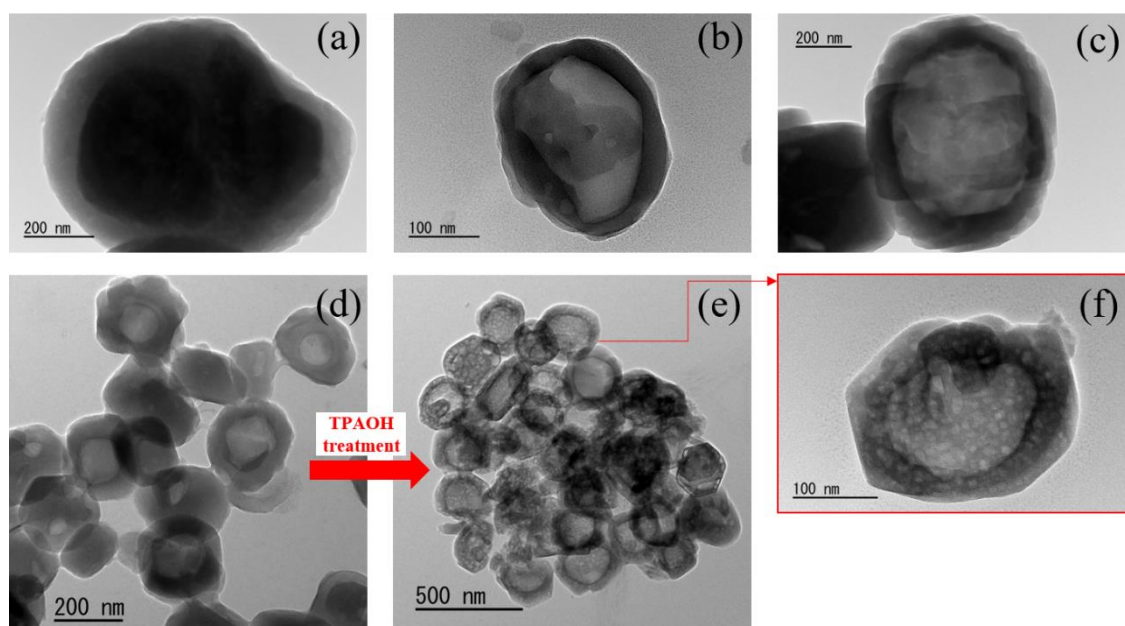
Fig. 4.2 TEM images of (a) Solid HZSM-5, (b) Hollow(40), (c) Hollow(60), (d) Hollow(30) and (e-f) Hollow(30)-TP
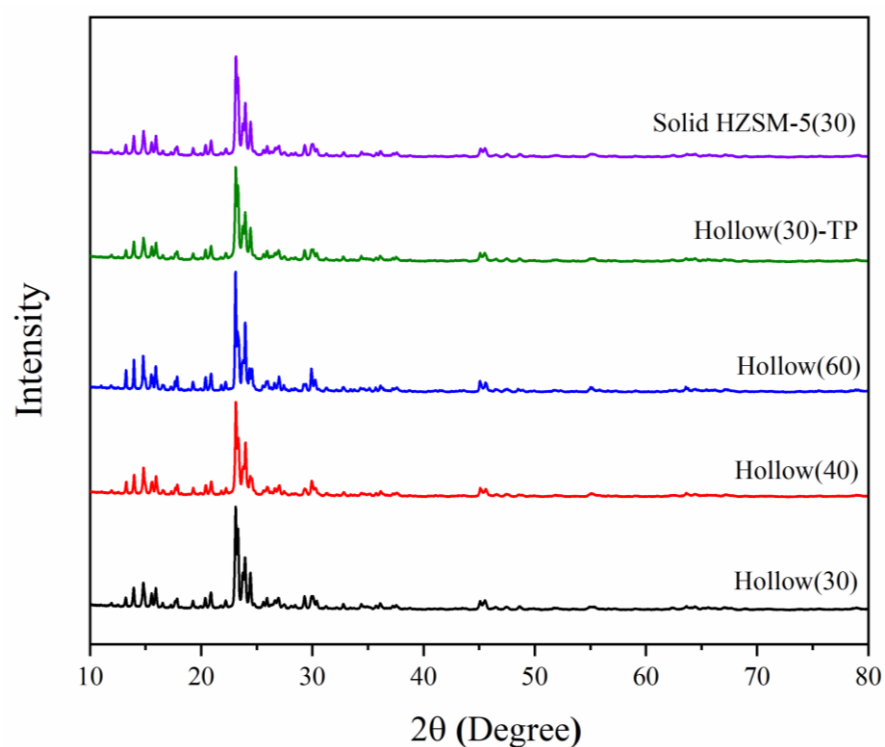
Fig. 4.3 XRD patterns of the hollow HZSM-5 catalysts

Fig. 4.3 exhibits XRD patterns of hollow HZSM-5 zeolites prepared with different initial Si/Al molar ratios. The strong diffraction peaks appeared at the 2θ range of 23-25º for all as-obtained zeolites confirmed the presence of a well-crystallized MFI structure (ZSM-5) [25],

which also indicated that the addition of NaOH in the precursor solution had no effect on the crystallization of ZSM-5, but it resulted in the hollow structure. **Fig. 4.4** shows the NH_3-TPD analysis results of hollow and solid HZSM-5 zeolite catalysts. There were two ammonia desorption peaks at the temperature ranges of 120-300 and 300-600℃, relating to weak acid sites and strong acid sites, respectively [25]. All catalysts showed almost the similar desorption temperatures. Herein, the acid strength can be inferred by the peak temperature whereas the peak area associates with the acid amount [28]. However, a small shift to the higher temperature was observed for all hollow ZSM-5 zeolite catalysts when compared with that of the solid HZSM-5. As summarized in **Table 4.1**, the total acid amount was decreased with the increasing of the initial Si/Al molar ratio owing to the partial removal of Al species from the framework accompanying with Si species during desilication [29]. In addition, the Hollow(30) exhibited a higher Lewis acid amount and a lower Brønsted acid amount than those of Solid HZSM-5(30). Herein, the Lewis acid site is normally associated with extra framework Al species. Thus, when partial Al species were extracted from the framework, to form an external framework, Lewis acid amounts were increased [25]. Moreover, it can be seen that the Hollow(30)-TP had the highest acid amount followed by the Hollow(30) and solid HZSM-5, successively. This suggested that the mesopores formed on the hollow ZSM-5 shell resulted in the generation of more acid amount, which can also provide more access channels for the reactants reaching the acid sites on the hollow zeolite. Normally, high acidity is benefit for the dehydrogenation, aromatization and cracking [30].

Table 4.1 Acidity of hollow HZSM-5 and solid HZSM-5 catalysts

Catalyst	Acid amount (mmol/g, low temp)	Acidity amount (mmol/g, high temp)	Total acid amount (mmol/g)
Hollow(30)	0.34	0.37	0.71
Hollow(40)	0.15	0.18	0.33
Hollow(60)	0.08	0.16	0.24
Hollow(30)-TP	0.36	0.36	0.72
Solid HZSM-5(30)	0.26	0.40	0.66
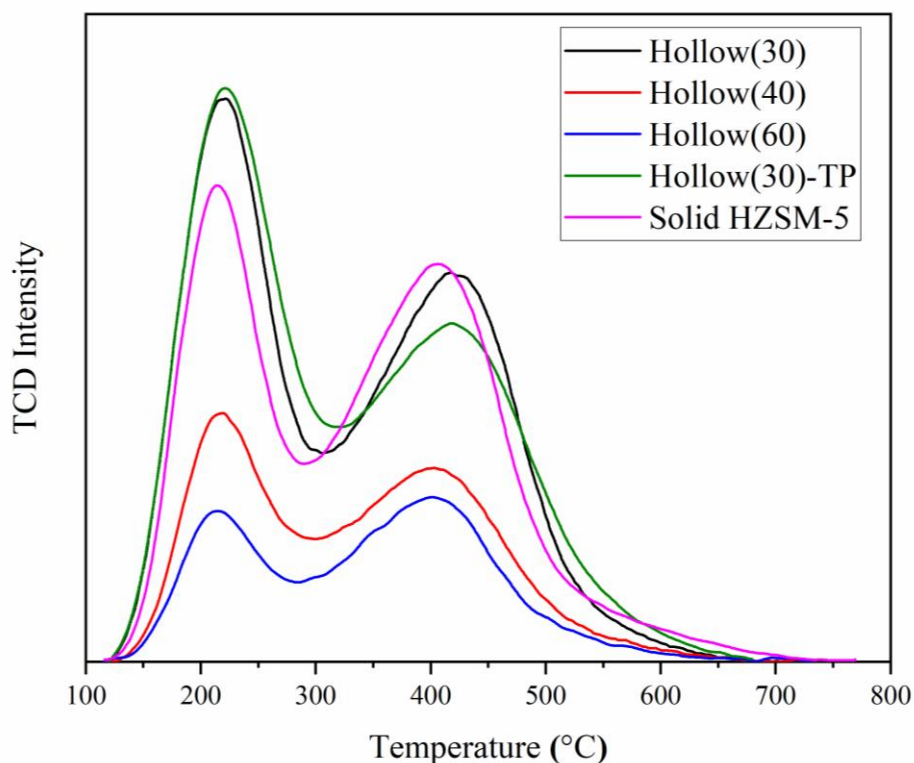
Fig. 4.4 NH_3-TPD profiles of the hollow HZSM-5 catalysts

  Fig. 4.5(a) shows BET isotherms of the hollow ZSM-5 samples prepared with various initial

Si/Al molar ratios and the Solid ZSM-5. For the Solid ZSM-5, a representative type I isotherm

based on the classification of IUPAC was obtained, which is the characteristics of microporous

materials [31]. In contrast, Hollow(30) exhibited a type I isotherm with a plateau at relative pressure $P/P_0 < 0.45$ and a H4-type hysteresis loop at $P/P_0 = 0.45$-1, revealing both micropores and mesopores were formed in the structure [32]. With the increasing of the initial Si/Al molar ratio during the synthesis of zeolite from 30 to 60, the progression of the hysteresis loop indicated the generation of larger mesopores [33]. Meanwhile, with the increase in the amount of Al in the ZSM-5 zeolite, further desilication could be inhibited to limit the generation of more mesopores [34]. On the other hand, when the Hollow(30) was further treated with TPAOH the type IV isotherm with a larger hysteresis loop was obtained, which indicated the presence of numerous mesopores in the catalyst at high relative pressures ($P/P_0=0.4$–1.0) [35]. As a result, a largest total pore volume of 0.49 cm^3/g was achieved. **Fig. 4.5(b)** shows the corresponding DFT pore size distributions. It can be observed that the Solid ZSM-5 had micropores (<2 nm) with a large volume and mesopores (2.5-4 nm) with a small amount. In comparison, for the hollow ZSM-5 zeolites, their main mesopores were distributed in two ranges, i.e., 2.5-4 and 15-30 nm. More specifically, the Hollow(30)-TP presented a large volume of mesopores in the narrow ranges of 3-4 and 15–30 nm. It can be inferred that the number of mesopores was greatly increased by the further treatment with TPAOH [21]. The surface areas and pore volumes are summarized in **Table 4.2**. Since the formation of hollow structure in the HZSM-5 catalyst could reduce the number of micropores in the zeolite, the surface area (S_{BET}) was slightly reduced when comparing with that of the Solid ZSM-5 sample. Among all the as-synthesized hollow catalysts, Hollow(30) had a highest surface area of 369.9 m^2/g. While, Hollow(60) showed a highest total pore volume but with a lowest micropore volume. Furthermore, the additional TPAOH treatment for hollow(30) maintained a similar high surface area (365.0 m^2/g) as the original hollow(30) but with a decrease of micropore surface area. This indicated that the TPAOH treatment increased the mesopore surface area.

Table 4.2 Textural properties of hollow HZSM-5 and solid HZSM-5 catalysts

Catalyst	S_{BET} (m^2/g)	S_{micro} (m^2/g)	V_{total} (cm^3/g)	V_{micro} (cm^3/g)
Hollow(30)	369.9	289.2	0.36	0.14
Hollow(40)	331.0	290.9	0.35	0.14
Hollow(60)	301.2	224.2	0.45	0.10
Hollow(30)-TP	365.0	208.4	0.49	0.10
Solid HZSM-5(30)	373.6	315.3	0.28	0.16
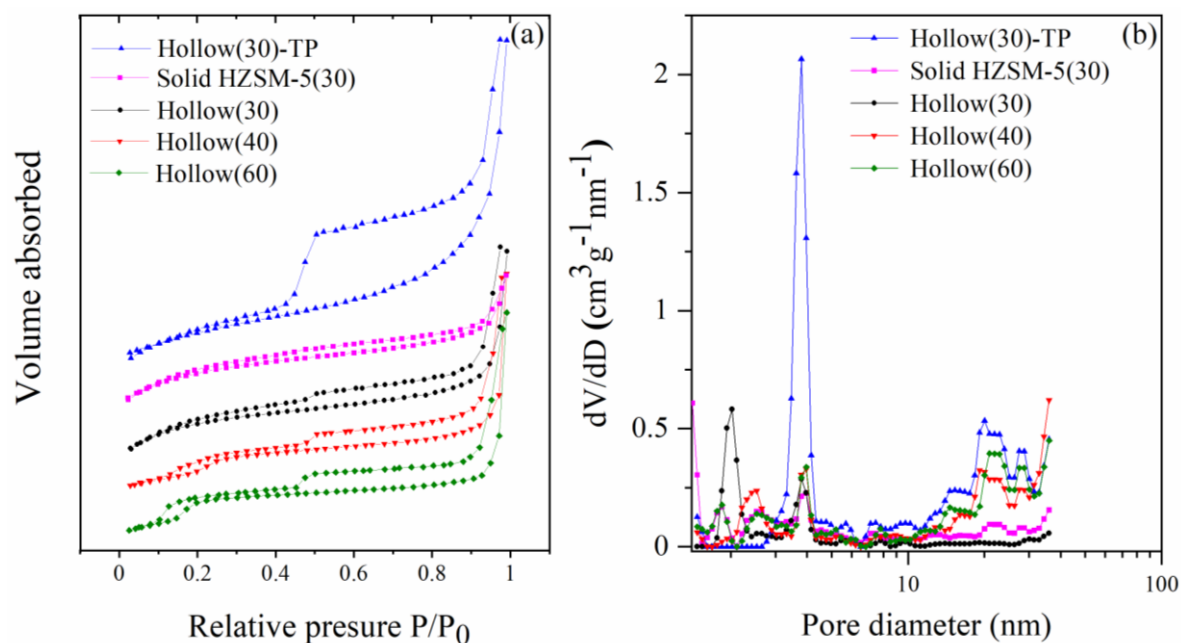
Fig. 4.5 N_2 adsorption/desorption isotherms (a) and DFT pore size distributions (b) of the hollow HZSM-5 catalysts

Based on the results shown above, **Scheme 4.1** illustrates the formation mechanism of the hollow ZSM-5 structure. As TEOS is mixed with the diluted TPAOH solution, hydrolysis of TEOS occurs, which was observed as a clear homogeneous solution, indicating that a colloidal solution was formed [36]. After the addition of mixture containing Al species, NaOH and H_2O, an amorphous aluminosilicate gel is formed in the aging period. Under the hydrothermal treatment process, the formation of nuclei surrounded by the organic structure-directing agent
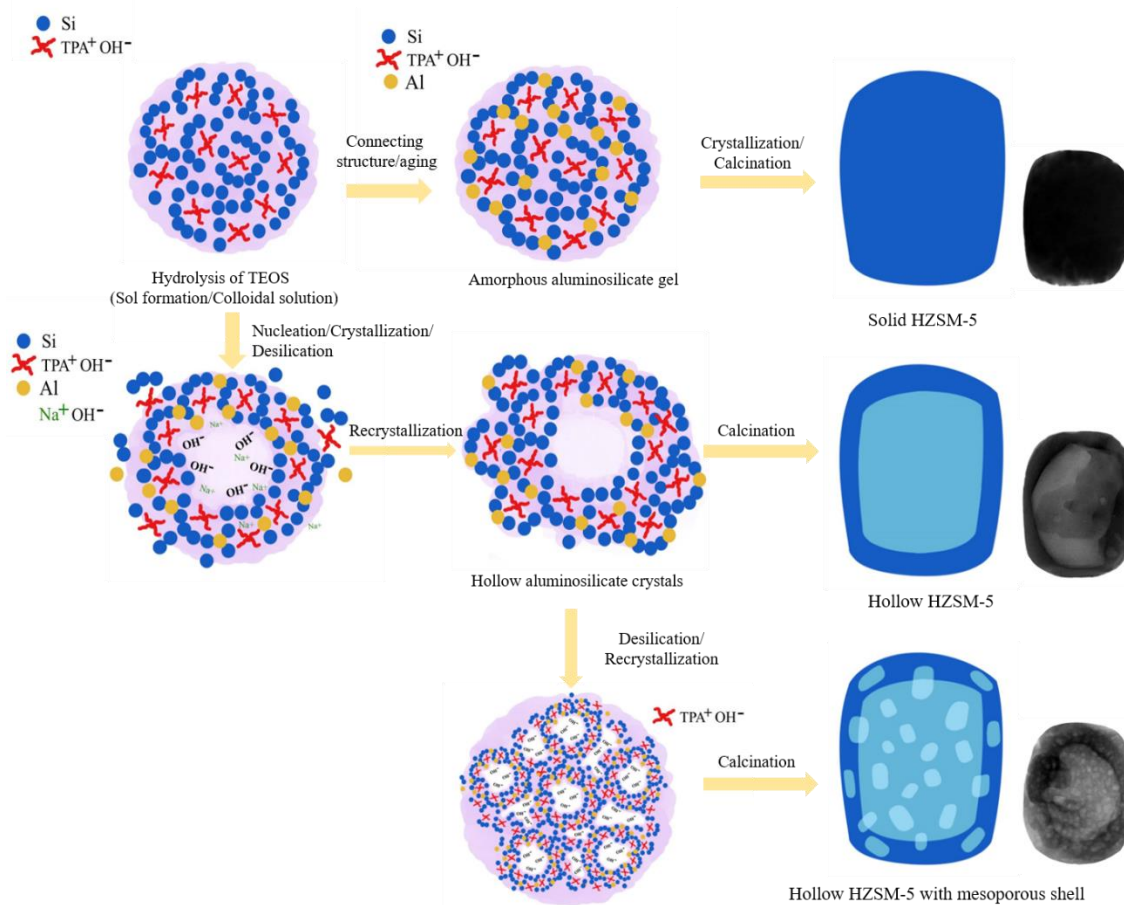
Scheme 4.1 Formation mechanism of hollow ZSM-5 structure

of TPA$^+$ will be formed with a connecting structure, followed by crystal growth [37]. Herein,

in the absence of NaOH, solid ZSM-5 crystal will be formed; however, in the presence of

NaOH, the formed solid ZSM-5 crystals were desilicated to form hollow crystals [38]. Since

most of the Si atoms on the shell are stabilized by the neighbour AlO$_4^-$ tetrahedron and

negatively charged OH$^-$ groups, the extraction of Si in the outer shell will be hindered.

However, since the Na$^+$ cation is smaller the TPA$^+$ cation so that it is usually located in the

internal structure of the zeolite crystal precursor, which can result in more favourable internal

dissolution of framework Si and prevent the recrystallization of desilicated Si with the partial

desilicated Al species around TPA$^+$, a hollow cavity could be formed in the zeolite crystal

precursor, and thereby obtaining hollow structure after the calcination [25]. Furthermore, when

the hollow HZSM-5 zeolite is treated by TPAOH again, the framework Si in the shell will be

mildly desilicated to form mesoporous structure on the shell with the secondary recrystallization [28].

4.3.2 TGA analysis of biomass

Fig. 4.6 shows the TGA profiles of cellulose, hemicellulose, lignin and cedar wood. The differences among these TG curves reflected the different pyrolysis behaviours of the components in biomass. The first stage of weight loss at the temperature less than 200 ºC for all the samples was resulted from the loss of water and weakly absorbed organic compound [39]. After that, for the hemicellulose, it started to decompose faster than other samples in the temperature range of 210-320 ºC, and then a slow weight loss was observed until dropped again in the 670-780 ºC range with a solid residue left of 6.5%.
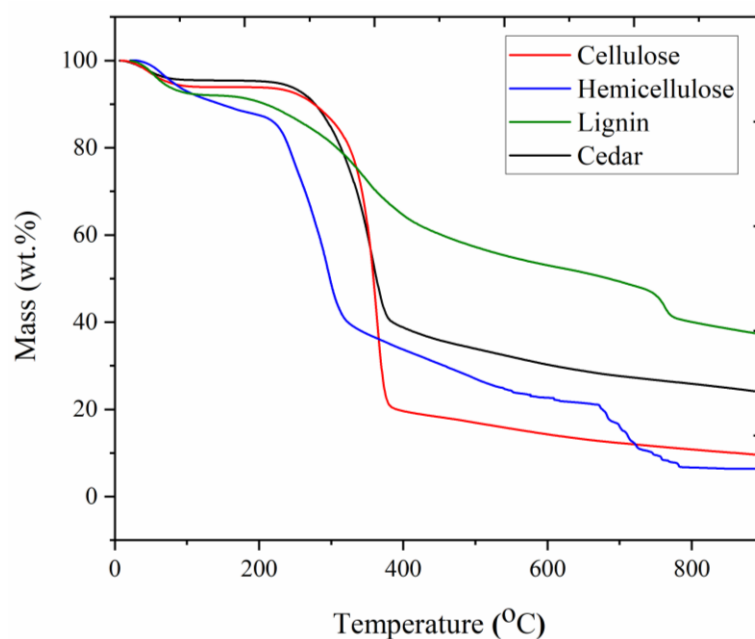
Fig. 4.6 TGA profiles of biomass materials.

While, the cellulose had the greatest weight loss temperature range of 250-380 ºC and after that, it showed a little weight loss with a final remaining residue of 9.5%. For the lignin, it exhibited a spontaneous decomposition slowly over a wide temperature range of 200-900 ºC with a highest remaining residue of 40%, indicating that lignin is the most difficult decomposition component in the biomass. Cedar wood was selected as the representative of

actual biomass in this study, and it exhibited a decomposing curve that is quite similar to that of cellulose but it had a lower decomposition rate with the remaining residue of 23.9%.

4.3.3 Catalysts screening

Fig. 3 compares the chemical compositions obtained in the upgraded bio-oils generated from the rapid pyrolysis of three biomass components using the as-prepared catalysts examined by Py-GC/MS. For the bio-oil derived from cellulose, as shown in **Fig. 4.7a**, in the case without catalysts, almost no aromatic hydrocarbons except ketones and other oxygenates. In the presences of catalysts, one can see that the Hollow(30) led to the highest aromatic hydrocarbon content. Generally, the zeolite catalyst with higher Si/Al molar ratio has lower catalytic cracking ability, which could result in the decrease in the yield of aromatic hydrocarbon yield [30]. In comparison, by using the Hollow(30)-TP, the formation of aromatic hydrocarbons was further promoted with an increase in the relative peak area of aromatic hydrocarbons to a maximum value of 78.67%. Herein, the highest aromatic hydrocarbon content obtained from the use of Hollow(30)-TP should be ascribed to its hollow structure with abundant mesopores on the shell since such a structure could obviously reduce the diffusion length to improve the mass transport of the reactants and products through the mesoporous structure to contact more active sites [27]. It can be concluded that a catalyst with more hollow spaces and thinner porous shell will promote the production of aromatic hydrocarbon. For the upgrading of bio-oil from hemicellulose (Fig. 3b), it showed similar result as that for the cellulose. That is, the Hollow(30)-TP also served as the best catalyst. Different from the cellulose and hemicellulose, since lignin consists of phenylpropanes, it can be typically pyrolyzed and cracked into aromatic compounds like phenolics, aromatic ethers, and other monomers [40]. It is found that the use of Hollow(30) resulted in the highest aromatic hydrocarbon content, but the application of Hollow(30)-TP decreased the aromatic hydrocarbon content. This might be due to that those components commonly found in the raw bio-oil such as phenol (guaiacol, creosol) and others (mainly vanillin) cannot effectively

diffused in the rich mesopore of Hollow(30)-TP, resulting in a negative effect on the final product. Possible reaction pathways during the in-situ upgrading of bio-oils from the fast pyrolysis of three biomass components are illustrated in **Scheme 4.2**. Herein, the pyrolysis of cellulose and hemicellulose have a similar mechanism. However, their different components in the bio-oil should have different primary decomposition pathways over the catalysts. That is, the cellulose would be cracked initially into anhydro-monosaccharides like levoglucosan, which is the main product in the pyrolysis of cellulose while the hemicellulose can be broken down to furfural and related derivatives at first [41]. Then, in the presence of catalysts, both levoglucosan and furfural could be broken down by ring scission, followed by rearrangement, and deacetylation to form 1-hydroxy-2-Propanone and acetic acid [42]. In addition, recyclization, dehydration and other reaction could also occur and further convert levoglucosan or smaller esters and ketones into aromatic hydrocarbons. While, furfural and related derivatives can be also converted to aromatics through those reactions on the outer and internal Brønsted acid sites of the hollow zeolite [43]. Thus, various reactions could occur during the upgrading of bio-oil by the significantly high degree of utilization of the internal surfaces within the hollow zeolite structure. In contrast, lignin is a complex polymer with three interconnected phenylpropanes enriched with aromatic rings. During the pyrolysis of lignin, macromolecule chains would be broken down to form free radicals containing a benzene ring, which are mainly phenolic compounds.
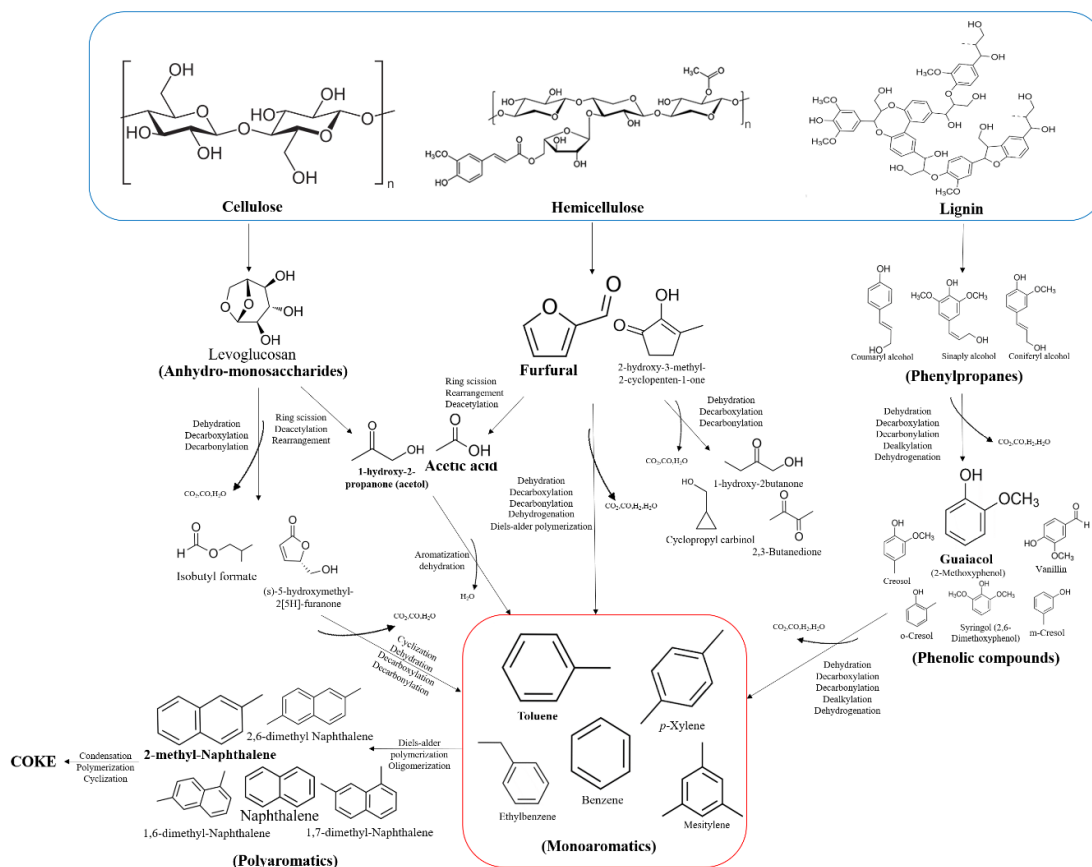
Scheme 4.2 Possible reaction pathways for the in-situ upgrading of bio-oils generated from the rapid pyrolysis of cellulose, hemicellulose and lignin over hollow HZSM-5 catalysts

Subsequently, in the presence of catalysts, various aromatic compounds could be generated. Moreover, coke could be also formed on the catalyst due to the improper acidity and improper diffusion distance in the zeolite structure. In this study, the use of both Hollow(30) and Hollow(30)-TP catalysts not only contribute to the reduction of coke but also accelerate the conversion of bio-oil into more aromatic hydrocarbons without altering the specific aromatics distributions since the high access ability to the acid sites on the zeolite improved the reaction rates and the reduced diffusion length led to the more coke deposition on the external surface.
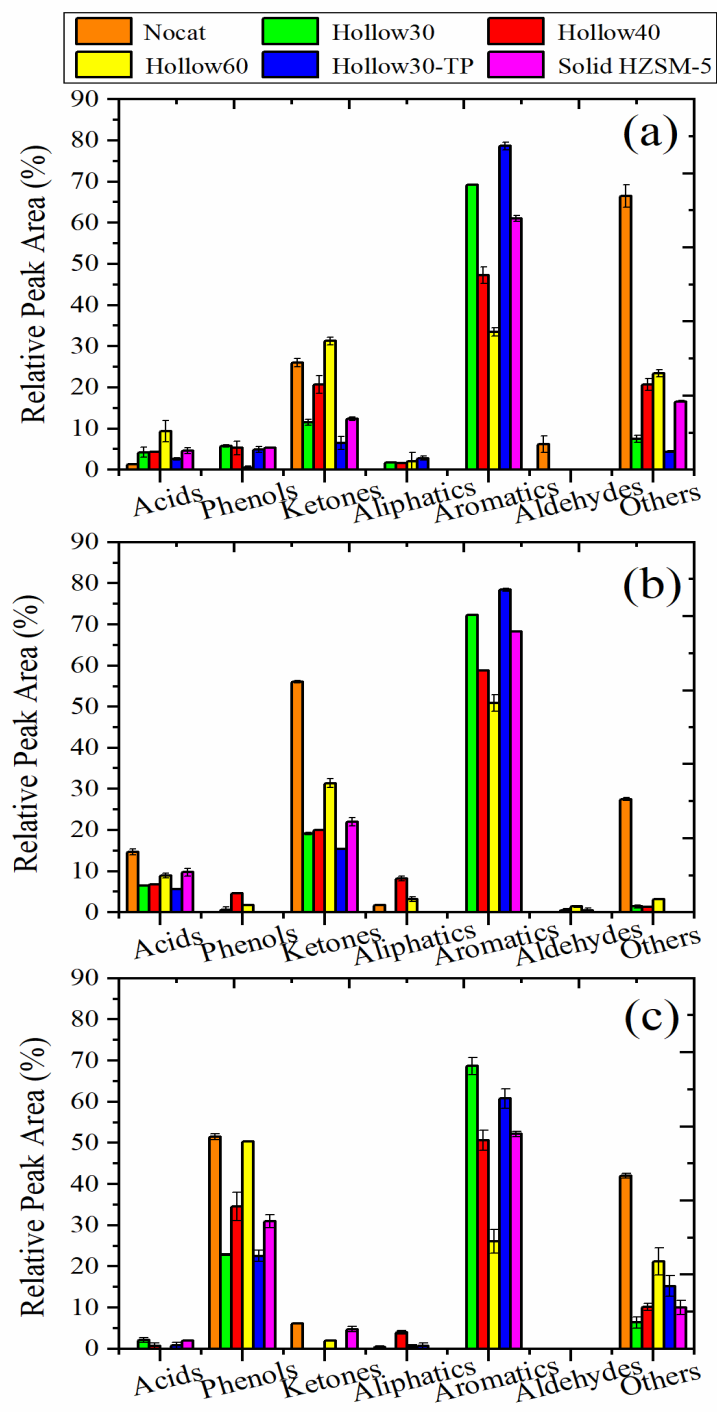
Fig. 4.7 Relative peak areas of compounds in the upgraded bio-oils from catalytic upgrading determined by Py-GC/MS for different biomass feedstocks: cellulose (a), hemicellulose (b) and lignin (c) with hollow HZSM-5 catalysts

4.3.4 *In-situ catalytic bio-oil upgrading in a fixed bed reactor*

4.3.3.1 *Effect of biomass to catalyst weight ratio*

In-situ catalytic bio-oil upgrading was also carried out in a fixed bed quartz reactor to verify

the performance of the catalyst in the Py-GC/MS analysis and obtain more information on coke, gases, water, and upgraded bio-oil composition. Herein, the best catalyst screened by the Py-GC/MS results was utilized and the effect of biomass to catalyst (B/C) weight ratio was investigated at first. **Fig. 4.8** shows the relative peak areas and peak areas of compounds using Hollow(30)-TP for cellulose and hemicellulose and Hollow(30) for lignin. By using a B/C weight ratio of 1:1 for cellulose, the relative peak area of aromatic hydrocarbons was 78.7%, and with the increasing of the B/C weight ratios to 1:2 and 1:4, as expected, the relative peak areas of aromatic hydrocarbons were increased to 88.0% and 99.7%, respectively. It has been reported that more catalysts addition can increase the conversion of oxygenates [44]. Similarly, for the hemicellulose, as the B/C weight ratio was increased to 1:2 and 1:4 from 1:1, the relative peak areas of aromatic hydrocarbons were increased to 83.8% and 100% from 74.2%. While, for the lignin, when the Hollow(30) catalyst, which was the best one during Py-GC/MS screening, was used, the same trend was observed. That is, the relative peak area of aromatic hydrocarbons were increased to 75.6% and 85.4% from 64.5% as the B/C weight ratio was raised to 1:2 and 1:4 from 1:1. Thus, the use of cellulose, hemicellulose, and lignin in combination with their corresponding best catalysts for the upgrading of bio-oil, the relative peak areas of aromatic hydrocarbons increased in the same way when increasing the B/C weight ratio from 1:1 to 1:4. While, it should be noted that the peak areas of aromatic hydrocarbons did not show significant change after increasing the B/C weight ratio of 1:2 to 1:4, however, the peak areas of other compounds decreased, especially for the cellulose and hemicellulose. Therefore, the highest aromatic hydrocarbon yield could be limited by increasing the catalyst amount in the reaction system.

On the other hand, it can be observed that the chemical distribution changed to some extent when comparing with the results obtained in the Py-GC/MS analysis (Fig. 4.7). That is, the order of chemical distribution for cellulose and hemicellulose with the use of Hollow(30)-TP was as follows: aromatics > ketones > phenols in the Py-GC/MS analysis, which was changed

to aromatics > acids > others obtained in the fixed bed reactor. While, for the lignin with the use of Hollow(30), it changed from aromatic > phenols > others (in the Py-GC/MS analysis) to aromatics > other > phenols (using fixed bed reactor). Such changes could be resulted from the different sample amounts in two reaction systems and different operation conditions, which could affect the heat and mass transfer in the reactors, thereby changing the product distributions.
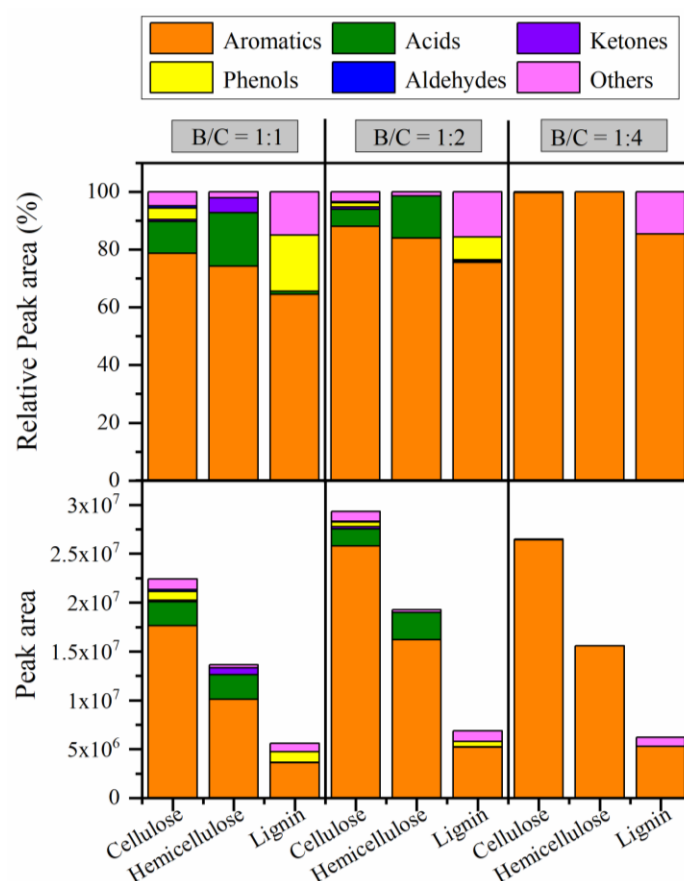
Fig. 4.8 Relative peak areas and peak areas of compounds obtained from the fixed bed reactor using the best catalysts for each biomass feedstock(cellulose+hollow(30)-TP, hemicellulose+ hollow(30)-TP, lignin+ hollow(30)) with various B/C weight ratios of 1:1, 1:2 and 1:4.

In this study, the disappearing of oxygenated compounds implied that they have been converted to aromatic hydrocarbons with the generation of water and/or CO and CO_2 gases. While, some generated aromatic hydrocarbons could be further converted to PAHs or coke through secondary reactions [45]. It is clearly seen in **Fig. 4.9** that the increasing use of the catalyst decreased monoaromatics (MAHs) including benzene, toluene and p-xylene while other alkylbenzenes and PAHs like naphthalene were increased. This suggested that the use of high amount of catalyst enhanced the conversion of oxygenated components in the bio-oil to PAHs by increasing a series of reactions among MAHs and other oxygenated compounds.
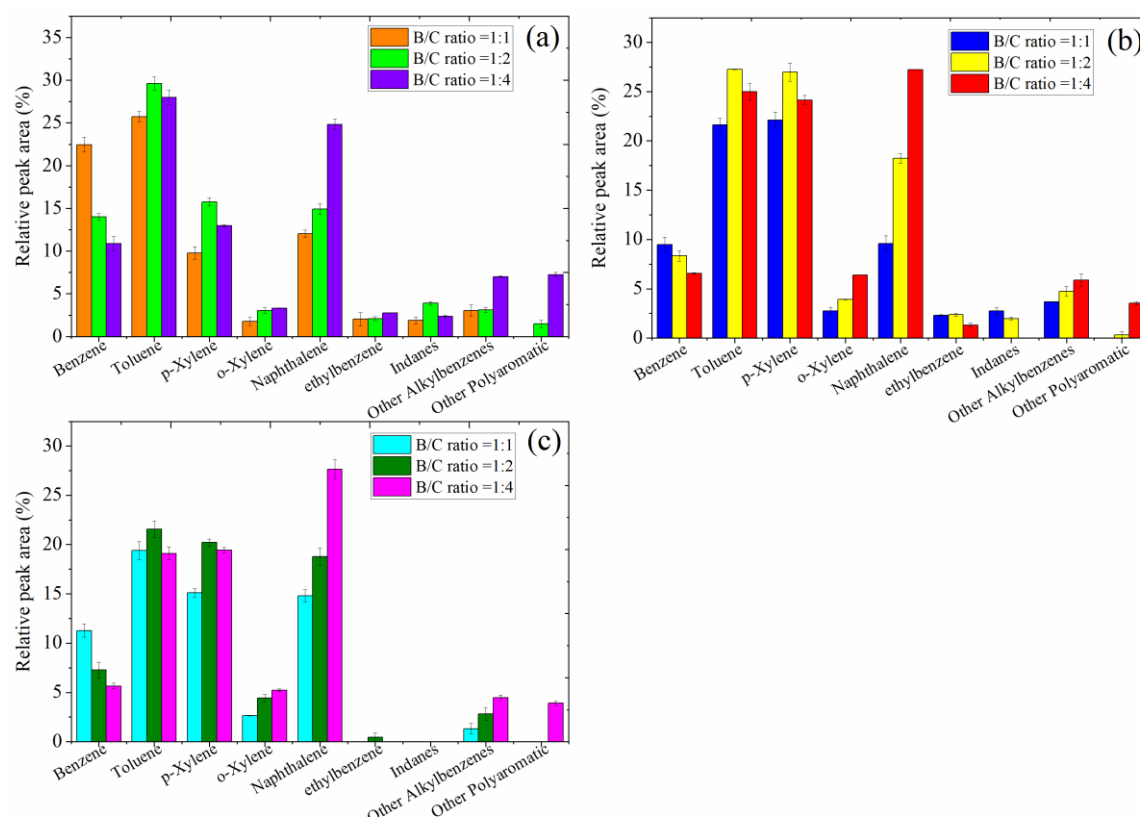
Fig. 4.9 Relative peak areas of specific aromatics in the upgraded bio-oils obtained from in-situ catalytic upgrading using the fixed bed reactor for different biomass feedstocks: cellulose (a), hemicellulose (b) and lignin (c) with their corresponding best hollow catalysts.

4.3.3.2 Mass balance and gas yields

Fig.4.10 shows the mass balance and gas yields during the in-situ catalytic upgrading of bio-oils generated from the rapid pyrolysis of cellulose, hemicellulos and lignin. Herein, the average data from 3 repeated experiments are shown. Bio-oil amount in each experiment was obtained from calculating the weight difference of original biomass mass and the generated water, coke, gas, and char weights after the reaction. As shown in Figs. 7(a) and (b), when the B/C weight ratio was raised to 1:2 and 1:4 from 1:1 for cellulose and hemicellulose, the gas and water yields increased while bio-oil significantly decreased since the increased amount of catalyst promoted decarbonylation, decarboxylation, and various hydrocarbon conversion reactions such as cracking and aromatization reactions [46]. That is, the high amount of acid sites available at higher catalyst mass loading enhanced these reactions to generate more gas, water, and coke. Interestingly, an opposite trend was observed when lignin was used, in which both bio-oil and gas yield were gradually decreased with the increasing of B/C weight ratio from 1:1 to 1:4 but the coke yield was obviously increased. At the highest catalyst loading (B/C ratio of 1:4), the coke formation significantly increased, which should be resulted from the re-polymerization of deoxygenated intermediates and the condensation of hydrocarbons [46], which is consistence with the results shown in **Fig. 4.9**, where more PAHs were produced. As shown in **Figs. 4.10 (d,e,f)**, the main gaseous products from the three cases were similar, including H_2, CO_2, and CO. One can see that the cellulose and hemicellulose are preferable to produce gaseous products while a higher coke generating rate was observed for the lignin. Thus, with the increasing of catalyst amount in the reaction system, more aromatic hydrocarbons could be condensed to form coke but it is unfavourable for the gas generation.
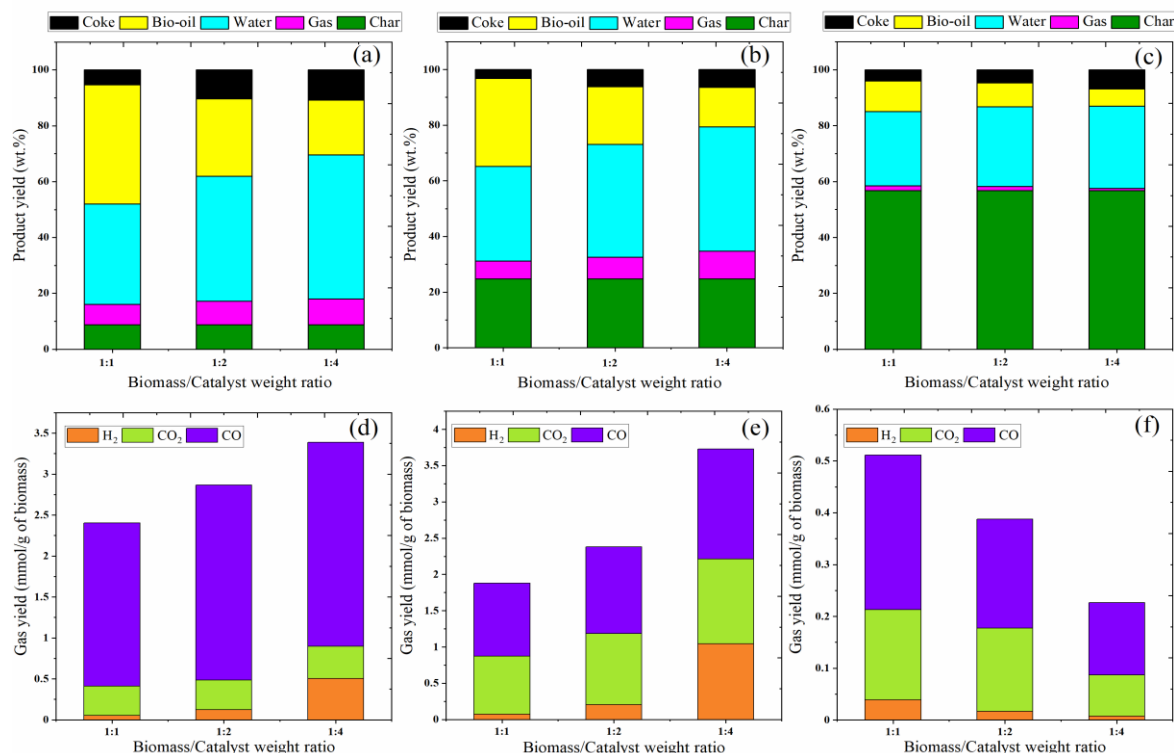
Fig. 4.10 Mass balances and gas yields obtained from the in-situ upgrading of bio-oils using the fixed bed reactor in the presence of the best catalyst of each biomass feedstock (a),(d) of (cellulose+hollow(30)-TP, (b),(e) of hemicellulose+ hollow(30)-TP and (c),(f) of lignin+ hollow(30)) with various B/C weight ratios of 1:1, 1:2 and 1:4.

4.3.3.3 Application for the real biomass

  Although the actual biomass consists of cellulose, hemicellulose and lignin, the interaction between these three components in the influence of the pyrolysis behavior of the biomass is still unclear [47]. In the above studies, it is found that the Hollow(30) was the best catalyst for the in-situ upgrading of bio-oils generated from the rapid pyrolysis of lignin but the Hollow(30)-TP was the best one in the case of using cellulose and hemicellulose, and meanwhile, the optimum B/C weight ratio was 1:2. In this section, a real biomass, i.e., cedar wood, was used as the representative to confirm the performance of these best catalysts for the in-situ upgrading of bio-oil generated from the rapid pyrolysis of real biomass. As shown in **Fig.4.11(a)**, it can be seen that the main components in the upgraded bio-oils with both Hollow(30) and Hollow(30)-TP were aromatic hydrocarbons, and the use of Hollow(30)-TP resulted in higher aromatic hydrocarbon content with a larger relative peak area of 80.16%

129

than that by using the Hollow(30) (75.53%) and also a much higher peak area of aromatics as displayed in **Fig. 4.11(b)**. The catalytic influence on the distributions of specific aromatics is shown in **Fig.4.11 (c)**. One can see that by using both Hollow(30) and Hollow(30)-TP, the obtained aromatic hydrocarbons were mainly MAHs such as toluene, p-xylene, and benzene and PAHs like naphthalene. Herein, the selectivity towards aromatic hydrocarbons was similar to the cases using pure chemicals (cellulose, hemicellulose and lignin).
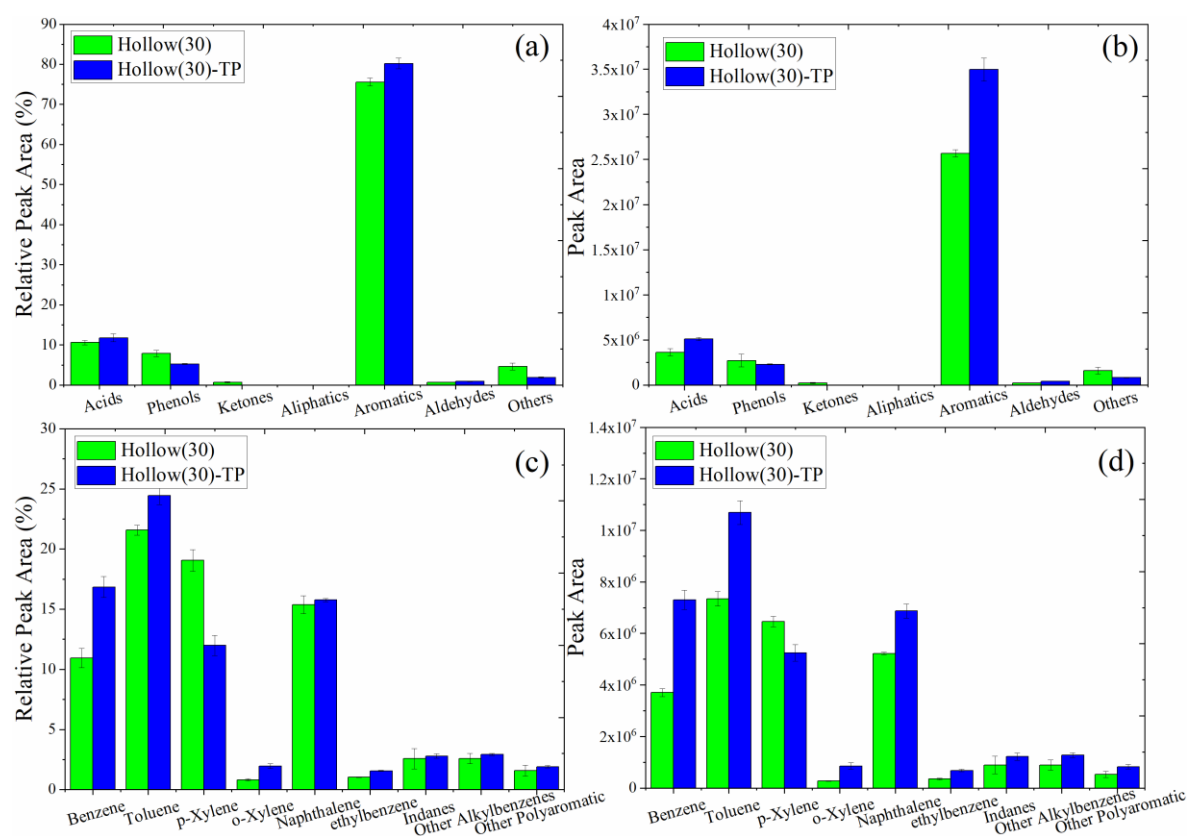
Fig. 4.11 (a-b) Relative peak areas and peak areas of compounds and (c-d) Relative peak areas and peak areas of specific aromatic hydrocarbons obtained from the use of the fixed bed reactor with a B/C weight ratio of 1:2.

Moreover, the Hollow(30)-TP exhibited a more excellent performance for the in-situ upgrading of bio-oil generated from the real biomass, also indicating that the increased mass

transfer capacity resulting from abundant mesopore on the hollow structure of HZSM-5 should be more benefit for the promoting the generation of MAHs and the inhibiting the reactions leading to larger alkylated aromatics and PAHs, thereby resulting in the production of the highest amount of MAHs in the upgraded bio-oil. **Fig. 4.12** shows the mass balance of products and gas production.
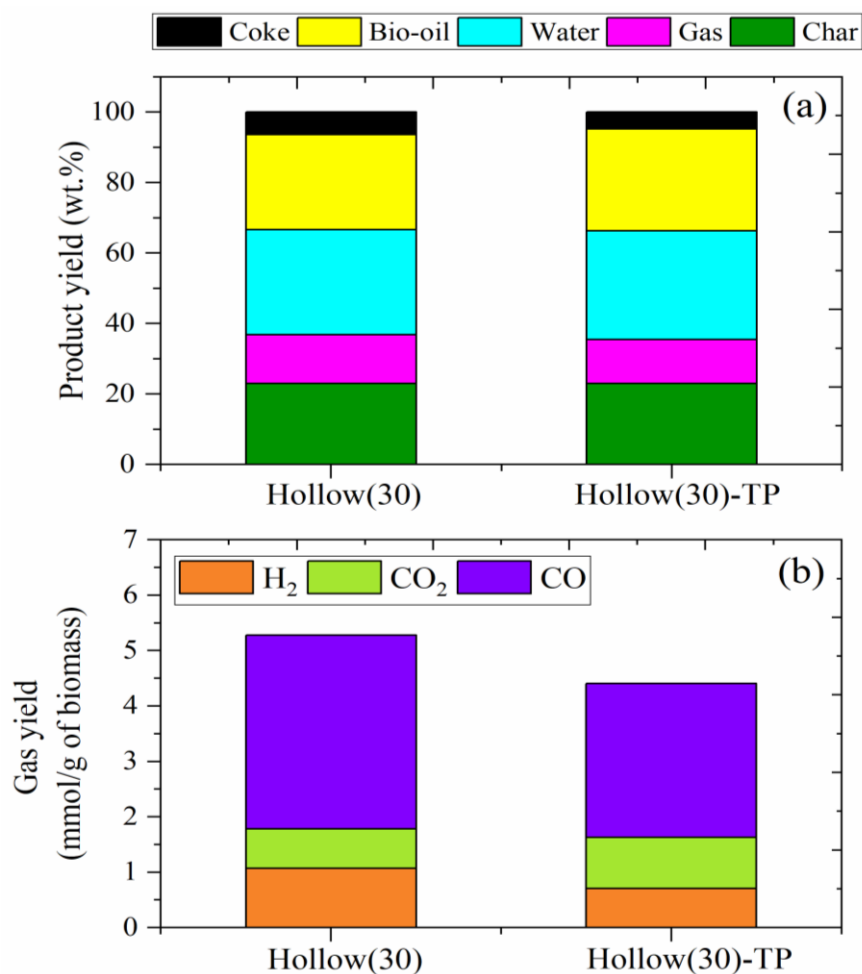
Fig. 4.12 Mass balances and gas yields obtained from the fixed bed reactor using cedar wood as the feedstock with a B/C weight ratio of 1:2.

One can see that the total gas yield (5.28 mmol/g) by the using of Hollow(30) was higher than that by using Hollow(30)-TP (4.40 mmol/g), indicating that the secondary cracking over the Hollow(30)-TP could be hindered to form more gases and coke, hence increasing the bio-oil yield. This also confirmed that the abundant mesopores and hollow structure of

Hollow(30)-TP allowed the reactants more accessible active sites and thus led the product leave out from the catalytic sites faster. In addition, it can be seen that the gas product compositions were mainly CO and CO_2 for the cases using either Hollow(30) or Hollow(30)-TP, indicating the deoxygenation occurred mainly via the decarbonylation and decarboxylation [48].

4.4 Conclusions

In this work, novel hollow HZSM-5 zeolites were prepared by a facile hydrothermal method, and applied for the in-situ catalytic upgrading of bio-oils generated from the rapid pyrolysis of cellulose, hemicellulose and lignin. From Py-GC/MS analysis, it is found that among the hollow HZSM-5 zeolite catalysts prepared with different initial Si/Al molar ratios, the Hollow(30) with the initial Si/Al molar ratio of 30 showed the best performance that can produce the highest aromatic hydrocarbon content. Furthermore, when the Hollow(30) was further treated with TPAOH (Hollow(30)-TP), abundant mesopores were found to be formed on the shell of the hollow HZSM-5, which exhibited the highest performance for the aromatic hydrocarbon production in the upgraded bio-oils generated from cellulose and hemicellulose but a decreased aromatic hydrocarbon amount when using lignin as the feedstock. Based on the experiments in a fixed bed reactor, the B/T weight ratio of 1:2 was found to be the optimum condition with the high aromatic selectivity. In addition, when the cedar wood was used as the representative of real biomass, by using the Hollow(30)-TP, the coke yield was reduced when compared to the parent Hollow(30), which led to a maximum aromatic hydrocarbon content of 80.16% in the upgraded bio-oil. It is believed that the improvement of reactants and products diffusion limitation of the zeolites and expose more active sites through the generation of hollow structure with mesoporous shell of the HZSM-5. In addition, the hollow structure and the presence of high mesopores also played crucial roles in determining the aromatics selectivity as well as solving the coke formation.

References

[1] Gómez, N., Banks, S.W., Nowakowski, D.J., Rosas, J.G., Cara, J., Sánchez, M.E., Bridgwater, A.V. 2018. Effect of temperature on product performance of a high ash biomass during fast pyrolysis and its bio-oil storage evaluation. Fuel Process. Technol., 172, 97-105.

[2] Zou, R., Wang, Y., Jiang, L., Yu, Z., Zhao, Y., Wu, Q., Dai, L., Ke, L., Liu, Y., Ruan, R. 2019. Microwave-assisted co-pyrolysis of lignin and waste oil catalyzed by hierarchical ZSM-5/MCM-41 catalyst to produce aromatic hydrocarbons. Bioresour. Technol., 289, 121609.

[3] Moogi, S., Jae, J., Kannapu, H.P.R., Ahmed, A., Park, E.D., Park, Y.K. 2020. Enhancement of aromatics from catalytic pyrolysis of yellow poplar: Role of hydrogen and methane decomposition. Bioresour. Technol., 315, 123835.

[4] Peng, J., Chen, P., Lou, H., Zheng, X. 2009. Catalytic upgrading of bio-oil by HZSM-5 in sub- and super-critical ethanol. Bioresour. Technol., 100(13), 3415-3418.

[5] Nishu, Liu, R., Rahman, M.M., Sarker, M., Chai, M., Li, C., Cai, J. 2020. A review on the catalytic pyrolysis of biomass for the bio-oil production with ZSM-5: Focus on structure. Fuel Process. Technol., 199, 106301.

[6] Zhang, Z., Liu, L., Shen, B., Wu, C. 2018. Preparation, modification and development of Ni-based catalysts for catalytic reforming of tar produced from biomass gasification. Renew. Sustain. Energy Rev., 94, 1086-1109.

[7] Ji, Y., Yang, H., Yan, W. 2017. Strategies to enhance the catalytic performance of ZSM-5 zeolite in hydrocarbon cracking: A Review. Catalysts, 7(12).

[8] Primo, A., Garcia, H. 2014. Zeolites as catalysts in oil refining. Chem. Soc. Rev., 43(22), 7548-7561.

[9] Mihalcik, D.J., Mullen, C.A., Boateng, A.A. 2011. Screening acidic zeolites for catalytic fast pyrolysis of biomass and its components. J. Anal. Appl. Pyrol., 92(1), 224-232.

[10] Wei, B., Jin, L., Wang, D., Xiong, Y., Hu, H., Bai, Z. 2020. Effect of different acid-leached USY zeolites on in-situ catalytic upgrading of lignite tar. Fuel, 266.

[11] Zhang, B., Zhong, Z., Min, M., Ding, K., Xie, Q., Ruan, R. 2015. Catalytic fast co-pyrolysis of biomass and food waste to produce aromatics: Analytical Py-GC/MS study. Bioresour. Technol., 189, 30-35.

[12] Li, W., Zheng, J., Luo, Y., Tu, C., Zhang, Y., Da, Z. 2017. Hierarchical zeolite Y with full crystallinity: formation mechanism and catalytic cracking performance. Energy Fuels, 31(4), 3804-3811.

[13] Chaihad, N., Situmorang, Y.A., Anniwaer, A., Kurnia, I., Karnjanakom, S., Kasai, Y., Abudula, A., Reubroycharoen, P., Guan, G. 2021. Preparation of various hierarchical HZSM-5 based catalysts for in-situ fast upgrading of bio-oil. Renew. Energy, 169, 283-292.

[14] Wan, W., Fu, T., Qi, R., Shao, J., Li, Z. 2016. Coeffect of Na+ and tetrapropylammonium (TPA+) in alkali treatment on the fabrication of mesoporous ZSM-5 catalyst for methanol-to-hydrocarbons reactions. Ind. Eng. Chem. Res., 55(51), 13040-13049.

[15] Ma, Q., Fu, T., Li, H., Cui, L., Li, Z. 2020. Insight into the selection of the post-treatment strategy for ZSM-5 zeolites for the improvement of catalytic stability in the conversion of methanol to hydrocarbons. Ind. Eng. Chem. Res., 59(24), 11125-11138.

[16] Novruzova, N., Tuel, A., Farrusseng, D., Meunier, F.C. 2016. Influence of crystal size on the uptake rate of isooctane in plain and hollow silicalite-1 crystals. Micropor. Mesopor. Mater., 228, 147-152.

[17] Chen, L.H., Sun, M.H., Wang, Z., Yang, W., Xie, Z., Su, B.L. 2020. Hierarchically structured zeolites: from design to application. Chem. Rev., 120(20), 11194-11294.

[18] Groen, J.C., Peffer, L.A.A., Moulijn, J.A., Pérez-Ramírez, J. 2004. Mesoporosity development in ZSM-5 zeolite upon optimized desilication conditions in alkaline medium. Colloids Surf. A Physicochem. Eng. Asp., 241(1-3), 53-58.

[19] Abelló, S., Bonilla, A., Pérez-Ramírez, J. 2009. Mesoporous ZSM-5 zeolite catalysts prepared by desilication with organic hydroxides and comparison with NaOH leaching. Appl. Catal. A: Gen., 364(1-2), 191-198.

[20] Li, X., Zhang, X., Shao, S., Dong, L., Zhang, J., Hu, C., Cai, Y. 2018. Catalytic upgrading of pyrolysis vapor from rape straw in a vacuum pyrolysis system over La/HZSM-5 with hierarchical structure. Bioresour. Technol., 259, 191-197.

[21] Ren, X.-Y., Cao, J.-P., Zhao, X.-Y., Yang, Z., Liu, S.-N., Wei, X.-Y. 2017. enhancement of aromatic products from catalytic fast pyrolysis of lignite over hierarchical HZSM-5 by piperidine-Assisted desilication. ACS Sustainable Chem. Eng., 6(2), 1792-1802.

[22] Deng, S., Wang, Z., Deng, D., Chen, Z., He, D., He, H., Ji, Y., Hou, G., Sun, W., Liu, L. 2021. One-pot synthesis of hollow single crystal SSZ-13 zeolite by creating aluminum gradients with excellent activity for NH3-SCR. Micropor. Mesopor. Mater., 314.

[23] Fodor, D., Pacosova, L., Krumeich, F., van Bokhoven, J.A. 2014. Facile synthesis of nano-sized hollow single crystal zeolites under mild conditions. Chem. Commun. (Camb), 50(1), 76-78.

[24] Xu, Y., Wang, J., Ma, G., Lin, J., Ding, M. 2019. Designing of hollow ZSM-5 with controlled mesopore sizes to boost gasoline production from syngas. ACS Sustainable Chem. Eng., 7(21), 18125-18132.

[25] Jin, W.-y., Qiao, J.-r., Yu, J.-p., Wang, Y.-l., Cao, J.-p. 2020. Influence of hollow ZSM-5 zeolites prepared by treatment with different alkalis on the catalytic conversion of methanol to aromatics. Energy Fuels, 34(11), 14633-14646.

[26] Niu, X., Sun, Y., Lei, Z., Qin, G., Yang, C. 2020. Facile synthesis of hierarchical hollow Mn-ZSM-5 zeolite for enhanced cyclohexane catalytic oxidation. Prog. Nat. Sci.: Mater. Int., 30(1), 35-40.

[27] Yang, Z., Cao, J.-P., Liu, T.-L., Zhu, C., Feng, X.-B., Zhao, X.-Y., Zhao, Y.-P., Bai, H.-C. 2021. Controllable hollow HZSM-5 for high shape-selectivity to light aromatics from

catalytic reforming of lignite pyrolysis volatiles. Fuel, 294.

[28] Ma, Z., Fu, T., Wang, Y., Shao, J., Ma, Q., Zhang, C., Cui, L., Li, Z. 2019. Silicalite-1 derivational desilication-recrystallization to prepare hollow nano-ZSM-5 and highly mesoporous micro-ZSM-5 catalyst for methanol to hydrocarbons. Ind. Eng. Chem. Res., 58(6), 2146-2158.

[29] Gao, Y., Zheng, B., Wu, G., Ma, F., Liu, C. 2016. Effect of the Si/Al ratio on the performance of hierarchical ZSM-5 zeolites for methanol aromatization. RSC Adv., 6(87), 83581-83588.

[30] Rahimi, N., Karimzadeh, R. 2011. Catalytic cracking of hydrocarbons over modified ZSM-5 zeolites to produce light olefins: A review. Appl. Catal. A: Gen., 398(1-2), 1-17.

[31] Xiao, W., Wang, F., Xiao, G. 2015. Performance of hierarchical HZSM-5 zeolites prepared by NaOH treatments in the aromatization of glycerol. RSC Adv., 5(78), 63697-63704.

[32] Song, G., Xue, D., Xue, J., Li, F. 2017. Synthesis and catalytic characterization of ZSM-5 zeolite with uniform mesopores prepared in the presence of a novel organosiloxane. Micropor. Mesopor. Mater., 248, 192-203.

[33] Zhang, K., Fernandez, S., Kobaslija, S., Pilyugina, T., O'Brien, J., Lawrence, J.A., Ostraat, M.L. 2016. Optimization of hierarchical structures for beta zeolites by post-synthetic base leaching. Ind. Eng. Chem. Res., 55(31), 8567-8575.

[34] Wu, J.-b., Zhang, X.-y., Sun, Z.-p., Li, H.-t., Zhou, W., Zhao, Y.-x. 2019. Effect of NaOH content in the synthesis gel on the catalytic performance of H-ZSM-5 zeolites in the gas phase carbonylation of dimethoxymethane. J. Fuel Chem. Technol., 47(10), 1226-1234.

[35] Wu, L., Xue, X., Yu, H., Zhang, C., Wei, X., Liang, J., Sun, Y. 2020. Catalytic pyrolysis of poplar sawdust: excellent hydrocarbon selectivity and activity of hollow zeolites. Bioresour. Technol., 317, 123954.

[36] Li, H., Wang, Y., Meng, F., Gao, F., Sun, C., Fan, C., Wang, X., Wang, S. 2017.

Controllable fabrication of single-crystalline, ultrafine and high-silica hierarchical ZSM-5 aggregates via solid-like state conversion. RSC Adv., 7(41), 25605-25620.

[37] Subotić, B., Bronić, J., Antonić Jelić, T. 2009. Theoretical and practical aspects of zeolite nucleation. in: Ordered Porous Solids, pp. 127-185.

[38] Zhang, Y., Zhang, W., Zhang, J., Dong, Z., Zhang, X., Ding, S. 2018. One-pot synthesis of cup-like ZSM-5 zeolite and its excellent oxidative desulfurization performance. RSC Adv., 8(56), 31979-31983.

[39] Uzun, B.B., Sarioğlu, N. 2009. Rapid and catalytic pyrolysis of corn stalks. Fuel Process. Technol., 90(5), 705-716.

[40] Zheng, Y., Tao, L., Yang, X., Huang, Y., Liu, C., Zheng, Z. 2018. Insights into pyrolysis and catalytic co-pyrolysis upgrading of biomass and waste rubber seed oil to promote the formation of aromatics hydrocarbon. Int. J. Hydrog. Energy, 43(34), 16479-16496.

[41] Kim, J.-S., Choi, G.-G. 2018. Pyrolysis of lignocellulosic biomass for biochemical production. in: Waste Biorefinery, pp. 323-348.

[42] Lu, Q., Zhang, Y., Tang, Z., Li, W.-z., Zhu, X.-f. 2010. Catalytic upgrading of biomass fast pyrolysis vapors with titania and zirconia/titania based catalysts. Fuel, 89(8), 2096-2103.

[43] Chaihad, N., Anniwaer, A., Karnjanakom, S., Kasai, Y., Kongparakul, S., Samart, C., Reubroycharoen, P., Abudula, A., Guan, G. 2021. In-situ catalytic upgrading of bio-oil derived from fast pyrolysis of sunflower stalk to aromatic hydrocarbons over bifunctional Cu-loaded HZSM-5. J. Anal. Appl. Pyrol., 155.

[44] Vichaphund, S., Aht-ong, D., Sricharoenchaikul, V., Atong, D. 2014. Catalytic upgrading pyrolysis vapors of Jatropha waste using metal promoted ZSM-5 catalysts: An analytical PY-GC/MS. Renew. Energy, 65, 70-77.

[45] Wang, J.-X., Cao, J.-P., Zhao, X.-Y., Liu, T.-L., Wei, F., Fan, X., Zhao, Y.-P., Wei, X.-Y. 2017. Study on pine sawdust pyrolysis behavior by fast pyrolysis under inert and

reductive atmospheres. J. Anal. Appl. Pyrol., 125, 279-288.

[46] Balasundram, V., Ibrahim, N., Kasmani, R.M., Isha, R., Hamid, M.K.A., Hasbullah, H., Ali, R.R. 2018. Catalytic upgrading of sugarcane bagasse pyrolysis vapours over rare earth metal (Ce) loaded HZSM-5: effect of catalyst to biomass ratio on the organic compounds in pyrolysis oil. Appl. Energy, 220, 787-799.

[47] Dhyani, V., Bhaskar, T. 2018. A comprehensive review on the pyrolysis of lignocellulosic biomass. Renew. Energy, 129, 695-716.

[48] Zhang, C., Zhang, Z., Zhang, L., Li, Q., Li, C., Chen, G., Zhang, S., Liu, Q., Hu, X. 2020. Evolution of the functionalities and structures of biochar in pyrolysis of poplar in a wide temperature range. Bioresour. Technol., 304, 123002.

Chapter 5 Conclusions and Future Perspectives

Catalytic pyrolysis is the fast pyrolysis of biomass to increase the quality of bio-oil by increasing valuable products such as benzene, toluene, xylene, and other aromatic chemicals in the bio-oil. The catalyst is the foundation of this process. Thus, it is necessary to ensure higher catalytic activity, better selectivity, and longer life-time. The ZSM-5 based catalysts are currently the most widely used catalysts for biomass conversion in aromatics production due to its outstanding acidity, heat-resistant properties, adequate pore size, and good catalytic activity. However, the mass transfer capacity of large reactants and products through the small pores of ZSM-5 is limited which had a significant negative impact on the catalytic activity. Due to the most cracking reaction occurring within the pore, products will be formed and spread out slowly from the pores, resulting in low-yield of product being obtained. In addition, the ZSM-5 based catalysts often suffer from coke formation due to its high acidity. As a result, ZSM-5 based catalysts should be more improved and modified.

In this dissertation, metal loading by wet impregnation method was chosen for loading Cu onto the ZSM-5 because it is a simple and low-cost procedure. It is found that the optimal amount of Cu loading on the HZSM-5 for maximum aromatic hydrocarbon production was found to be 0.5 wt.% with a relative content of 73.2% and a yield of specific aromatic hydrocarbons (mostly including BTX) was up to 56.5 mg/g-biomass (daf), which is higher than the original HZSM-5 (55.0% and 26.0 mg/g-biomass (daf)). Despite metal loading improves the acidity and unique nature of the metal, leading to enhanced catalytic activity, diffusion limitation concerns remain due to its small pore size, which has yet to be resolved.

Therefore, further research was performed to overcome diffusion limitations and simultaneously, metal loading was carried out to further improve the performance of the developed catalyst. Hierarchical zeolite, which has properties significantly different from that of conventional ZSM-5 in terms of reactants and product diffusions, mass transfer ability and

resistance to deactivation, was prepared and studied for its catalytic activity. In this research, the commercial HZSM-5 catalyst was desilicated by post treatment method to obtain the hierarchical HZSM-5 zeolite. It is found that a mixture of 0.2 M NaOH and 0.25 M TPAOH was the optimal condition that gave the best catalytic performance. The production of aromatic hydrocarbons up to 45.2 mg/g-bio-oil was achieved with 65.8% of relative total peak area related to the obtained aromatic hydrocarbons. However, the coking on the catalyst surface was not inhibited. Thus, the hierarchical HZSM-5 zeolites were further modified by Cu, Ag, and Mg to solve the coking problem and enhance aromatic hydrocarbon production. As a result, the appropriate amount for these three metals was 0.25 wt. % Cu, 0.25 wt.%Ag, and 0.1 wt.% Mg for the avoiding severe coking.

To further improve the catalytic performance of the HZSM-5 based catalysts, the preparation of a hollow HZSM-5 structure and its application in catalytic upgrading of bio-oil were further investigated to gain knowledge and benefit in the development of hollow ZSM-5 based catalysts for the bio-oil upgrading in the future. This structure is challenging and novel since it is considered another class of material that can reduce diffusion limitation problem and there hasn't been much reported on its application in catalytic upgrading of bio-oil. The hollow structure of the ZSM-5 using the facile hydrothermal method, coupled with post treatment with TPAOH, resulting in a special hollow structure ZSM-5 with mesoporous shell was synthesized and applied for in-situ catalytic upgrading of bio-oils generated from the rapid pyrolysis of biomass components (i.e., cellulose, hemicellulose and lignin). It is found that hollow ZSM-5 exhibited a higher aromatic production capacity than the original ZSM-5 due to the hollow structure and high presence of mesopores, which play an important role in determining the aromatic selectivity as well as solving the problem of coke formation.

Each of the strategies investigated in this dissertation has its combination of advantages and disadvantages. It should take the advantages of each technique and continue to improve the HZSM-5 based catalyst to make it more efficient. According to our findings, short diffusion

path and acidity properties should be moderately modified to preserve catalytic activity and meanwhile to avoid secondary reactions that lead to coke and catalyst deactivation. Above all, these proposed studies for the development of HZSM-5 based catalysts to optimize catalytic upgrading of bio-oil remain at a laboratory scale. Therefore, it would be of great benefit to the industrial application if it is cost-effectively scaled up. In addition, other structured ZSM-5 catalysts with properties to shorten diffusion length, such as core/shell ZSM-5@mesoporous material and nanosheet structured ZSM-5, are also expected to improve the catalytic upgrading of bio-oil to produce value product.

Finally, the improved ZSM-5 catalysts were not only suitable for the catalytic upgrading of bio-oil, as the original ZSM-5, they should be also served as the excellent catalysts for a variety of other processes. It is expected that this research will assist not only those who are interested in catalytic upgrading of bio-oil processes, but also those who are interested in applying my findings to other research areas.

CURRICULUM VITAE

Personal Details

    Name: Nichaboon Chaihad

    Nationality: Thai

    Sex: Female

    Marital Status: Single

    Date of birth: 25 April, 1993

    Hobbies: Exercising, watching movies, travelling

Language Known: Thai, English, and Japanese

Education background

2019-2022   **Doctor of Engineering (Safety Science and Engineering)**

               The graduate school of Science and Technology, Hirosaki University, Aomori, Japan

2016-2018   **Master of Science in Petrochemistry and Polymer science**

               Faculty of Science, Chulalongkorn University, Bangkok, Thailand

2011-2015   **Bachelor of Science in Chemistry**

               Faculty of Science, Chulalongkorn University, Bangkok, Thailand

Scholarships and Awards

    Japanese Government (MEXT, Monbukagakusho) Scholarship, *Doctoral Degree*,

        Hirosaki University, Japan (2019-2022)

    Best Oral Presentation Award, The Second International Symposium of Young Scholars

        on Carbon Resources Conversion (2021)

Work Experiences

    2015- 2016   Kao Consumer Products (Southeast) Co.,Ltd.

               Position: Fragrance Evaluator (Research & Development)

List of First Author Publications

1) **Nichaboon Chaihad**, Aisikaer Anniwaer, Aghietyas Choirun Az Zahra, Yutaka Kasai, Prasert Reubroycharoen, Katsuki Kusakabe, Abuliti Abudula and Guoqing Guan, In-situ catalytic upgrading of bio-oil from rapid pyrolysis of biomass over hollow HZSM-5 with mesoporous shell, Bioresoure Technology, 341 (2021) 125874.

2) **Nichaboon Chaihad**, Yohanes Andre Situmorang, Aisikaer Anniwaer, Irwan Kurnia, Surachai Karnjanakon, Yutaka Kasai, Abuliti Abudula, Prasert Reubroycharoen and Guoqing Guan, Preparation of various hierarchical HZSM-5 based catalysts for in-situ fast upgrading of bio-oil, Renewable Energy, 169 (2021) 283-292.

3) **Nichaboon Chaihad**, Aisikaer Anniwaer, Surachai Karnjanakom, Yutaka Kasai, Suwadee Kongparakul, Chanatip Samart, Prasert Reubroycharoen, Abuliti Abudula and Guoqing Guan, In-situ catalytic upgrading of bio-oil derived from fast pyrolysis of sunflower stalk to aromatic hydrocarbons over bifunctional Cu-loaded HZSM-5, Journal of Analysis and Applied Pyrolysis, 155 (2021) 105079.

4) **Nichaboon Chaihad**, Irwan Kurnia, Akihiro Yoshida, Chuichi Watanabe, Koji Tei, Prasert Reubroycharoen, Yutaka Kasai, Abuliti Abudula, and Guoqing Guan, Catalytic pyrolysis of wasted fishing net over calcined scallop shells: Analytical Py-GC/MS study, Journal of Analysis and Applied Pyrolysis, 146 (2020) 104750.

5) **Nichaboon Chaihad**, Surachai Karnjanakom, Irwan Kurnia, Akihiro Yoshida, Abuliti Abudula, Prasert Reubroycharoen, and Guoqing Guan, Catalytic upgrading ofbio-oils over high-alumina zeolites, Renewable Energy, 136 (2019) 1304-1310.

6) **Nichaboon Chaihad**, Surachai Karnjanakom, Irwan Kurnia, Akihiro Yoshida, Abuliti Abudula, Prasert Reubroycharoen, Guoqing Guan, In-situ Catalytic Upgrading of Bio-oils Derived from Fast Pyrolysis of Cellulose, Hemicellulose, and Lignin over Various Zeolites, Journal of Japan Institute of Energy, 98（2019）254-258.

List of Co-Author Publications

1) Aisikaer Anniwaer, **Nichaboon Chaihad**, Aghietyas Choirun Az Zahra, Tao Yu, Yutaka Kasai, Suwadee Kongparakul, Chanatip Samart, Abuliti Abudula, Steam co-gasification of Japanese cedarwood and its commercial biochar for hydrogen-rich gas production, Int. J. Hydrog. Energy, 46 (2021) 34587-34598.

2) Aisikaer Anniwaer, **Nichaboon Chaihad**, Mengjuan Zhang, Chao Wang, Tao Yu, Yutaka Kasai, Abuliti Abudula, Guoqing Guan, Hydrogen-rich gas production from steam co-gasification of banana peel with agricultural residues and woody biomass, Waste Manag., 125 (2021) 204-214.

3) Yohanes Andre Situmorang, Zhongkai Zhao, **Nichaboon Chaihad**, Chao Wang, Aisikaer Anniwaer, Yutaka Kasai, Abuliti Abudula, and Guoqing Guan, Steam Gasification of Co-pyrolysis Chars from Various Types of Biomass, Int. J. Hydrog. Energy, 46 (2021) 3640-3650.

4) Aisikaer Anniwaer, Tao Yu, **Nichaboon Chaihad**, Yohanes Andre Situmorang , Chao Wang, Yutaka Kasai, Abuliti Abudula, Guoqing Guan, Steam gasification of marine biomass and its biochars for hydrogen-rich gas production, Biomass Convers. Biorefinery, 2020.

5) Irwan Kurnia, Akihiro Yoshida, **Nichaboon Chaihad**, Tirto Prakoso, Shasha Li, Xiao Du, Xiaogang Hao, Abuliti Abudula and Guoqing Guan, Synthesis of p-Menthane-3,8-diol from from Citronellal over Lignin-Derived Carbon Acid Catalysts, New J. Chem., 44 (2020) 10441-10447.

6) Irwan Kurnia, Akihiro Yoshida, **Nichaboon Chaihad**, Asep Bayu, Yutaka Kasai, Abuliti Abudula, and Guoqing Guan, Hydrolysis of Cellulose and Woody Biomass over Sustainable Weak-Acid Carbon Catalysts from Alkaline Lignin, Fuel Process. Technol., 196 (2019) 106175.

List of International Conferences

1) **<u>Nichaboon Chaihad</u>**, Aisikaer Anniwaer, Abuliti Abuliti, Guoqing Guan, In-situ Catalytic Upgrading of Bio-oil Derived from Pyrolysis of Biomass over Hollow H-ZSM-5 Zeolites. *Second International Symposium of Young Scholars on Carbon Resources Conversion (YSCRC-2021),* Thammasat University, Thailand, October 14th-16th, 2021.

List of Domestic Conferences in Japan

1) **<u>Nichaboon Chaihad</u>**, Aiaikaer Anniwaer, 阿布 里提, 官 国清, In-situ catalytic upgrading of bio-oil derived from pyrolysis of cellulose over hollow H-ZSM-5 zeolites. 日本エネルギー学会第 30 回大会, 2021 年 8 月 4-5 日.

2) **<u>Nichaboon Chaihad</u>**, Aisikaer Anniwaer, 于涛, 葛西裕, 吉田 曉弘, 阿布里提, 官国清, Cu で修飾した H-ZSM-5 を用いたバイオオイルの in-situ アップグレードによる軽質芳香族生成物の増加. 第 16 回バイオマス科学会議, 2021 年 1 月 20-21 日.

3) **<u>Nichaboon Chaihad</u>**, Aiaikaer Anniwaer, Irwan Kurnia, 吉田 曉弘, 阿布 里提, 官国清, Enhancement of aromatics production from catalytic upgrading of bio-oil over hierarchical HZSM-5. 2020 年度化学系学協会東北大会（八戸）, 2020 年 9 月 26-27 日.

4) **<u>Nichaboon Chaihad</u>**, Aiaikaer Anniwaer, Wang Chao, Kasai Yutaka, 吉田 曉弘, 阿布 里提, 官 国清, In-situ catalytic upgrading of bio-oil over metal-doped hierarchical HZSM-5 catalyst. 化学工学会第 51 回秋季大会, 2020 年 9 月 24-26 日.

5) **<u>Nichaboon Chaihad</u>**, Irwan Kurnia, 于涛, 吉田 曉弘, Yutaka Kasai, 阿布 里提, 官国清, Enhancement of aromatics production from catalytic upgrading of bio-oil over hierarchical HZSM-5 catalyst. 化学工学会第 85 年会, 関西大学　千里山キャンパス, 2020 年 3 月 15-17 日.

6) **<u>Nichaboon Chaihad</u>**, 吉田 曉弘, Tei Koji, Watanabe Chuichi, 阿布 里提, 官 国清, Catalytic pyrolysis of wasted fishing nets over environmentally friendly scallop shell catalyst. 化学工学会第 84 年会、芝浦工業大学、2019 年 3 月 13-15 日.